FUZZY AND OBSERVER-BASED CONTROL DESIGNS WITH APPLICATION TO POWER SYSTEMS

BY

ADEEL SABIR

A Dissertation Presented to the

DEANSHIP OF GRADUATE STUDIES

KING FAHD UNIVERSITY OF PETROLEUM & MINERALS

DHAHRAN, SAUDI ARABIA

In Partial Fulfillment of the

Requirements for the Degree of

DOCTOR OF PHILOSOPHY

In

ELECTRICAL ENGINEERING

DECEMBER 2015

KING FAHD UNIVERSITY OF PETROLEUM & MINERALS
DHAHRAN 31261, SAUDI ARABIA

DEANSHIP OF GRADUATE STUDIES

This thesis, written by **ADEEL SABIR** under the direction of his thesis adviser and approved by his thesis committee, has been presented to and accepted by the Dean of Graduate Studies, in partial fulfillment of the requirements for the degree of **DOCTOR OF PHILOSOPHY IN ELECTRICAL ENGINEERING**.

Dissertation Committee

Dr. Mahmoud Kassas (Adviser)

Dr. Salim Ibrir (Co-adviser)

Dr. Mohammed Abido (Member)

Dr. Ibrahim M. El-Amin (Member)

Dr. Ibrahim O. Habiballah (Member)

Dr. Ali Ahmad Al-Shaikhi
Department Chairman

Dr. Salam A. Zummo
Dean of Graduate Studies

24/1/16
Date

This dissertation is dedicated to my parents and my family.

ACKNOWLEDGMENTS

In the name of Allah, the Most Beneficient, the Most Merciful

I am thankful to Allah Almighty for His blessings, mercy and support, and for carrying me through this arduous and challenging phase of my life's journey.

I would like to deeply thank my supervisor Dr. Mahmoud Kassas for the continuous support of my doctoral research, and for his patience, enthusiasm and encouragement. His precious advice, valuable knowledge and thorough guidance played a crucial role in the completion of this thesis. I especially acknowledge the encouragement and physical resources that Dr. Kassas provided in completing the experimental part of my thesis. It would not have been possible without him facilitating the necessary hardware.

I would like to express my sincere gratitude to my co-supervisor Dr. Salim Ibrir for his intellectual support and guidance, and for sharing his knowledge and valuable ideas with me. His advice and counsel have an invaluable and integral contribution in the pursuit and accomplishment of the research objectives of this work. I am deeply indebted to him for his guidance.

I would also like to thank my dissertation committee members Dr. Mohammad A. Abido, Dr. Ibrahim M. ElAmin, and Dr. Ibrahim O. Habiballah for their guidance, insightful comments and constructive feedback.

I am thankful to the King Fahd University of Petroleum and Minerals (KFUPM) for providing me with the research facilities, precious resources, and an environment conducive to intellectual growth for my doctoral research.

I would like to thank a number of other people from the Electrical Engineering Department who have made my years at KFUPM unforgettable and cherished. They include Alam Zaib, Dr. Naveed Iqbal, Waqas Afzal, Hussain Ali, Dr. Raza Umer, Mohamed Mamdouh, Asjad Amin, M.A. Qureshi. I'd like to thank these individuals for their friendship, support and most importantly, being there for me in the time of need and difficulty.

Finally, I would like to thank some people with whom I have a much deeper relationship, not directly linked to this thesis. Among them are my parents who brought me up and supported me through my education. I thank them for their unconditional love and always remembering me in their prayers. I'd like to thank my siblings for sincerely caring about my well-being and for their love and affection. Finally, thanks goes to my wife for being tolerant of my difficult schedule, being understanding, patient and caring, providing a carefree environment at our home, and sharing my life.

TABLE OF CONTENTS

LIST OF TABLES

LIST OF FIGURES

Nomenclature

Abbreviations

ADC	:	Analog-to-Digital Converter
ANFIS	:	Artificial Neuro-Fuzzy Inference System
ANN	:	Artificial Neural Networks
BLDC	:	Brushless DC
CPU	:	Central Processing Unit
D-STATCOM	:	Distribution STATCOM
DE	:	Differential Evolution
DFIG	:	Doubly-fed Induction Generator
DG	:	Distributed Generation
DSP	:	Digital Signal Processor
FACTS	:	Flexible AC Transmission System
FL	:	Fuzzy Logic
GA	:	Genetic Algorithm
LMI	:	Linear Matrix Inequality
LPV	:	Linear Parameter Varying
LQR	:	Linear Quadratic Regulator
MCU	:	Microcontroller

PI	:	Proportional plus Integral
PID	:	Proportional plus Integral plus Derivative
PIL	:	Processor-in-the-loop
PMSM	:	Permanent Magnet Synchronous Motor
PSO	:	Particle Swarm Optimization
pu	:	Per Unit
PV	:	Photovoltaic
PWM	:	Pulsewidth Modulation
RTDS	:	Real Time Digital Simulator
s.t.	:	Subject to
SM	:	Sliding Mode
SMIB	:	Single-machine-infinite-bus
SOF	:	Static Output Feedback
STATCOM	:	Static Compensator
VSC	:	Voltage Source Converter

Notations

$\mathbb{R}$	:	Set of real numbers, the real space
$\mathbb{R}^n$	:	Set of real-valued vectors of length n
$\mathbb{R}^{m\times n}$	:	Set of real-valued matrices of size $m \times n$
$\in$	:	is an element of
$\|u(t)\|_{\mathcal{L}_2}$	:	$\mathcal{L}_2$ norm of the signal $u(t)$
$\|T(s)\|_\infty$	:	$\mathcal{H}_\infty$ norm of the transfer matrix $T(s)$
$\|T(s)\|_2$	:	$\mathcal{H}_2$ norm of the transfer matrix $T(s)$
I	:	Identity matrix of the appropriate dimension
$f_0 : \mathbb{R}^n \to \mathbb{R}$	:	Function f_0 maps real-valued vectors of length n to the real space

THESIS ABSTRACT

NAME:	Adeel Sabir
TITLE OF STUDY:	Fuzzy and Observer-Based Control Designs With Application to Power Systems
MAJOR FIELD:	Electrical Engineering
DATE OF DEGREE:	December 2015

Full state feedback offers a convenient way to impose a desired behavior on the closed loop performance of controllable systems. However, in real life systems, all of the states may not be available. Moreover, the mathematical model chosen for controller synthesis may contain uncertain elements and inaccuracies due to unmodeled dynamics. Thus the controller must exhibit a satisfactory closed loop performance in the presence of these uncertainties and inaccuracies, making the control design a challenge. It has motivated several research efforts on observer and output based control of uncertain systems.

New linear matrix inequality (LMI) based results on observer based controller design for uncertain linear systems subject to polytopic uncertainties and exogenous disturbance under single and multiobjective performance constraints are presented. A

matched Luenberger type observer is designed for state estimation, whose gain and state matrices are synthesized using a single-step solution to a convex optimization problem involving LMI constraints with a guaranteed performance index. The results are shown to be less conservative and have lower computational complexity than some existing solutions.

Additionally, a novel output based hybrid fuzzy/PI controller is designed for robust control of uncertain systems without using any knowledge of the system model. The proposed controller is computationally simpler than the existing designs and results in improved system performance.

The effectiveness of proposed control techniques is demonstrated through simulation and processor-in-the-loop configuration results in MATLAB®/Simulink environment on robust speed control of a brushless DC (BLDC) motor drive and stabilization of static compensator (STATCOM) installed power system under parametric uncertainties and external disturbances. The results show the validity and performance gains of the proposed techniques.

Finally, experimental validation of the hybrid fuzzy/PI controller is carried out on speed control of the BLDC motor drive. The control algorithm is implemented on low-cost microcontroller (MCU) and its performance is compared with those of the conventional PI and fuzzy logic controllers to demonstrate the complexity reduction and performance improvement achieved by it. The details of hardware implementation are also given.

ملخص الرسالة

الاسم: عديل صابر

عنوان الدراسة: تصاميم وتطبيقات لأنظمة التحكم المراقبة الضبابية

التخصص: هندسة كهربائية

تاريخ المناقشة: ديسمبر 2015

التغذية الرجعية الكاملة تقدم وسيلة مريحة لفرض السلوك المطلوب على أداء الحلقات حلقة مغلقة من نظم السيطرة عليها. ومع ذلك، في أنظمة الحياة الحقيقية، كل من الفروض قد لا تكون متاحة. بالإضافة، فإن النموذج الرياضي الذي تم اختياره لتجميع تحكم قد تحتوي على عناصر غير مؤكدة وغير دقيقة بسبب ديناميات unmodeled . وبالتالي فإن وحدة التحكم يجب أن تحمل أداء أفضل للحلقة المغلقة في وجود هذه الشكوك وعدم الدقة، مما يجعل التحكم في هذا السياق تحديا. وقد حفز ذلك عدد من الجهود البحثية على مراقبة المخرجات على أساس السيطرة على أنظمة غير مؤكدة.

في هذا البحث، يتم عرض مصفوفة جديدة التفاوتات الخطية (LMI) النتائجة على أساس يعتم على تصميم جهاز تحكم النظم الخطية غير مؤكدة تخضع للشكوك polytopic واضطرابات خارجية في ظل قيود multiobjective . ثم تم تصميم يقابل Luenberger نوع المراقب عن تقدير القيود، الذي ربح والمصفوفات دولة تم تجميعها باستخدام محلول خطوة واحدة لإيجاد الحل الأمثل لمحدبة تنطوي على قيود LMI مع مؤشر أداء مضمون. وأظهرت النتائج أن أقل تحفظا وتعاني من انخفاض التعقيد الحسابي من بعض الحلول القائمة.

بالإضافة إلى ذلك، تم تصميم هجين ناتج رواية تقوم تحكم غامض PI / للسيطرة قوية من النظم غير مؤكدة دون استخدام أي معرفة من نموذج النظام. وحدة تحكم المقترح هو أبسط حسابيا من التصاميم والنتائج الحالية في تحسين أداء النظام.

وأظهرت فعالية تقنيات الرقابة المقترحة من خلال المحاكاة والمعالجات في حلقة النتائج التكوين في MATLAB / Simulink البيئة السيميولينك على قوة السيطرة على سرعة فرش DC (BLDC) محرك السيارات واستقرار المعوض ثابت (STATCOM) تثبيت نظام السلطة في ظل الشكوك حدودي والاضطرابات الخارجية. أظهرت النتائج صحة وأداء مكاسب التقنيات المقترحة.

وأخيرا، ويتم التحقق التجريبي من وحدة تحكم غامض PI / الهجين من على التحكم في سرعة محرك السيارات .BLDC يتم تطبيق خوارزمية التحكم في منخفض التكلفة متحكم (MCU) ومقارنة أدائها مع تلك PI التقليدي وتحكم المنطق الضبابي للتدليل على الحد من التعقيد وتحسين الأداء التي حققتها. وترد أيضا تفاصيل التنفيذ الأجهزة.

CHAPTER 1

INTRODUCTION

Robust control is a branch of control systems theory addressing uncertainties. A controller can be classified as robust if under its action, the performance of the controlled system is within some prescribed limits despite the presence of uncertainties and disturbances. The performance can be characterized in terms of fulfilling goals such as closed loop stability, reference tracking ability, disturbance and sensor noise rejection, avoidance of actuator saturation and effectively dealing with model mismatches. However, in practice all of these goals may not be simultaneously achievable and may often be contradictory to each other. As a result, the final controller can only attain a trade-off between these goals [1].

The requirement on the output signals of a specific system asymptotically tracking a set of desired reference signals is frequently encountered in many practical situations. From a robust control perspective, this requirement entails finding a control law ensuring satisfactory tracking behavior despite the presence of uncertainties and external disturbances. In the context of linear systems, full state feedback offers a convenient

way to effectively synthesize a control law and impose desired behavior on the system being controlled. However, in practical systems, all of the states may not be available. Furthermore, the mathematical model chosen for control synthesis may contain uncertain elements due to additive noise, operating environment, nonlinearities, inadequate plant knowledge, unmodeled dynamics and uncertain or slowly varying parameters [2]. The unavailability of states and undesired model uncertainties make the control design a challenge. It has lead the designers to seek control laws based merely on the available output of the system.

Output based control can be broadly categorized into two major categories: (1) model-based control and (2) model-free control. Model-based control techniques utilize information from the system's model in control design while in model-free approaches, controller synthesis is independent of the system model. In recent years, a number of works have emerged addressing robust model-based output feedback control; utilizing observer based state feedback control where the missing state information is reconstructed through observer design (see for example [2–27]), and static output feedback (SOF) control where the controller is synthesized using the output alone (see for example [28–40]). In the model-free control domain also, several control techniques have been proposed for different practical systems where model-based techniques encounter limitations or a working model is unavailable. A number of these techniques involve intelligent control based on fuzzy logic, artificial neural networks (ANN), artificial neuro-fuzzy inference system (ANFIS), and hybrid of intelligent and classical control, due to the convenience and performance gains they offer, and their similarity

to human reasoning and naturally occurring systems. Control of flexible-link robots [41–47], speed control of brushless dc motors [48–54] and control of static compensator (STATCOM) based power systems [55–64] are some examples.

With this brief introduction, this work aims to develop new techniques in each domain i.e., model-based and model-free (intelligent) robust control, targeting the areas of observer-based control and fuzzy logic control. In the model-based control area, novel results for robust observer based control using linear matrix inequality (LMI) formulation are developed for a class of uncertain linear systems. In the model-free intelligent control domain, a new hybrid control technique combining the classical proportional plus integral (PI) control and fuzzy logic control is developed. To demonstrate the effectiveness of the proposed control techniques, two different applications are selected due to their widespread practical usage; speed control of brushless dc (BLDC) motor drive and stabilization of oscillations in a STATCOM installed power system. An account of the literature in the relevant subject areas is provided, followed by an overview of the gaps in the existing literature to establish the motivation behind this research work and highlight the contributions of this dissertation.

1.1 Robust Observer Based Control using LMIs

Over the past few years, a large amount of research effort has been contributed toward formulating complex control problems as convex optimization involving LMI constraints. LMI formulations greatly simplify complex problems due to their numerical tractability and availability of efficient LMI solving tools. In the absence of full

state information, one way to synthesize the controller is to reconstruct the state information using an observer. In general, finding the observer and controller gains for the the closed loop configuration leads to a nonconvex problem [14]. In the domain of robust control, the derivation of convex optimization conditions for observer based control design is still an open and active research topic.

In control engineering, the design of a robust controller often requires that the controller not only be robustly stabilizing in the presence of uncertainties and disturbances, but also optimizes a certain performance index under worst case disturbances. The $\mathcal{H}_\infty/\mathcal{L}_2$ constraint is an important robust control design constraint for cogently minimizing the effect of disturbances and uncertainties, while the $\mathcal{H}_2$ constraint is effective in imposing certain optimal performance requirements on the controller. Consequently, the combination of the $\mathcal{H}_2$ and $\mathcal{H}_\infty$ constraints into a single mixed performance $\mathcal{H}_2/\mathcal{H}_\infty$ constraint enables the controller to have the combined strengths of both performance indexes [65–68].

The literature on convex optimization based synthesis of robust observer and observer based controller design for uncertain systems can be broadly categorized into two major categories: parameter-dependent and parameter-independent approach. The former is widely employed in the framework of linear parameter varying (LPV) systems (see for example [3–12, 17, 69–75]; specifically [4–6, 8, 9, 11, 12] for $\mathcal{H}_\infty/\mathcal{L}_2$ performance and [69–74] for mixed $\mathcal{H}_2/\mathcal{H}_\infty$ performance). This approach is based on the assumption that some measure of the varying parameters is available and utilizes it in synthesizing parameter dependent gains and Lyapunov functions, subsequently reliev-

ing the degree of conservatism [70]. However, it can not be applied in cases where the varying parameters are not online measurable or, are unmeasurable. Additionally, in many cases rate limitation constraints are placed on varying parameters [72, 75]. On the other hand, parameter-independent approach using the concept of quadratic stability, employs constant gains and a fixed Lyapunov function for the entire operating range of parameters (see for example [2, 13, 14, 67, 68, 76–80]; specifically [67, 68, 77, 78, 80] for mixed $\mathcal{H}_2/\mathcal{H}_\infty$ performance). It is well-suited for cases where the varying parameters are not online measurable, and can accommodate arbitrarily fast time-varying parameters at the expense of added conservatism [69, 70, 81].

The observer based convex optimization approaches presented in this dissertation utilize the notion of quadratic stability. For discrete time systems, LMI conditions for a parameter varying Luenberger observer design are proposed in [3] by interpolating several invariant observer gains tuned for different operating points using nonlinear interpolating functions. Parametrized observer-controller design for the same class of systems and similar observer gain synthesis approach as in [3] is treated in [10] with uncertainty in varying parameters. A stabilization approach with $\mathcal{L}_2$ gain performance using Kalman style observer and optimal control theory has been proposed in [5]. The concepts of *superstability* and *superdetectability* for observer based stabilization of switched linear discrete time systems with equalized performance have been employed in [7]. Both [5, 7] use iterative LMI solution. The observer based stabilization of switched discrete time systems has also been treated in [15], subject to time varying uncertainties under $\mathcal{H}_\infty$ performance framework. Convex optimization

approaches have been employed for observer-controller synthesis of uncertain linear systems with structured uncertainties in [2, 13, 14] and with polytopic uncertainties in [17]. In [2] and [13], equality constraints are used to formulate the problem in terms of convex constraints. Then in [14], LMI conditions for observer-controller design for the same class of uncertain linear systems are proposed using a decoupling approach without any equality constraints, to obtain less conservative results as compared to [2, 13]. LMI conditions for tracking control of linear time invariant systems with mixed $\mathcal{H}_2/\mathcal{H}_\infty$ performance are proposed in [80] assuming perfect knowledge of system matrices. The authors of [34] propose convex optimization techniques for stabilization of uncertain continuous-time linear systems with polytopic uncertainties through static output feedback, and extend the results to $\mathcal{H}_\infty$ performance. Similarly, those in [78] propose observer based controller design for discrete time linear systems with structured uncertainties and mixed $\mathcal{H}_2/\mathcal{H}_\infty$ performance, in terms of LMI conditions. Robust tracking control approaches for systems with polytopic uncertainties with full state feedback are reported in [82–84]. In [85] the authors propose an output feedback based iterative solution to robust tracking control of systems with polytopic uncertainties, solving an originally bilinear problem as LMIs. The observer based controller reported in [21] also relies on an iterative solution involving particle swarm optimization to seek optimal gain values and carefully choosing a search space to achieve convergence. The robust $\mathcal{H}_\infty$ controller reported by the authors of [86] for system with polytopic uncertainties also takes on an observer-based state feedback formulation with an asymptotic observer designed independently. In a recent work [87], LMI aided synthesis of an

obsever-based controller for fractional-order uncertain systems has been addressed.

1.2 Fuzzy Logic Control

The idea of fuzzy sets was introduced by Zadeh in [88]. In the recent years, fuzzy logic has been used in many applications such as subways, washing machines, biomedical systems, industrial process systems, medical instrumentation and finance applications [53, 89]. It allows the control system designer to make the controller behave intuitively; like an expert on the system being controlled. The input-output relationship is defined through a number of linguistic rules in the form of *if-else* statements. This makes fuzzy logic control similar to the reasoning ability of humans and facilitates the handling of nonlinearities and complex phenomena in the system.

A fuzzy logic controller offers several advantages over other types of controllers. In comparison to a neural network based controller, a rule-based fuzzy controller provides a heuristic approach for controlling the plant, giving the control designer a clear understanding of different parameters and their effect on system performance. Similar to the analytical approaches, it characterizes the input-output relationship in terms of physical rules governing system behavior. Unlike the conventional PI controller, it is not operating point dependant. Finally, in contrast to the analytical nonlinear controllers, it does not necessarily require a mathematical model for the system to be controlled [59].

1.3 Applications

Two distinct applications, one from power systems and the other from power electronic drives, are selected for demonstrating the performance of the proposed control techniques; due to their advantages, desirable features and widespread usage. Their significance and an overview of the existing literature on their control are given here.

1.3.1 The Brushless DC Motor

A BLDC motor is essentially a permanent magnet synchronous motor (PMSM) with trapezoidal shaped back-emf waveforms. Its rotor is a permanent magnet, fitted with position sensors and a commutation module that could be independent or integrated into the motor. The shape of the back-EMF is dictated by the rotor magnets' shape and the stator winding distribution. In contrast to the PMSM which requires a high resolution position sensor, a low resolution position sensor can be utilized in the BLDC motor drive for generating commutation signals. The stator structure of the BLDC motor is similar to that of a synchronous or an induction motor. The armature winding is installed on the stator side to reduce heating. The permanent magnets producing the excitation field are on the rotor. Due to this reason, the BLDC motor is also referred to as the 'inside out dc machine' [90–92].

The BLDC motor offers several advantages in comparison to the conventional dc motor and the induction motor. Compared to a conventional dc motor, it has lighter construction, higher power density, lower maintenance and cooling requirements, longer lifespan, spark-freeness and ability to operate in explosive environments. Compared to

an induction motor, it has higher efficiency, higher-speed operation capability, better power factor performance and lower control complexity [90, 93]. However, unlike the conventional dc and induction motors, a BLDC motor can not be driven directly from a power source. Torque production in a BLDC is dependant on energizing the appropriate phase winding relative to the rotor position. This adds the requirement of driving circuitry and information about the rotor position, eventually adding to the overall cost of the system. Nevertheless, owing to its advantages, employing a BLDC motor instead of a conventional dc motor or an induction motor can result in a lower overall life-cycle cost of the system [90]. Common applications of BLDC motor drives include industrial variable speed drives, electric vehicles, robotics, heating, ventilation and air conditioning (HVAC) systems, water pumps, refrigerators and washing machines [94–97].

Speed Control of BLDC Motor

Over the recent years, a number of ideas have been proposed in the literature for speed control of BLDC motor drive namely the classical PI and proportional plus integral plus derivative (PID) control [98, 99] and their combination [100], fuzzy logic control [48, 49, 52, 53], ANFIS [54], combined fuzzy and neural network control [51], nonlinear control theory based techniques like input-output linearization, sliding mode control and backstepping control [101–105], model reference adaptive control [106], and others [107,108] to name a few. These speed control techniques can also be broadly categorized into: (1) model-based (see [51, 94, 96, 100, 102, 106–114]) and (2) model-free (see [48–50, 52–54, 97, 115]). Model-based techniques usually employ the simplified dc motor model for controller design (see [51, 96, 102, 104, 112, 113, 116]).

Many of the above-mentioned speed control schemes involve sensing one or more current signals for controlling the speed through current (see for instance [50, 51, 96, 107, 109, 110, 114]). This requires additional current sensors and clean measurement signals to achieve satisfactory performance. In case of a noisy signal due to sensor or process noise, additional filtering circuitry may be required to clean up the feedback signals.

Fuzzy Logic Based Speed Control

Fuzzy logic based control, hybrid fuzzy control and a combination of fuzzy logic and other types of control has been applied for speed control of the BLDC motor drive in [48–54, 117]. The authors of [48] employed a fuzzy logic based controller that acts on the error between actual speed and its set-point to obtain current set-point, and enforcing it through the phases using hysteresis control. A large rule base is employed resulting in a total of 49 rules. In [117] the authors presented a fuzzy proportional plus integral derivative controller for speed control of BLDC motor drive, by replacing only the proportional part of a conventional PID controller with fuzzy logic control. In [49] the authors proposed a hybrid fuzzy/PI controller that switches between fuzzy and PI control structure based on oscillations, overshoot and large disturbances, and generating the output switching logic based on the control signal through pulsewidth modulation (PWM). A fuzzy logic controller for the speed loop is employed in [51] with neural network assisted reference current generation, resulting in a fairly complex overall control structure. In [52] a composite controller combining the classical PID and a fuzzy PID is proposed with online tunable parameters. Implementation of fuzzy

logic based speed control is also demonstrated in [53], while subjecting the drive system to different operating conditions like change in speed reference, rotor inertia and load.

1.3.2 STATCOM Based Power System

The STATCOM is a family of flexible AC transmission system (FACTS) devices that is employed to regulate the reactive current by controlling the generation and absorption of reactive power through switching of solid-state devices. The power electronic voltage source converter (VSC) is the backbone of this device. The STATCOM consists of a six pulse VSC whose DC side is connected to an energy storage device (e.g., a capacitor), coupling devices (e.g., transformers) to electrically couple the STATCOM output and system voltage, and a controller. The primary objective of the STATCOM is to control the flow of reactive power and voltage support. However, the real power flow can also be controlled through the control of phase angle between STATCOM output voltage and the system's voltage. Due to the integration of solid-state devices, the STATCOM allows for a fast transient response, compact construction, optimum voltage characteristics, operational flexibility and good dynamic performance under a variety of operating conditions [118, 119].

Applications of STATCOM and Control Techniques

The STATCOM has been used in many applications relevant to power system stability. Due to its power control and voltage support abilities, it is continually being employed in the latest state-of-the-art applications. Some prominent applications of STATCOM

include damping of power system oscillations [120–124], subsynchronous damping control [125], voltage unbalance compensation [126], low voltage ride-through [127] and subsynchronous resonance (SSR) alleviation [128] in wind farms, voltage fluctuation control under high levels of distributed generation (DG) penetration [129], stability of fixed-speed wind farms [130], unbalanced currents compensation for self-excited induction generators [131] and improving power transfer limits in photovoltaic (PV) solar farms [132] until very recently.

A number of diverse control techniques have been used in the literature on STATCOM-integrated power systems. In [122] a PI based damping stabilizer is presented for power system stability using STATCOM; the gains are designed using particle swarm optimization (PSO). In [124] the gains for the PI damping stabilizer for STATCOM power system are designed using differential evolution (DE) and real-time digital simulator (RTDS) implementation results are presented. A nonlinear $\mathcal{H}_\infty$ damping stabilizer is proposed in [123] using feedback linearization design approach. In [133] the authors have proposed an adaptive PI controller for power system voltage stability with self-adjusting controller gains. A state-feedback STATCOM controller for voltage regulation is proposed in [134] in the presence of load uncertainty and voltage flicker. In [135] the authors have proposed a STATCOM controller designed by pole placement to mitigate unbalanced faults. The linear quadratic regulator (LQR) based pole placement approach is employed in [136] for designing a STATCOM controller with optimization of LQR coefficients using genetic algorithm (GA). State feedback based controllers have also been employed in other works such as [137–139] and until

very recently in [140].

Fuzzy Logic Control in STATCOM Based Power Systems

Along with numerous other applications, fuzzy logic control has also been applied to STATCOM based power systems in order to improve stability and provide voltage support. An overview of some very recent works in this area is given here.

In [61] a STATCOM is used in multimachine power system stability using adaptive neuro-fuzzy based PI controllers. Action dependent heuristic dynamic programming approach is adopted and the proposed controller is compared with the conventional PI controller to demonstrate its performance. In [59] the same authors have proposed a STATCOM controller for multimachine power systems using type-II fuzzy systems to deal with uncertainties and noise, and improve voltage stability and dynamic performance in comparison to the traditional PI controller. In [55] the results of a fuzzy logic controller used as the main and supplementary controller for a STATCOM based AC power system are demonstrated in the context of transient stability. The authors of [58] have employed a fuzzy logic based controller for the STATCOM for reactive power compensation in distribution networks. In [60] the authors demonstrate the hardware implementation results of a model-free, Mamdani structure fuzzy logic controller for the STATCOM in a multimachine power system and compare its performance with the conventional PI controller. An ANFIS based STATCOM controller is proposed in [56] for the stability of a single-machine-infinite-bus (SMIB) system under fault conditions. The authors of [63] have demonstrated the use of a fuzzy logic STATCOM controller in reactive power control and power quality improvement. In [62] the fuzzy logic con-

trol has been employed for STATCOM to damp out SSR oscillations. In a very recent work [64], a PID damping controller and a hybrid PID plus fuzzy logic controller for STATCOM are employed in a multimachine power system connected with a doubly-fed induction generator (DFIG) based wind farm for improving power system stability and damping oscillations. A frequency-domain approach based on a linearized system model using root-loci technique is employed and nonlinear time domain simulations under three phase faults are carried out, comparing the performance of the proposed controller with the conventional PID controller to examine its effectiveness. A fuzzy logic controller for a five-level inverter based distribution STATCOM (D-STATCOM) for power quality improvement in distribution power system is proposed recently in [57].

1.4 Summary of Literature

The literature overview of different control techniques in the context of this research is summarized in the following table:

Model-based output feedback control	Observer-based control	LPV	[3–12, 17, 69–75, 85]
		Quadratic stability	[2, 13, 14, 67, 68, 76–80, 86]
	Static output feedback control		[28–40]
Model-free output feedback control	Fuzzy logic control		[48, 53, 55, 57–60, 63]
	Hybrid fuzzy control		[49, 51, 52, 54, 61, 64, 117]
	Other model-free control techniques		[50, 56, 97, 115, 122, 124, 133]

Table 1.1: Summary of literature

1.5 Motivation and Objectives

The motivation behind this research work stems from the gaps in the existing literature on robust model-based and model-free control. The objectives are to address some of these gaps and develop improved control techniques.

There is a growing tendency in contemporary literature to utilize convex optimization techniques involving LMI constraints [141] to formulate complex control problems. It is underscored by the numerical tractability of LMIs along with the availability of a variety of efficient computer tools for solving them.

The robust observer based solutions proposed in [2, 13] rely on equality constraints, introducing conservatism in the presence of significant uncertainties. Neither of [2, 13, 14] impose any performance or optimality constraints on the controller. The mixed $\mathcal{H}_2/\mathcal{H}_\infty$ controller proposed in [80] assumes perfect knowledge of system ma-

trices and does not consider uncertainties. The ideas recently proposed in [34] and [78] consider the $\mathcal{H}_\infty$ and mixed $\mathcal{H}_2/\mathcal{H}_\infty$ performance constraints respectively, in the presence of polytopic uncertainties, but the proposed conditions are nonconvex in some scaler parameters that are found separately and treated as constants in order to realize a convex optimization problem. This makes the solution multistep and convex, and may introduce conservatism in the solution. The works [82–84] assume that full state information is available for feedback, and can not be adopted in cases where full state information is unavailable. The works [137–140] have the same limitation. The iterative LMI technique reported in [85] is highly computationally intensive. The particle swarm optimization (PSO) based observer-controller solution reported in [21] relies on a properly chosen search space to attain convergence. Finding such a search space of across a wide range of systems may become a non-trivial and cumbersome task. In the robust $\mathcal{H}_\infty$ control solution reported by the authors of [86], the missing states for full state feedback control are estimated from an asymptotic observer formulated separately from the controller dynamics. Proof of stability of the collective observer-controller dynamics is not given thus, significantly narrowing down the scope of this solution.

In model-free intelligent control utilizing fuzzy logic, the majority of techniques proposed in literature use at least nine or more fuzzy rules [48–64]. The complex nonlinear function resulting from the fuzzy inference process can be computationally intensive when implemented on a low cost microcontroller (MCU) and can slow down the processing speed. Alternatively, the fuzzy logic controller can be implemented on MCU as a lookup table to speed up calculations. However, it must be ensured that

the lookup table represents the fuzzy logic function with adequate accuracy. Implementation of a fuzzy inference system with a large number of rules and membership functions requires a large sized lookup table with many entries to be programmed on limited MCU memory. The hybrid fuzzy/PI/PID techniques reported in [49,52,117] use a large rule-set and are hence computationally intensive and memory-inefficient. The scheme in [52] requires experimental trial and error for tuning the fuzzy controller's parameters which can be a cumbersome task. These shortcomings are summarized in the following table:

Control Type	Shortcoming
Model-based output feedback control	- Full state availability assumption [82–84, 137–140] - Uncertainties or performance constraints not considered [2, 13, 14, 80] - Equality constraints, added conservatism [2, 13] - Non-convex parameter dependence, multistep and complex solution [34, 78] - Closed-loop stability of observer-controller not proven [86]
Model-free fuzzy logic control	- Techniques reported use large number of rules, computationally complex and memory intensive [48–64] - Tuning by experimental trial and error, cumbersome process [52] - Insufficient operating range coverage, finite steady state error [53]

Table 1.2: Literature shortcomings

These aforementioned factors have motivated the research presented in this thesis. From an overview of the identified gaps in the technical literature, it is clear that the issue of observer based control of uncertain linear systems subject to external perturbations and parametric uncertainties under performance constraints has not been fully addressed. Moreover, there is also room for the development of a computationally sim-

pler fuzzy logic based controller whose implementation on limited MCU memory is easier than the ones presently reported. Keeping this in mind, the broader objectives of this thesis can be stated as follows:

- To develop a generalized single-step convex optimization solution to the robust observer based controller design problem for uncertain systems with polytopic uncertainties and external disturbances under single and multiobjective performance constraints
- To develop a generalized model-free robust fuzzy logic based controller for systems with uncertainties and unknown disturbances that is computationally more efficient than the existing approaches and does not compromise performance
- To develop these techniques in a generalized framework, making them applicable to multiple practical systems

1.6 Thesis Contribution

In this research, novel ideas are developed in the fields of robust observer based control and fuzzy logic control. The contributions of this thesis are summarized as follows:

- The original ideas presented in [14] for uncertain linear systems with structured uncertainties are extended to uncertain systems with polytopic uncertainties. A novel, minimally restrictive, single-step LMI-based solution with the $\mathcal{L}_2$-gain performance constraint is developed for the observer-controller gain synthesis using the notion of quadratic stability.

- A new single-step LMI-based observer-controller solution with the mixed $\mathcal{H}_2/\mathcal{H}_\infty$ performance constraint is developed for the same class of uncertain systems with polytopic uncertainties and unknown disturbances under the quadratic stability framework.

- A novel, simplified fuzzy logic/PI based hybrid control technique is proposed with improved performance in comparison to the conventional PI control and fuzzy logic control. Fuzzy logic and hybrid fuzzy/PI techniques proposed in the existing literature use a minimum of 9 fuzzy rules. In comparison, the proposed technique uses only 3 fuzzy rules, resulting in a lower computational load on the central processing unit (CPU) in MCU implementation.

- It is demonstrated that when fuzzy logic is implemented as a lookup table stored in the MCU memory, the proposed controller, owing to its low rule-count, can be implemented using a much smaller sized lookup table as compared to those with higher number of rules. Thus, it has much lower requirements on limited MCU memory.

- The generality of the proposed control techniques is demonstrated through application to two distinct practical systems using MATLAB®/Simulink digital simulations i.e., speed control of BLDC motor drive and power system stability using STATCOM.

- The functionality of the proposed control techniques is demonstrated by implementing them on a digital signal processor (DSP) chip under processor-in-the-

loop (PIL) configuration.

- Hardware implementation results of the hybrid fuzzy/PI controller are demonstrated for the speed control of BLDC motor drive on low cost MCU. A number of the schemes proposed in literature for speed control of BLDC motor drive involve sensing one or more current signals for controlling the speed (see for example [50, 51, 96, 107, 109, 110, 114]), requiring additional sensors and clean current measurements to achieve satisfactory performance. In case of a noisy signal due to sensor or process noise, additional filtering circuitry may be required to clean up the feedback signals. The proposed technique does not require current sensing thus, avoiding the need for additional sensors and filtering circuitry in practical implementation and reducing cost and complexity.

1.7 Thesis Organization

The thesis is organized into six chapters. Chapter 2 gives the formulation and derivation of convex optimization solution to the robust observer based controller design problem for an uncertain linear system with $\mathcal{L}_2$-gain performance. Chapter 3 treats the same class of systems with mixed $\mathcal{H}_2/\mathcal{H}_\infty$ performance. In Chapter 4, the design procedure and results of the hybrid fuzzy/PI controller are discussed. Experimental implementation of the hybrid fuzzy/PI controller for speed control of a BLDC motor drive is presented in Chapter 5. Chapter 6 gives the discussion and comparative analysis, conclusion and future work.

CHAPTER 2

ROBUST OBSERVER-BASED CONTROL OF UNCERTAIN LINEAR SYSTEMS WITH $\mathcal{L}_2$-GAIN PERFORMANCE

In this chapter, the observer-controller design for a class of uncertain linear systems with polytopic uncertainties subject to exogenous disturbance is treated. Sufficient LMI conditions are developed for the synthesis of controller and observer gains that can be solved in a single step without using any multistep or iterative techniques. Our objective is to robustly stabilize the uncertain system using output feedback with a certain guaranteed $\mathcal{L}_2$ gain performance from observation error to the unknown disturbance. The uncertain parameters are assumed to be unknown but lie between an upper and lower value. No other restrictions are placed on the uncertain parameters. A full-order

Luenberger type observer [142] guaranteeing the desired $\mathcal{L}_2$-gain performance is synthesized using LMIs. The effectiveness of the developed results is demonstrated by robust speed control of a BLDC motor drive under parametric uncertainties and exogenous load torque disturbance, and robust stabilization of a STATCOM based power system under uncertain parameters and disturbance conditions.

Notation: Throughout this chapter and the rest of this thesis, the matrix notations $M > 0$ and $M < 0$ impliy that a matrix M is positive definitive and negative definite, respectively. The transpose of a matrix M is denoted by M^T. Notations I and $\mathbf{0}$ represent the identity and null matrices of appropriate dimensions, respectively. $\mathbb{R}$ stands for the set of real numbers, and $*$ denotes the transpose entries in a matrix.

2.1 Definitions

The following definitions will be used in this chapter and the subsequent chapters [143, 144]:

Definition 2.1. *A set C is defined as a convex set if a line segment between any two points in C also lies in C. In other words, for any two points $x_1, x_2 \in C$ and any θ with $0 \leq \theta \leq 1$, we have*

$$\theta x_1 + (1 - \theta)x_2 \in C. \tag{2.1}$$

Definition 2.2. *An optimization problem of the form*

$$\begin{aligned} &\text{minimize } f_0(x) \\ &\text{subject to } f_i(x) \leq b_i, \qquad i = 1, \ldots, m, \end{aligned} \tag{2.2}$$

where the functions $f_0, f_1, \ldots, f_m : \mathbb{R}^n \to \mathbb{R}$ *are convex, is a convex optimization problem.*

Definition 2.3. *A set of square-integrable signals is defined as the* $\mathcal{L}_2$*-space i.e.,*

$$\mathcal{L}_2 := \left\{ u(t) \in \mathbb{R} : \int_0^\infty u(t)^2 dt < \infty \right\}. \tag{2.3}$$

Definition 2.4. *The* $\mathcal{L}_2$*-norm of a signal* $u(t) \in \mathcal{L}_2$ *is defined as*

$$\|u(t)\|_{\mathcal{L}_2} = \left(\int_0^\infty u(t)^2 dt \right)^{\frac{1}{2}}. \tag{2.4}$$

Definition 2.5. *For a multidimensional signal* $u(t) = \{u_t(t),\ u_2(t),\ \ldots,\ u_{n_u}(t)\}^T$ *with* $u_i(t) \in \mathcal{L}_2$ *for* $i = 1,\ 2,\ \ldots,\ n_u$*, the* $\mathcal{L}_2$*-norm is defined as*

$$\|u(t)\|_{\mathcal{L}_2} = \left(\int_0^\infty u(t)^T u(t) dt \right)^{\frac{1}{2}} = \left(\int_0^\infty \sum_{i=1}^{n_u} u_i(t)^2 dt \right)^{\frac{1}{2}}. \tag{2.5}$$

2.2 Problem Statement and Main Results

Consider the following uncertain linear system:

$$\begin{aligned} \dot{x}(t) &= A(\rho)x(t) + Bu(t) + D\xi(t) \\ y(t) &= Cx(t) \end{aligned} \tag{2.6}$$

where $x(t) \in \mathbb{R}^n$ is the state vector, $u(t) \in \mathbb{R}^m$ is the control input vector, $\xi(t) \in \mathbb{R}^d$ is the unknown disturbance input vector and $y(t) \in \mathbb{R}^p$ is the system output vector. The

matrices $B \in \mathbb{R}^{n\times m}$, $D \in \mathbb{R}^{n\times d}$ and $C \in \mathbb{R}^{p\times n}$ are the input, disturbance and output matrices, respectively. The matrix $A(\rho) \in \mathbb{R}^{n\times n}$ is given by:

$$A(\rho) = \sum_{i=1}^{\mu} \zeta_i A_i, \tag{2.7}$$

where $\zeta = [\zeta_1\ \zeta_2\ \cdots\ \zeta_\mu]^T \in \mathbb{R}^\mu$ is the uncertain constant parameter vector satisfying

$$\zeta \in \Omega := \left\{ \zeta \in \mathbb{R}^\mu : \zeta_i \geq 0\ (i = 1, \cdots, \mu),\ \sum_{i=1}^{\mu} \zeta_i = 1 \right\}. \tag{2.8}$$

It is assumed that the pairs (A_i, B) and (A_i, C) are controllable and observable, respectively for all $i = 1, 2, \cdots, \mu$. Let $\hat{x}(t)$ represent the observer state vector with dynamical equation:

$$\dot{\hat{x}}(t) = A_o\hat{x}(t) + Bu + P_2Y_2(C\hat{x}(t) - y(t)) \tag{2.9}$$

where $A_o \in \mathbb{R}^{n\times n}$ is the observer matrix to be found. Our aim is to find a stabilizing controller $u(t) = Y_1P_1\hat{x}(t)$ such that the system (2.6) is globally asymptotically stable when $\xi(t) = 0$. Additionally, when $\xi(t) \neq 0$, our objective is to minimize the following $\mathcal{L}_2$-gain:

$$\frac{\|C\hat{x}(t) - y(t)\|_{\mathcal{L}_2}}{\|\xi(t)\|_{\mathcal{L}_2}} < \gamma \tag{2.10}$$

where γ is a certain positive performance scaler. The matrices $P_1 \in \mathbb{R}^{n\times n}$, $P_2 \in \mathbb{R}^{n\times n}$ are symmetric and positive definite matrices; $Y_1 \in \mathbb{R}^{m\times n}$ and $Y_2 \in \mathbb{R}^{n\times p}$ are arbitrary real matrices to be determined. The design of the controller and observer gains is

summarized in the following theorem:

Theorem 2.1. *Consider system (2.6) and observer (2.9). Then, if there exist two symmetric and positive definite matrices* $X_1 \in \mathbb{R}^{n\times n}$, $X_2 \in \mathbb{R}^{n\times n}$, *three real matrices* $Y_1 \in \mathbb{R}^{m\times n}$, $Y_2 \in \mathbb{R}^{n\times p}$, $Z \in \mathbb{R}^{n\times n}$ *and six strictly positive constants* α, β, δ, λ_1, λ_2 *and* λ_3 *such that the following convex optimization problem is solvable for* $0 < \lambda_1 < 1$*:*

$$\text{minimize } \eta \text{ s.t.}$$

$$\begin{bmatrix} -X_1 & I \\ I & -(2\beta-\alpha)I \end{bmatrix} < 0, \tag{2.11}$$

$$\begin{bmatrix} \Phi_{1i} & X_1 & D & -BY_1 \\ * & -(2-\lambda_1)I & \mathbf{0} & \mathbf{0} \\ * & * & -\delta I & \mathbf{0} \\ * & * & * & -\alpha I \end{bmatrix} < 0, \ \forall\, i=1,2,\cdots,\mu. \tag{2.12}$$

$$\Phi_{1i}=X_1A_i^T+A_iX_1+Y_1^TB^T+BY_1,$$

$$\begin{bmatrix} \Phi_2 & \beta I & X_2D \\ * & -X_1 & \mathbf{0} \\ * & * & -(\eta-\lambda_3-\delta)I \end{bmatrix} < 0, \tag{2.13}$$

$$\Phi_2 = Y_2C+C^TY_2^T+C^TC+Z^T+Z+\lambda_2 I,$$

$$\begin{bmatrix} -\lambda_1 I & A_i^T X_2 - Z^T & \mathbf{0} \\ * & -\lambda_2 I & \mathbf{0} \\ * & * & -\lambda_3 I \end{bmatrix} < 0, \ \forall\, i = 1, 2, \cdots, \mu. \tag{2.14}$$

with $X_1 = P_1^{-1}$, $X_2 = P_2^{-1}$, $\eta = \gamma^2$ *then, the observer based controller with* $u(t) = Y_1 P_1 \hat{x}(t)$ *and* $A_o = X_2^{-1} Z = P_2 Z$, *is an asymptotically stabilizing controller for system (2.6) when* $\xi(t) = 0$ *and verifies the objective (2.10) when* $\xi(t) \neq 0$.

Proof. Let $e(t) = x(t) - \hat{x}(t)$ be the observer error. Then we can write the original system (2.6), with $u(t) = Y_1 P_1 \hat{x}(t)$ in terms of observer error as:

$$\dot{x}(t) = (A(\rho) + BY_1 P_1) x(t) - BY_1 P_1 e(t) + D\xi(t) \tag{2.15}$$

The observer dynamics (2.9) can be written in terms of $x(t)$ and $e(t)$ as:

$$\dot{\hat{x}}(t) = (A_o + BY_1 P_1) x(t) - (A_o + BY_1 P_1 + P_2 Y_2 C) e(t) \tag{2.16}$$

Since $\dot{e}(t) = \dot{x}(t) - \dot{\hat{x}}(t)$, the observer error dynamic is written as:

$$\dot{e}(t) = (A(\rho) - A_o) x(t) + (A_o + P_2 Y_2 C) e(t) + D\xi(t) \tag{2.17}$$

Combining (2.15) and (2.17), we can write the dynamics of the states and the observer

error in matrix form as:

$$\begin{bmatrix} \dot{x}(t) \\ \dot{e}(t) \end{bmatrix} = \begin{bmatrix} A(\rho)+BY_1P_1 & -BY_1P_1 \\ A(\rho)-A_o & A_o+P_2Y_2C \end{bmatrix} \begin{bmatrix} x(t) \\ e(t) \end{bmatrix} + \begin{bmatrix} D \\ D \end{bmatrix} \xi(t) \tag{2.18}$$

Define the Lyapunov candidate function:

$$V(x(t), e(t)) = \begin{bmatrix} x(t) \\ e(t) \end{bmatrix}^T \begin{bmatrix} P_1 & \mathbf{0} \\ \mathbf{0} & P_2^{-1} \end{bmatrix} \begin{bmatrix} x(t) \\ e(t) \end{bmatrix}. \tag{2.19}$$

Then, by differentiating (2.19) we get

$$\dot{V}(x(t), e(t)) = \begin{bmatrix} x(t) \\ e(t) \\ \xi(t) \end{bmatrix}^T \begin{bmatrix} \mathcal{M}_{11} & \mathcal{M}_{12} & P_1D \\ \mathcal{M}_{12}^T & \mathcal{M}_{22} & P_2^{-1}D \\ D^TP_1 & D^TP_2^{-1} & \mathbf{0} \end{bmatrix} \begin{bmatrix} x(t) \\ e(t) \\ \xi(t) \end{bmatrix}, \tag{2.20}$$

where

$$\begin{aligned} \mathcal{M}_{11} &= A(\rho)^TP_1 + P_1A(\rho) + P_1(Y_1^TB^T + BY_1)P_1 \\ \mathcal{M}_{12} &= -P_1BY_1P_1 + (A(\rho)-A_o)^TP_2^{-1} \\ \mathcal{M}_{22} &= A_o^TP_2^{-1} + P_2^{-1}A_o + C^TY_2^T + Y_2C \end{aligned} \tag{2.21}$$

Since $e(t) = x(t) - \hat{x}(t)$, using the definition of $\mathcal{L}_2$ norm, squaring both sides and after some mathematical manipulation we can write (2.10) as

$$\int_0^\infty (e(t)^TC^TCe(t) - \gamma^2\xi(t)^T\xi(t))dt < 0. \tag{2.22}$$

Imposing the condition on (2.22) as

$$\int_0^\infty (e(t)^T C^T C e(t) - \gamma^2 \xi(t)^T \xi(t)) dt < -V(x(t), e(t)). \tag{2.23}$$

Letting $V(0,0) = 0$, we can write

$$\begin{aligned} \int_0^\infty (e(t)^T C^T C e(t) - \gamma^2 \xi(t)^T \xi(t)) dt \\ + \int_0^\infty \dot{V}(x(t), e(t)) dt < 0. \end{aligned} \tag{2.24}$$

Inequality (2.24) is satisfied if the following is satisfied:

$$(e(t)^T C^T C e(t) - \gamma^2 \xi(t)^T \xi(t) + \dot{V}(x(t), e(t)) < 0. \tag{2.25}$$

Substituting (2.20) in (2.25), we get the matrix inequality

$$\begin{bmatrix} x(t) \\ e(t) \\ \xi(t) \end{bmatrix}^T \begin{bmatrix} \mathcal{M}_{11} & \mathcal{M}_{12} & P_1 D \\ \mathcal{M}_{12}^T & \mathcal{M}_{22} + C^T C & P_2^{-1} D \\ D^T P_1 & D^T P_2^{-1} & -\gamma^2 I \end{bmatrix} \begin{bmatrix} x(t) \\ e(t) \\ \xi(t) \end{bmatrix} < 0, \tag{2.26}$$

where $\mathcal{M}_{ii}$ are defined in (2.21). A sufficient condition for the matrix inequality (2.26) to hold is

$$\begin{bmatrix} \mathcal{M}_{11} & \mathcal{M}_{12} & P_1 D \\ \mathcal{M}_{12}^T & \mathcal{M}_{22} + C^T C & P_2^{-1} D \\ D^T P_1 & D^T P_2^{-1} & -\gamma^2 I \end{bmatrix} < 0. \tag{2.27}$$

Inequality (2.27) can be written as a sum of matrix inequalities as follows:

$$\begin{bmatrix} \mathcal{M}_{11}+\lambda_1 I & -P_1 B Y_1 P_1 & P_1 D \\ -P_1 Y_1^T B^T P_1 & \mathcal{M}_{22}+C^T C+\lambda_2 I & P_2^{-1} D \\ D^T P_1 & D^T P_2^{-1} & -(\gamma^2-\lambda_3) I \end{bmatrix} + \begin{bmatrix} -\lambda_1 I & (A(\rho)-A_o)^T P_2^{-1} & \mathbf{0} \\ P_2^{-1}(A(\rho)-A_o) & -\lambda_2 I & \mathbf{0} \\ \mathbf{0} & \mathbf{0} & -\lambda_3 I \end{bmatrix} < 0 \tag{2.28}$$

for some positive scalers λ_1, λ_2 and λ_3. Then, sufficient conditions for satisfying (2.28) are met if the following two matrix inequalities hold:

$$\begin{bmatrix} \mathcal{M}_{11}+\lambda_1 I & -P_1 B Y_1 P_1 & P_1 D \\ -P_1 Y_1^T B^T P_1 & \mathcal{M}_{22}+C^T C+\lambda_2 I & P_2^{-1} D \\ D^T P_1 & D^T P_2^{-1} & -(\gamma^2-\lambda_3) I \end{bmatrix} < 0 \tag{2.29}$$

and

$$\begin{bmatrix} -\lambda_1 I & (A(\rho)-A_o)^T P_2^{-1} & \mathbf{0} \\ P_2^{-1}(A(\rho)-A_o) & -\lambda_2 I & \mathbf{0} \\ \mathbf{0} & \mathbf{0} & -\lambda_3 I \end{bmatrix} < 0. \tag{2.30}$$

Now, multiplying (2.29) on both sides by the matrix $\begin{bmatrix} P_1^{-1} & \mathbf{0} & \mathbf{0} \\ \mathbf{0} & I & \mathbf{0} \\ \mathbf{0} & \mathbf{0} & I \end{bmatrix}$ we get

$$\begin{bmatrix} \mathcal{G}_{11} & -BY_1P_1 & D \\ -P_1Y_1^TB^T & \mathcal{G}_{22} & P_2^{-1}D \\ D^T & D^TP_2^{-1} & -(\gamma^2-\lambda_3)I \end{bmatrix} < 0 \tag{2.31}$$

where

$$\begin{aligned} \mathcal{G}_{11} &= P_1^{-1}\mathcal{M}_{11}P_1^{-1} + \lambda_1 P_1^{-1}P_1^{-1} \\ \mathcal{G}_{22} &= \mathcal{M}_{22} + C^TC + \lambda_2 I \end{aligned} \tag{2.32}$$

Inequality (2.31) can be rewritten as (2.33), for some positive scalers δ and α.

$$
\begin{bmatrix}
I & \mathbf{0} & \mathbf{0} & -\frac{D}{\sqrt{\delta}} & \mathbf{0} \\
\mathbf{0} & P_1 & I & \mathbf{0} & \mathbf{0} \\
\mathbf{0} & \mathbf{0} & \mathbf{0} & \sqrt{\delta} I & I
\end{bmatrix} \cdot
$$

$$
\begin{bmatrix}
\mathcal{G}_{11}+\delta^{-1}DD^T & -BY_1 & \mathbf{0} & \mathbf{0} & \mathbf{0} \\
-Y_1^T B^T & -\alpha I & \mathbf{0} & \mathbf{0} & \mathbf{0} \\
\mathbf{0} & \mathbf{0} & \mathcal{G}_{22}+\alpha P_1 P_1 & \mathbf{0} & P_2^{-1}D \\
\mathbf{0} & \mathbf{0} & \mathbf{0} & -I & \mathbf{0} \\
\mathbf{0} & \mathbf{0} & D^T P_2^{-1} & \mathbf{0} & -(\gamma^2-\lambda_3-\delta)I
\end{bmatrix} \cdot \tag{2.33}
$$

$$
\begin{bmatrix}
I & \mathbf{0} & \mathbf{0} \\
\mathbf{0} & P_1 & \mathbf{0} \\
\mathbf{0} & I & \mathbf{0} \\
-\frac{D^T}{\sqrt{\delta}} & \mathbf{0} & \sqrt{\delta} I \\
\mathbf{0} & \mathbf{0} & I
\end{bmatrix} < 0.
$$

Therefore a sufficient condition for (2.33) to hold is

$$
\begin{bmatrix}
\mathcal{G}_\delta & -BY_1 & \mathbf{0} & \mathbf{0} & \mathbf{0} \\
-Y_1^T B^T & -\alpha I & \mathbf{0} & \mathbf{0} & \mathbf{0} \\
\mathbf{0} & \mathbf{0} & \mathcal{G}_\alpha & \mathbf{0} & P_2^{-1}D \\
\mathbf{0} & \mathbf{0} & \mathbf{0} & -I & \mathbf{0} \\
\mathbf{0} & \mathbf{0} & D^T P_2^{-1} & \mathbf{0} & -(\gamma^2-\lambda_3-\delta)I
\end{bmatrix} < 0 \tag{2.34}
$$

where

$$\begin{aligned} \mathcal{G}_\delta &= \mathcal{G}_{11} + \delta^{-1} D D^T \\ \mathcal{G}_\alpha &= \mathcal{G}_{22} + \alpha P_1 P_1 \end{aligned} \tag{2.35}$$

Due to its decoupled structure (2.34) can be written as the following individual matrix inequalities:

$$\begin{bmatrix} \mathcal{G}_{11} + \delta^{-1} D D^T & -B Y_1 \\ -Y_1^T B^T & -\alpha I \end{bmatrix} < 0, \tag{2.36}$$

$$\begin{bmatrix} \mathcal{G}_{22} + \alpha P_1 P_1 & \mathbf{0} & P_2^{-1} D \\ \mathbf{0} & -I & \mathbf{0} \\ D^T P_2^{-1} & \mathbf{0} & -(\gamma^2 - \lambda_3 - \delta) I \end{bmatrix} < 0. \tag{2.37}$$

Expanding (2.36) by Schur's complement, we get

$$\mathcal{G}_{11} + \delta^{-1} D D^T + \alpha^{-1} B Y_1 Y_1^T B^T < 0. \tag{2.38}$$

Let $X_1 = P_1^{-1}$. Then by substituting the value of $\mathcal{G}_{11}$ from (2.32) and the value of $\mathcal{M}_{11}$ from (2.21) into (2.38), after simplification the matrix inequality (2.38) becomes

$$\begin{aligned} X_1 A(\rho)^T + A(\rho) X_1 + Y_1^T B^T + B Y_1 \\ + \lambda_1 X_1 X_1 + \delta^{-1} D D^T + \alpha^{-1} B Y_1 Y_1^T B^T < 0. \end{aligned} \tag{2.39}$$

Since $A(\rho) = \sum_{i=1}^{\mu} \zeta_i A_i$, (2.39) can be written as

$$\begin{aligned} X_1 \sum_{i=1}^{\mu} \zeta_i A_i^T + \sum_{i=1}^{\mu} \zeta_i A_i X_1 + Y_1^T B^T + B Y_1 \\ + \lambda_1 X_1 X_1 + \delta^{-1} D D^T + \alpha^{-1} B Y_1 Y_1^T B^T < 0. \end{aligned} \tag{2.40}$$

Since and $\sum_{i=1}^{\mu} \zeta_i = 1$, we can write (2.40) as,

$$\begin{aligned} X_1 \sum_{i=1}^{\mu} \zeta_i A_i^T + \sum_{i=1}^{\mu} \zeta_i A_i X_1 + \sum_{i=1}^{\mu} \zeta_i (Y_1^T B^T + B Y_1 \\ + \lambda_1 X_1 X_1 + \delta^{-1} D D^T + \alpha^{-1} B Y_1 Y_1^T B^T) < 0 \end{aligned} \tag{2.41}$$

which is equivalent to

$$\begin{aligned} \sum_{i=1}^{\mu} \zeta_i (X_1 A_i^T + A_i X_1 + Y_1^T B^T + B Y_1 \\ + \lambda_1 X_1 X_1 + \delta^{-1} D D^T + \alpha^{-1} B Y_1 Y_1^T B^T) < 0. \end{aligned} \tag{2.42}$$

Therefore, a sufficient condition for (2.42) to hold is

$$\begin{aligned} X_1 A_i^T + A_i X_1 + Y_1^T B^T + B Y_1 \\ + \lambda_1 X_1 X_1 + \delta^{-1} D D^T + \alpha^{-1} B Y_1 Y_1^T B^T < 0 \end{aligned} \tag{2.43}$$

for all $i = 1, 2, \cdots, \mu$. The inequality (2.43) is equivalent by the Schur's complement

to

$$\begin{bmatrix} \Phi_{1i} & X_1 & D & -BY_1 \\ * & -\lambda_1^{-1}I & \mathbf{0} & \mathbf{0} \\ * & * & -\delta I & \mathbf{0} \\ * & * & * & -\alpha I \end{bmatrix} < 0, \ \forall\, i = 1, 2, \cdots, \mu. \tag{2.44}$$

with $\Phi_{1i} = X_1 A_i^T + A_i X_1 + Y_1^T B^T + BY_1$, and the entries $*$ induced by transposition. If λ_1 is chosen such that $0 < \lambda_1 < 1$, then we always have $-\lambda_1^{-1}I \leq -(2-\lambda_1)I$. Therefore, (2.29) is satisfied if the following linear matrix inequality holds:

$$\begin{bmatrix} \Phi_{1i} & X_1 & D & -BY_1 \\ * & -(2-\lambda_1)I & \mathbf{0} & \mathbf{0} \\ * & * & -\delta I & \mathbf{0} \\ * & * & * & -\alpha I \end{bmatrix} < 0, \ \forall\, i = 1, 2, \cdots, \mu. \tag{2.45}$$

which proves (2.12) in Theorem 2.1. Now, (2.37) can be written by Schur's complement as

$$\begin{bmatrix} \mathcal{G}_{22} + \alpha P_1 P_1 & \mathbf{0} \\ \mathbf{0} & -I \end{bmatrix} + \begin{bmatrix} X_2 D \\ \mathbf{0} \end{bmatrix} \begin{bmatrix} \chi^{-1} I \end{bmatrix} \begin{bmatrix} D^T X_2 & \mathbf{0} \end{bmatrix} < 0 \tag{2.46}$$

where $X_2 = P_2^{-1}$, $\eta = \gamma^2$ and $\chi = \eta - \lambda_3 - \delta$. Simplifying (2.46), we get

$$\begin{bmatrix} \mathcal{G}_{22} + \alpha P_1 P_1 + \chi^{-1} X_2 D D^T X_2 & \mathbf{0} \\ \mathbf{0} & -I \end{bmatrix} < 0. \tag{2.47}$$

It is clear that a sufficient condition for (2.47) to hold is

$$\mathcal{G}_{22} + \alpha P_1 P_1 + \chi^{-1} X_2 D D^T X_2 < 0. \tag{2.48}$$

Substituting the value of $\mathcal{G}_{22}$ from (2.32) and the value of $\mathcal{M}_{22}$ from (2.21), (2.48) becomes

$$\begin{aligned} A_o^T X_2 + X_2 A_o + C^T Y_2^T + Y_2 C + \\ C^T C + \alpha P_1 P_1 + \chi^{-1} X_2 D D^T X_2 + \lambda_2 I < 0. \end{aligned} \tag{2.49}$$

Using lemma 4 in [14], if the following LMI holds

$$\begin{bmatrix} -P_1^{-1} & I \\ I & -(2\beta - \alpha) I \end{bmatrix} < 0 \tag{2.50}$$

for some positive scaler β, then $\alpha P_1 P_1 < \beta^2 P_1$. Therefore (2.49) holds if the following holds

$$\begin{aligned} A_o^T X_2 + X_2 A_o + C^T Y_2^T + Y_2 C + \\ C^T C + \beta^2 P_1 + \chi^{-1} X_2 D D^T X_2 + \lambda_2 I < 0. \end{aligned} \tag{2.51}$$

By letting $Z = X_2 A_o$ and using the Schur's complement lemma (2.51) can be written as the following matrix inequality

$$\begin{bmatrix} \Phi_2 & \beta I & X_2 D \\ \beta I & -P_1^{-1} & \mathbf{0} \\ D^T X_2 & \mathbf{0} & -(\eta - \lambda_3 - \delta) I \end{bmatrix} < 0 \tag{2.52}$$

where $\Phi_2 = Z^T + Z + C^T Y_2^T + Y_2 C + C^T C + \lambda_2 I$. Using $X_1 = P_1^{-1}$, (2.52) can be

written as the LMI

$$\begin{bmatrix} \Phi_2 & \beta I & X_2 D \\ * & -X_1 & \mathbf{0} \\ * & * & -(\eta - \lambda_3 - \delta) I \end{bmatrix} < 0, \tag{2.53}$$

which proves (2.13) in Theorem 2.1. Now from (2.30), since $A(\rho) = \sum_{i=1}^{\mu} \zeta_i A_i$, we can write

$$\begin{bmatrix} -\lambda_1 I & (\sum_{i=1}^{\mu} \zeta_i A_i - A_o)^T X_2 & \mathbf{0} \\ X_2(\sum_{i=1}^{\mu} \zeta_i A_i - A_o) & -\lambda_2 I & \mathbf{0} \\ \mathbf{0} & \mathbf{0} & -\lambda_3 I \end{bmatrix} < 0. \tag{2.54}$$

Since $\sum_{i=1}^{\mu} \zeta_i = 1$, we can write (2.54) as

$$\sum_{i=1}^{\mu} \zeta_i \begin{bmatrix} -\lambda_1 I & (A_i - A_o)^T X_2 & \mathbf{0} \\ X_2(A_i - A_o) & -\lambda_2 I & \mathbf{0} \\ \mathbf{0} & \mathbf{0} & -\lambda_3 I \end{bmatrix} < 0. \tag{2.55}$$

With $Z = X_2 A_o$ defined already, a sufficient condition for (2.55) to hold is then

$$\begin{bmatrix} -\lambda_1 I & A_i^T X_2 - Z^T & \mathbf{0} \\ X_2 A_i - Z & -\lambda_2 I & \mathbf{0} \\ \mathbf{0} & \mathbf{0} & -\lambda_3 I \end{bmatrix} < 0, \ \forall i = 1, 2, \cdots, \mu. \tag{2.56}$$

which proves (2.14) in Theorem 2.1. This completes the proof. ∎

Remark 2.1. *The decoupling steps to obtain sufficient conditions (2.36) and (2.37) from (2.31) introduce some conservatism. However, the introduction of positive con-*

stants α and β, and the fact that no restrictive assumptions are placed on them, relieves the degree of conservatism of the LMIs. The constants also facilitate in making the sufficient conditions (2.36) and (2.37) linear with respect to the LMI variables.

2.3 Application of Results

In this section, the performance of the developed observer based controller are demonstrated through numerical examples. Two examples from practical systems are selected; (1) speed control of the BLDC motor drive and, (2) damping power system oscillations using STATCOM. The results are compared with the $\mathcal{H}_\infty$ performance SOF based controller reported in [145].

2.3.1 Speed Control of the BLDC Motor Drive

The equivalent dynamic model of a BLDC motor is given as follows [51, 96, 102, 112]:

$$\begin{aligned} \frac{d\omega}{dt} &= -\frac{b}{J_m}\omega + \frac{K_m}{J_m}I - \frac{1}{J_m}\tau \\ \frac{dI}{dt} &= -\frac{K_m}{L_a}\omega - \frac{R_a}{L_a}I + \frac{1}{L_a}V_{dc} \end{aligned} \tag{2.57}$$

where b, J_m, K_m, R_a and L_a are respectively the friction coefficient $(N.m.s)$, rotor inertia $(kg.m^2)$, motor constant $(V.s.rad^{-1})$, armature resistance (Ω) and armature inductance (H). The state variables are the speed ω (rad/s) and the current I (A). V_{dc} is the control input in (V) and τ is the load torque disturbance in $(N.m)$. Equation (2.57)

can be rewritten as

$$\dot{x}(t)=\begin{bmatrix}\dot{\omega}(t)\\ \dot{I}(t)\end{bmatrix}=\begin{bmatrix}-\frac{b}{J_m} & \frac{K_m}{J_m}\\ -\frac{K_m}{L_a} & -\frac{R_a}{L_a}\end{bmatrix}\begin{bmatrix}\omega(t)\\ I(t)\end{bmatrix}+\begin{bmatrix}0\\ \frac{1}{L_a}\end{bmatrix}u(t)+\begin{bmatrix}0\\ -\frac{1}{J_m}\end{bmatrix}\tau(t), \tag{2.58}$$
$$y(t)=\begin{bmatrix}1 & 0\end{bmatrix}x(t).$$

with $u(t) = V_{dc}$. Let us denote

$$\frac{b}{J_m}=\rho_1,\ \frac{K_m}{J_m}=\rho_2,\ \frac{K_m}{L_a}=\rho_3,\ \frac{R_a}{L_a}=\rho_4,\ \frac{1}{L_a}=\rho_5. \tag{2.59}$$

Assuming that parameters R_a, L_a, b and K_m are not precisely known but lie between an upper and lower value, we have

$$\rho_i^{min}\leq\rho_i\leq\rho_i^{max},\ i=1,\ldots,5. \tag{2.60}$$

Define $\tilde{\omega}(t) = \omega(t) - \omega_r(t)$ as the desired speed in rad/s, and a new state as $z(t) = \dot{x}(t) = \begin{bmatrix}\dot{\omega}(t) & \dot{I}(t)\end{bmatrix}^T$. Letting $\omega_r(t) = \omega_r$ constant, we have $\dot{\tilde{\omega}}(t) = \dot{\omega}(t) = \begin{bmatrix}1 & 0\end{bmatrix}\cdot\begin{bmatrix}\dot{\omega}(t) & \dot{I}(t)\end{bmatrix}^T$. We can write

$$\begin{aligned}\dot{\tilde{\omega}}(t) &= Cz(t),\\ \dot{z}(t) &= A(\rho)z(t)+B(\rho)v(t)+D\dot{\tau}(t),\end{aligned} \tag{2.61}$$

where $v(t)$ is a new control input defined as $v(t) = \dot{u}(t)$. The matrices $A(\rho)$, $B(\rho)$, D and C are:

$$A(\rho) = \begin{bmatrix} -\rho_1 & \rho_2 \\ -\rho_3 & -\rho_4 \end{bmatrix}, B(\rho) = \begin{bmatrix} 0 \\ \rho_5 \end{bmatrix}, D = \begin{bmatrix} 0 \\ -\frac{1}{J_m} \end{bmatrix}, \tag{2.62}$$
$$C = \begin{bmatrix} 1 & 0 \end{bmatrix}.$$

Defining another control input $w(t)$ such that $\dot{v}(t) = w(t) - v(t)$, and a new output $y_a(t) = \tilde{\omega}(t)$, we can write the following matrix equations:

$$\begin{aligned} \dot{x}_a(t) = \begin{bmatrix} \dot{\tilde{\omega}}(t) \\ \dot{z}(t) \\ \dot{v}(t) \end{bmatrix} &= \underbrace{\begin{bmatrix} \mathbf{0} & C & \mathbf{0} \\ \mathbf{0} & A(\rho) & B(\rho) \\ \mathbf{0} & \mathbf{0} & -I \end{bmatrix}}_{A_a(\rho)} \begin{bmatrix} \tilde{\omega}(t) \\ z(t) \\ v(t) \end{bmatrix} + \underbrace{\begin{bmatrix} \mathbf{0} \\ \mathbf{0} \\ I \end{bmatrix}}_{B_a} w(t) + \underbrace{\begin{bmatrix} \mathbf{0} \\ D \\ \mathbf{0} \end{bmatrix}}_{D_a} \xi(t), \\ y_a(t) &= \underbrace{\begin{bmatrix} I & \mathbf{0} & \mathbf{0} \end{bmatrix}}_{C_a} x_a(t). \end{aligned} \tag{2.63}$$

where $\xi(t) = \dot{\tau}(t)$. Equation (2.63) can be written compactly as

$$\begin{aligned} \dot{x}_a(t) &= A_a(\rho)x_a(t) + B_a w(t) + D_a \xi(t), \\ y_a(t) &= C_a x_a(t). \end{aligned} \tag{2.64}$$

Equation (2.64) is in the form of (2.6) hence the results of Theorem 2.1 can be readily applied.

Remark 2.2. *It must be pointed out that using the formulations in equations (2.63) and (2.64), uncertainties in the output and direct feedthrough matrices (if present) can also*

be considered.

Numerical Solution

Using the YALMIP toolbox [146] of MATLAB® [147], the convex optimization problem in Theorem 2.1 is solved for the system (2.64) with the following uncertain parameters limits, representing approximately $20-30\%$ uncertainty around the nominal values:

$$\begin{aligned}
&\rho_1^{min} = 1.00,\ \rho_1^{max} = 1.625,\\
&\rho_2^{min} = 1400.00,\ \rho_2^{max} = 2275.00,\\
&\rho_3^{min} = 65.882,\ \rho_3^{max} = 107.06,\\
&\rho_4^{min} = 270.59,\ \rho_4^{max} = 439.71,\\
&\rho_5^{min} = 47.059,\ \rho_5^{max} = 76.471.
\end{aligned} \tag{2.65}$$

The following numerical solution is obtained for the $\mathcal{H}_\infty$ controller:

$$X_1 = \begin{bmatrix} 0.3478 & -0.2436 & -0.0459 & -0.3242 \\ -0.2436 & 116.7727 & -9.5113 & 0.6653 \\ -0.0459 & -9.5113 & 5.4809 & -0.0707 \\ -0.3242 & 0.6653 & -0.0707 & 0.8587 \end{bmatrix} \tag{2.66}$$

$$X_2 = \begin{bmatrix} 1647.8 & -0.0004024 & -0.0015844 & 0.10621 \\ -0.0004024 & 3.1588\times10^{5} & -0.00020949 & -6.8452\times10^{-6} \\ -0.0015844 & -0.00020949 & 0.0034973 & -2.6043\times10^{-5} \\ 0.10621 & -6.8452\times10^{-6} & -2.6043\times10^{-5} & 1138.1 \end{bmatrix} \tag{2.67}$$

$$Y_1 = \begin{bmatrix} -0.41669 & -0.013185 & -0.048931 & -1.6634 \end{bmatrix}, \tag{2.68}$$

$$Y_2 = \begin{bmatrix} -929.52 \\ -1648 \\ -0.73588 \\ -29.386 \end{bmatrix} \tag{2.69}$$

$$Z = \begin{bmatrix} 4.5974\times10^{-8} & 1647.9 & -0.17642 & -0.20407 \\ 1.0008\times10^{-11} & -0.37733 & 0.13244 & -0.012932 \\ -4.0346\times10^{-11} & -0.33426 & -1.627 & 0.21603 \\ 2.2663\times10^{-8} & 0.10844 & -0.0033235 & -1138.1 \end{bmatrix} \tag{2.70}$$

$$\begin{aligned} &\alpha = 1.6634,\ \beta = 3.4705,\ \delta = 0.00016588,\ \gamma = 0.012915, \\ &\lambda_1 = 0.29476,\ \lambda_2 = 0.63294, \lambda_3 = 3.7717 \times 10^{-9}. \end{aligned} \tag{2.71}$$

The SOF $\mathcal{H}_\infty$ problem of [145] is feasible for the system (2.64). However, the numerical results are omitted for brevity.

Time-Domain Simulation Results

The designed observer-controller is tested for the speed control of a $1\ kW$ BLDC motor, whose schematic, dynamic model and commutation logic are given in section A.1 while its parameters are given in Table A.2 in Appendix A. The controller is also programmed on a DSP and the closed loop system is run in PIL configuration. The experimental setup for PIL testing is shown in fig. 2.1. The controller is discretized and run on the Microchip's 16-bit dsPIC33EP256MC502 microcontroller (MCU) with

a sampling time of $1\ ms$. The plant is run in Simulink on the host computer. The communication between the plant and controller takes place over a serial link. The results of the proposed controller in simulation and PIL modes of operation for speed regulation and tracking performance test cases are compared.

The simulation is run for $t = 50\ s$. Two test cases are run; one for speed regulation and the other for speed tracking. For the speed regulation test case, rated speed command of $\omega_r = 3000\ rpm$ is given. The motor is started under no load with rated load torque of $\tau = 3\ N.m$ applied at $t = 10\ s$ and removed at $t = 25\ s$. For the speed tracking test case, a constant load torque disturbance of $\tau = 1.5\ N.m$ is applied throughout the simulation. The actual paramters used in the time domain simulation are $R_a = R_a^{min}$, $L_a = L_a^{max}$, $K_m = K_m^{min}$ and $b = b^{max}$. They correspond to $\rho_1 = 1.375$, $\rho_2 = 1575$, $\rho_3 = 66.706$, $\rho_4 = 273.97$ and $\rho_5 = 52.941$. A step changing speed reference is used for speed tracking. The results of speed regulation and tracking test cases along with control voltage plots are shown in are shown in fig. 2.2 and fig. 2.3.

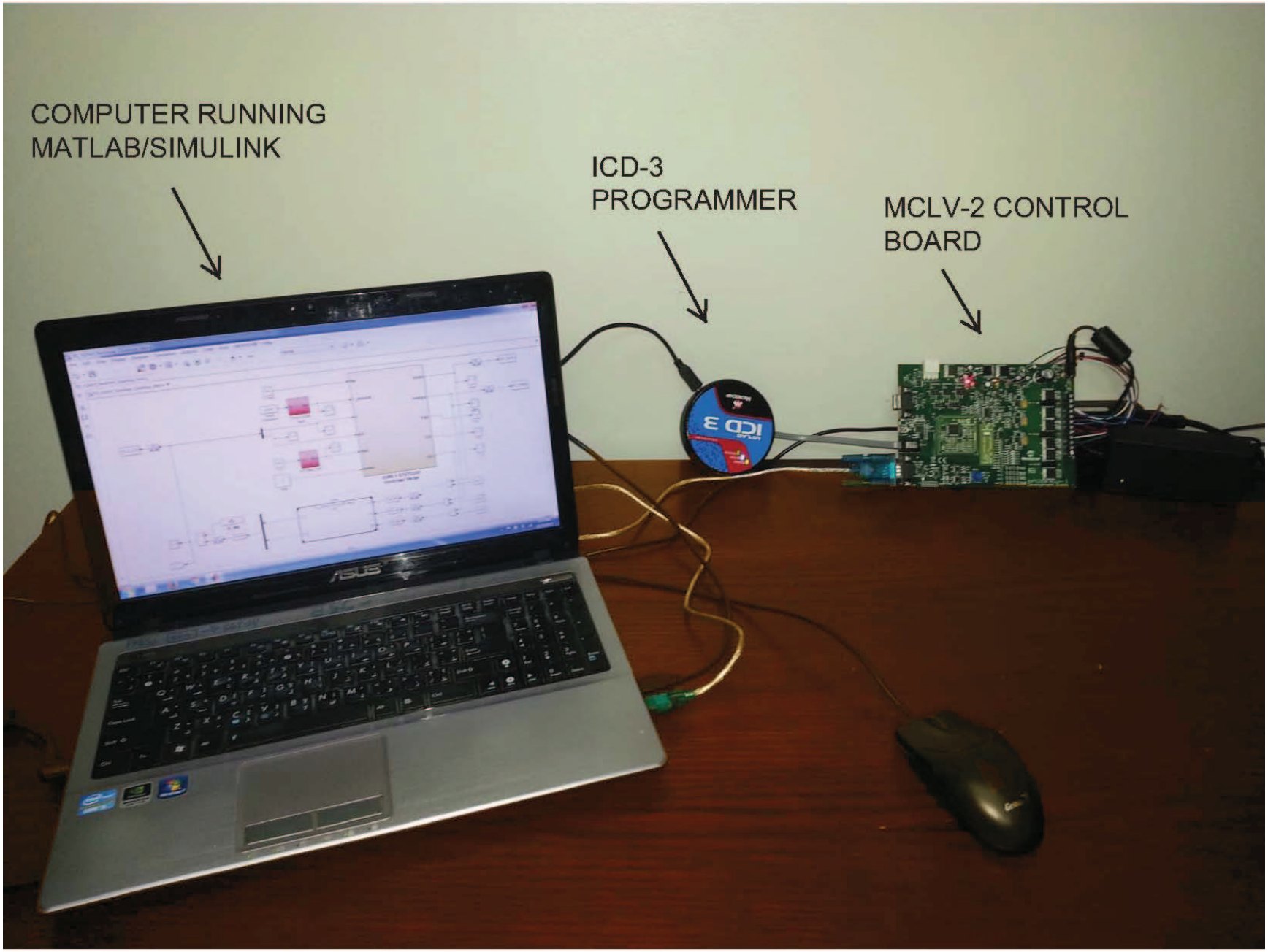

Figure 2.1: Processor-in-the-loop test setup

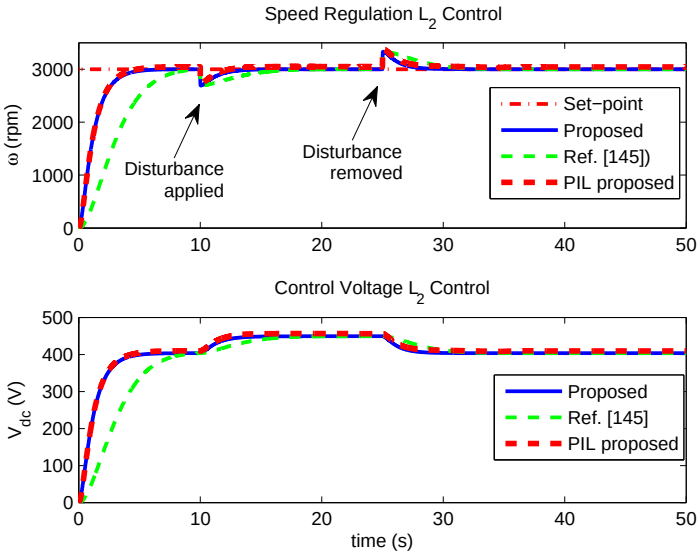

Figure 2.2: Speed regulation results for the $\mathcal{H}_\infty$ controller under rated load application

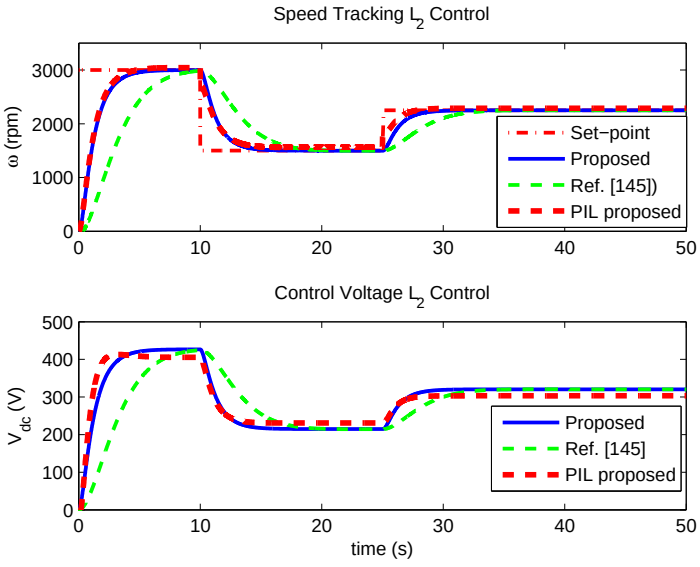

Figure 2.3: Speed tracking results for the $\mathcal{H}_\infty$ controller under 50% rated load application

2.3.2 Power System Stabilization using STATCOM

The linearized system model of a single machine infinite bus system installed with a static synchronous compensator (STATCOM) [120] is given in the form $\dot{x} = Ax + Bu + D\xi_1$ with

$$
\begin{aligned}
x &= \begin{bmatrix} \Delta\phi & \Delta\omega & \Delta E'_q & \Delta E_{fd} & \Delta V_{DC} \end{bmatrix}^T, \\
u &= \begin{bmatrix} \Delta c & \Delta\psi \end{bmatrix}^T, \ \xi_1 = \Delta P_m \\
A &= \begin{bmatrix}
\mathbf{0} & \omega_b & \mathbf{0} & \mathbf{0} & \mathbf{0} \\
-\frac{K_1}{M} & \mathbf{0} & -\frac{K_2}{M} & \mathbf{0} & -\frac{K_{10}}{M} \\
-\frac{K_4}{T'_{do}} & \mathbf{0} & -\frac{K_3}{T'_{do}} & \frac{1}{T'_{do}} & -\frac{K_{11}}{T'_{do}} \\
-\frac{K_A K_5}{T_A} & \mathbf{0} & -\frac{K_A K_6}{T_A} & -\frac{1}{T_A} & -\frac{K_A K_{12}}{T_A} \\
\frac{K_7}{C_{DC}} & \mathbf{0} & \frac{K_8}{C_{DC}} & \mathbf{0} & \frac{K_9}{C_{DC}}
\end{bmatrix}, \\
B &= \begin{bmatrix}
\mathbf{0} & \mathbf{0} \\
-\frac{K_{13}}{M} & -\frac{K_{14}}{M} \\
-\frac{K_{15}}{T'_{do}} & -\frac{K_{16}}{T'_{do}} \\
-\frac{K_A K_{17}}{T_A} & -\frac{K_A K_{18}}{T_A} \\
-\frac{K_{19}}{C_{DC}} & -\frac{K_{20}}{C_{DC}}
\end{bmatrix}, \ D = \begin{bmatrix} \mathbf{0} \\ \frac{1}{M} \\ \mathbf{0} \\ \mathbf{0} \\ \mathbf{0} \end{bmatrix}
\end{aligned}
\tag{2.72}
$$

where $\phi\ (rad)$ is the rotor angle, ω is the angular frequency, E'_q is the q-axis voltage behind transient reactance, E_{fd} is the field voltage, V_{DC} is the STATCOM capacitor voltage, c is the PWM modulation index, ψ is the angle of the STATCOM output voltage

referenced to the generator's terminal voltage, $M\ (s)$ is the machine inertia coefficient, $T'_{do}\ (s)$ is the open circuit field time constant, $\omega_b\ (\frac{rad}{s})$ is the base frequency, K_A is the gain of the excitation system while $T_A\ (s)$ is its time constant, C_{DC} is the capacitance of the STATCOM storage capacitor. The signal ξ_1 is change in mechanical input power P_m, treated as an external disturbance. All the quantities are in per unit (pu) unless specified otherwise. The constants $K_i\ , i = 1, \ldots, 20$, are introduced by linearization. The nominal parameter values and the single-line diagram are given in Appendix A section A.3, taken from [120]. We assume that measures of the states $\Delta\phi$, $\Delta\omega$ and ΔV_{DC} are available. The remote signal ω can be synthesized using locally available signals [148], while ϕ can be readily obtained from ω. The signal V_{DC} is also available for feedback [120]. We have the following output matrix:

$$C = \begin{bmatrix} 1 & 0 & 0 & 0 & 0 \\ 0 & 1 & 0 & 0 & 0 \\ 0 & 0 & 0 & 0 & 1 \end{bmatrix}. \tag{2.73}$$

Assuming that the parameters M and C_{DC} are not precisely known but lie between an upper and lower limit, and letting

$$\begin{aligned} \frac{1}{M} &= \theta_1, \\ \frac{1}{C_{DC}} &= \theta_2, \end{aligned} \tag{2.74}$$

we can write

$$\theta_i^{min} \leq \theta_i \leq \theta_i^{max}, \qquad i = 1, 2, \tag{2.75}$$

with $\theta_1^{min} = \frac{1}{M^{max}}$, $\theta_1^{max} = \frac{1}{M^{min}}$, $\theta_2^{min} = \frac{1}{C_{DC}^{max}}$ and $\theta_2^{max} = \frac{1}{C_{DC}^{min}}$. Let M^{min}, M^{max}, C_{DC}^{min} and C_{DC}^{max} represent the minimum and maximum values of M and C_{DC}. Under heavy loading conditions with the generator delivering real and reactive powers of $(P, Q) = (1.2, 0.4)\ pu$, we obtain the following uncertain model, in the form of $\dot{x} = A(\theta)x + B(\theta)u + D(\theta)\xi_1$ with $\theta = \begin{bmatrix} \theta_1 & \theta_2 \end{bmatrix}^T$:

$$
\begin{aligned}
A(\theta) &= \begin{bmatrix} \mathbf{0} & 377 & \mathbf{0} & \mathbf{0} & \mathbf{0} \\ -0.2614\theta_1 & \mathbf{0} & -1.1956\theta_1 & \mathbf{0} & -0.1528\theta_1 \\ -0.0664 & \mathbf{0} & -0.3965 & 0.1983 & 0.0202 \\ 94.3724 & \mathbf{0} & -494.1651 & -100 & -77.4758 \\ -0.4691\theta_2 & \mathbf{0} & 0.1886\theta_2 & \mathbf{0} & -0.0058\theta_2 \end{bmatrix}, \\
B(\theta) &= \begin{bmatrix} \mathbf{0} & \mathbf{0} \\ -2.3250\theta_1 & 0.7348\theta_1 \\ 0.3068 & 0.0996 \\ -1178.6 & -69.5586 \\ -0.0876\theta_2 & -0.6623\theta_2 \end{bmatrix}, \ D(\theta) = \begin{bmatrix} \mathbf{0} \\ \theta_1 \\ \mathbf{0} \\ \mathbf{0} \\ \mathbf{0} \end{bmatrix}
\end{aligned}
\tag{2.76}
$$

In order to derive a form consistent with (2.6), the second term θ_1 in the $D(\theta)$ matrix of (2.76) is replaced by $\frac{1}{M^{min}}$ corresponding to the worst case disturbance, resulting in the constant matrix D. Therefore, $D(\theta)$ in (2.76) is replaced by the constant matrix D. To write the system in the form of (2.6), let us introduce a new control input v such

that $\dot{u} = -u + v$. Let the new state vector $x_a = \begin{bmatrix} x & u \end{bmatrix}^T$. Then we can write the the dynamics of the augmented system as

$$\begin{aligned} \dot{x}_a(t) &= A_a(\theta)x_a(t) + B_a v(t) + D_a \xi(t) \\ y &= C_a x_a(t) \end{aligned} \tag{2.77}$$

The augmented matrices $A_a(\theta) \in \mathbb{R}^{7\times7}$, $B_a \in \mathbb{R}^{7\times2}$, $D_a \in \mathbb{R}^{7\times1}$ and $C_a \in \mathbb{R}^{3\times7}$ are

$$\begin{aligned} A_a(\theta) &= \begin{bmatrix} A(\theta) & B(\theta) \\ \mathbf{0} & -I \end{bmatrix}, B_a = \begin{bmatrix} \mathbf{0} \\ I \end{bmatrix}, D_a = \begin{bmatrix} D \\ \mathbf{0} \end{bmatrix} \\ C_a &= \begin{bmatrix} C & \mathbf{0} \end{bmatrix}. \end{aligned} \tag{2.78}$$

The equation system (2.77) is in the form of (2.6) thus, the results of Theorem 2.1 can readily be applied.

Numerical Solution

The following minimum and maximum values for θ_1 and θ_2 are used for the numerical solution, representing $20 - 30\%$ uncertainty around a nominal value:

$$\begin{aligned} \theta_1^{min} &= 0.13,\ \theta_1^{max} = 0.20, \\ \theta_2^{min} &= 0.80,\ \theta_2^{max} = 1.20. \end{aligned} \tag{2.79}$$

They correspond to $M^{min} = 5$, $M^{max} = 7.5$, $C_{DC}^{min} = 0.83$ and $C_{DC}^{max} = 1.25$. The nominal values of M and C_{DC} are 6 and 1 (pu), respectively. At the heavy loading operating point $(P, Q) = (1.2, 0.4)\ pu$, using the YALMIP toolbox [146] of MATLAB®,

the solution to the linear matrix inequalities (2.11), (2.12), (2.13) and (2.14) using the matrices of (2.77) is

$$X_1 = \begin{bmatrix} 9.8489 & -0.0777 & -0.4530 & -0.7960 & 1.0693 & 0.9245 & -1.3491 \\ -0.0777 & 0.0033 & 0.0092 & 0.0758 & -0.0061 & 0.0035 & -0.0849 \\ -0.4530 & 0.0092 & 1.5883 & -0.3585 & -0.2409 & -0.6517 & 0.1308 \\ -0.7960 & 0.0758 & -0.3585 & 466.8131 & 0.0111 & 12.5693 & 2.4570 \\ 1.0693 & -0.0061 & -0.2409 & 0.0111 & 0.8271 & 0.1194 & 0.2522 \\ 0.9245 & 0.0035 & -0.6517 & 12.5693 & 0.1194 & 2.6973 & -0.7578 \\ -1.3491 & -0.0849 & 0.1308 & 2.4570 & 0.2522 & -0.7578 & 15.5954 \end{bmatrix}, \tag{2.80}$$

$$X_2 = \begin{bmatrix} 0.4273 & -0.0000 & 0.0038 & 0.0003 & -0.0000 & 0.0017 & -0.0003 \\ -0.0000 & 0.0000 & -0.0000 & 0.0000 & 0.0000 & -0.0000 & -0.0000 \\ 0.0038 & -0.0000 & 0.2883 & 0.0017 & -0.0000 & 0.4591 & -0.1060 \\ 0.0003 & 0.0000 & 0.0017 & 0.0004 & -0.0000 & -0.0073 & -0.0005 \\ -0.0000 & 0.0000 & -0.0000 & -0.0000 & 0.0000 & -0.0000 & -0.0000 \\ 0.0017 & -0.0000 & 0.4591 & -0.0073 & -0.0000 & 9.8490 & 0.6611 \\ -0.0003 & -0.0000 & -0.1060 & -0.0005 & -0.0000 & 0.6611 & 0.3934 \end{bmatrix} \times 10^6, \tag{2.81}$$

$$Y_1 = \begin{bmatrix} -7.0809 & 0.2346 & -0.6680 & 11.9511 & -0.7441 & -166.1803 & -0.0008 \\ 60.7167 & -1.5721 & -2.1488 & 1.7101 & 8.4430 & -0.0058 & -166.1432 \end{bmatrix}, \tag{2.82}$$

$$Y_2 = \begin{bmatrix} -0.0049 & 0.0000 & 0.0000 \\ -1.6186 & -0.3051 & 0.0000 \\ -0.0020 & -0.0051 & -0.0009 \\ -0.0009 & -0.0001 & 0.0002 \\ 0.0002 & 0.0049 & -0.0041 \\ 0.0101 & -0.0035 & -0.0051 \\ 0.0012 & -0.0023 & 0.0002 \end{bmatrix} \times 10^8, \tag{2.83}$$

$$Z = \begin{bmatrix} 0.0003 & 1.6107 & -0.0014 & -0.0003 & -0.0002 & -0.0033 & -0.0002 \\ 0.0000 & -0.0001 & -0.0001 & -0.0000 & -0.0000 & -0.0001 & -0.0000 \\ 0.0014 & 0.0143 & -0.0097 & -0.0012 & -0.0013 & -0.0242 & 0.0001 \\ 0.0004 & 0.0011 & -0.0021 & -0.0004 & -0.0003 & -0.0050 & -0.0003 \\ -0.0000 & -0.0000 & 0.0000 & 0.0000 & 0.0000 & 0.0000 & 0.0000 \\ -0.0072 & 0.0063 & 0.0343 & 0.0082 & 0.0058 & -0.0108 & -0.0011 \\ -0.0004 & -0.0013 & 0.0030 & 0.0003 & 0.0004 & -0.0008 & -0.0037 \end{bmatrix} \times 10^8, \tag{2.84}$$

$$\begin{gathered} \alpha = 166.1421,\ \beta = 341.5227,\ \delta = 0.0016,\ \gamma = 0.0793 \\ \lambda_1 = 0.0081,\ \lambda_2 = 484.7565, \lambda_3 = 4.8111 \times 10^{-6}. \end{gathered} \tag{2.85}$$

The SOF based LMIs of [145] are infeasible for this problem.

Remark 2.3. *An alternative to the replacement of the second term θ_1 of the matrix $D(\theta)$ in (2.76) by $\frac{1}{M^{min}}$ to facilitate the application of Theorem 2.1 is to leave $D(\theta)$ as it is and apply the results of Theorem 2.1 on (2.77) with the matrix D_a replaced by $D_a(\theta)$. This would require a slight modification to the original results to include uncertainties*

in the D_a matrix. Nevertheless, the modified results still lead to a feasible solution to the given problem.

Time-Domain Simulation

Time domain simulations in MATLAB®/Simulink are run on the nonlinear power system model installed with STATCOM at two different operating points to validate the performance of the designed observer based controller. The operating points are $(P, Q) = (1.2, 0.4)$ and $(P, Q) = (0.8, 0.2)$ for heavy and nominal loading, respectively. The performance of the controller in PIL, under the same configuration setup as the BLDC motor speed control case, is also validated against the simulation. Numerical results for the nominal operating point are omitted for conciseness. The parameters M and C_{DC} are set to M^{min} and C_{DC}^{max}, and simulations are run for $t = 5\ s$ with a 15% step torque disturbance and a 3-phase fault at the infinite bus, applied at $t = 1\ s$ instant, lasting three cycles [122]. The results of the simulations under torque disturbance are shown in figs. 2.4, 2.5, 2.6, 2.7 and 2.8, while for the 3-phase fault are shown in figs. 2.9, 2.10, 2.11 and 2.12. Notice that under no control, after the disturbance application, the system becomes unstable. This is true for both disturbance types at all operating points. However, the results of instability are depicted in fig. 2.4 only for the heavy loading operating point under torque fault, for conciseness.

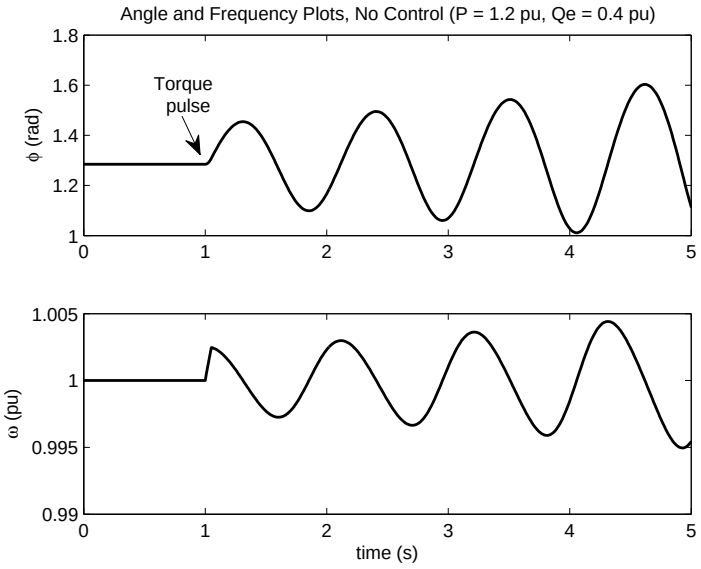

Figure 2.4: Rotor angle and angular frequency plots with no controller under heavy loading, 15% torque disturbance

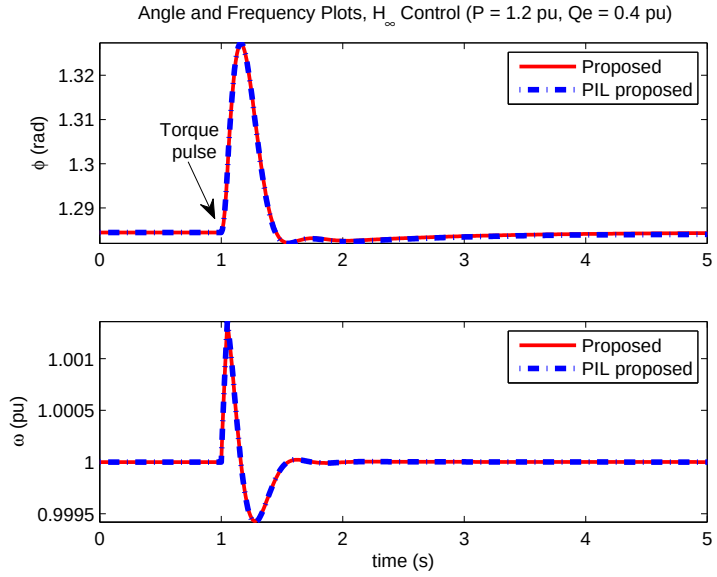

Figure 2.5: Rotor angle and angular frequency plots with the $\mathcal{H}_\infty$ controller under heavy loading, 15% torque disturbance

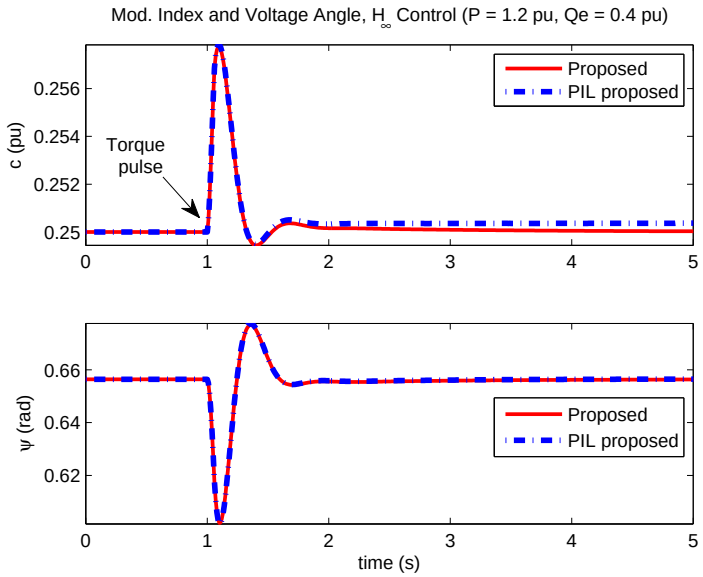

Figure 2.6: Modulation index and STATCOM output voltage angle plots with the $\mathcal{H}_\infty$ controller under heavy loading, 15% torque disturbance

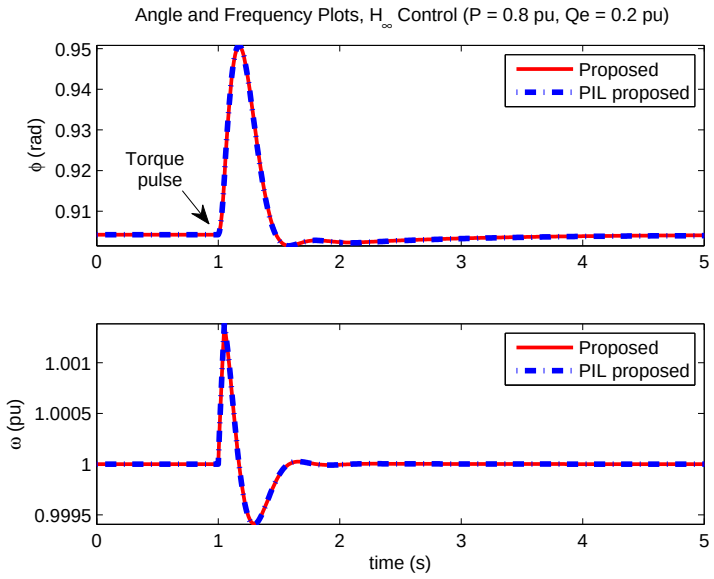

Figure 2.7: Rotor angle and angular frequency plots with the $\mathcal{H}_\infty$ controller under nominal loading, 15% torque disturbance

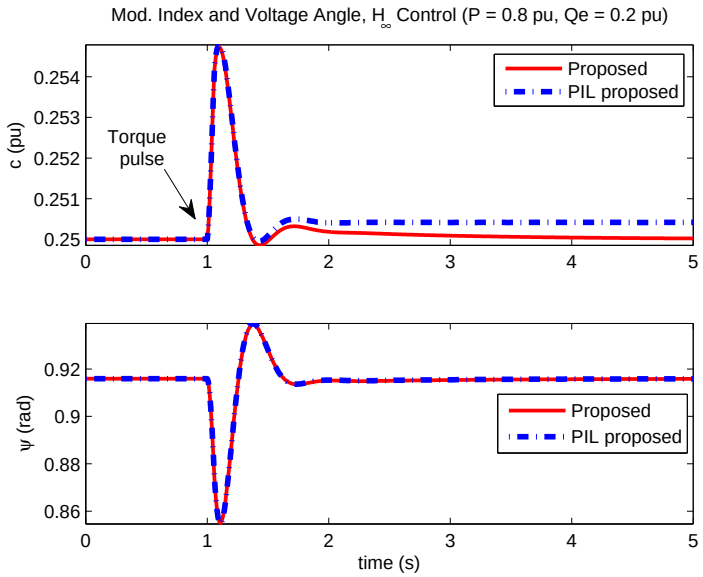

Figure 2.8: Modulation index and STATCOM output voltage angle plots with the $\mathcal{H}_\infty$ controller under nominal loading, 15% torque disturbance

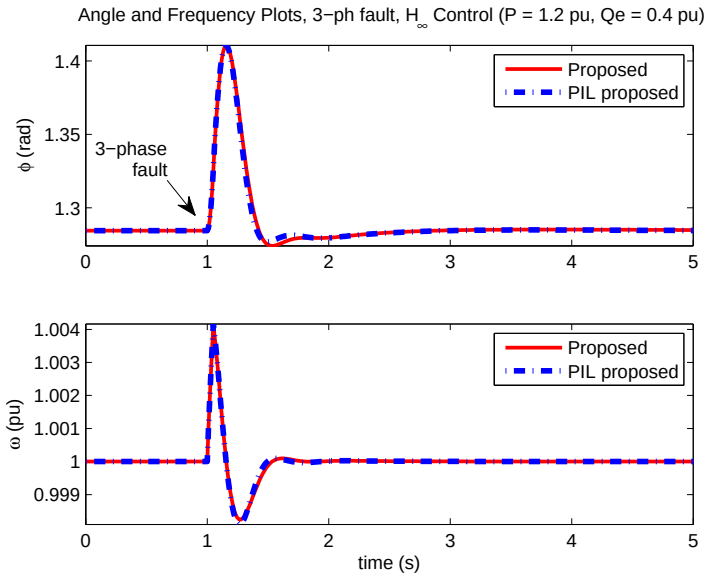

Figure 2.9: Rotor angle and angular frequency plots with the $\mathcal{H}_\infty$ controller under heavy loading, 3-phase fault for three cycles

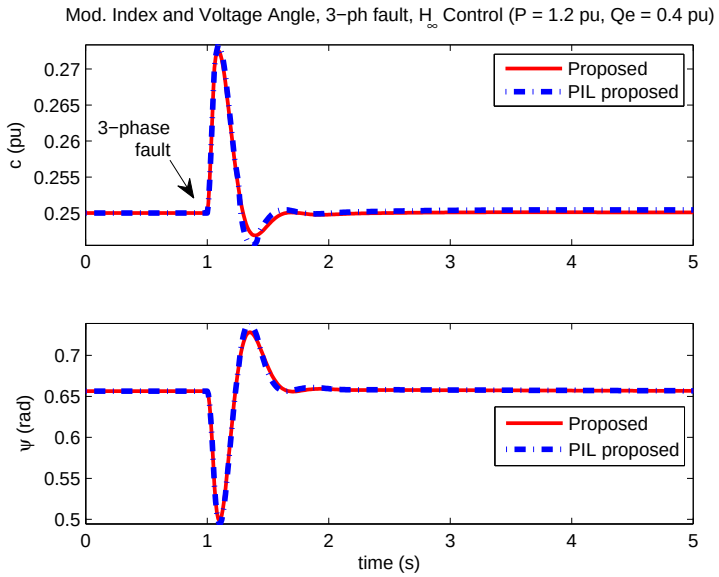

Figure 2.10: Modulation index and STATCOM output voltage angle plots with the $\mathcal{H}_\infty$ controller under heavy loading, 3-phase fault for three cycles

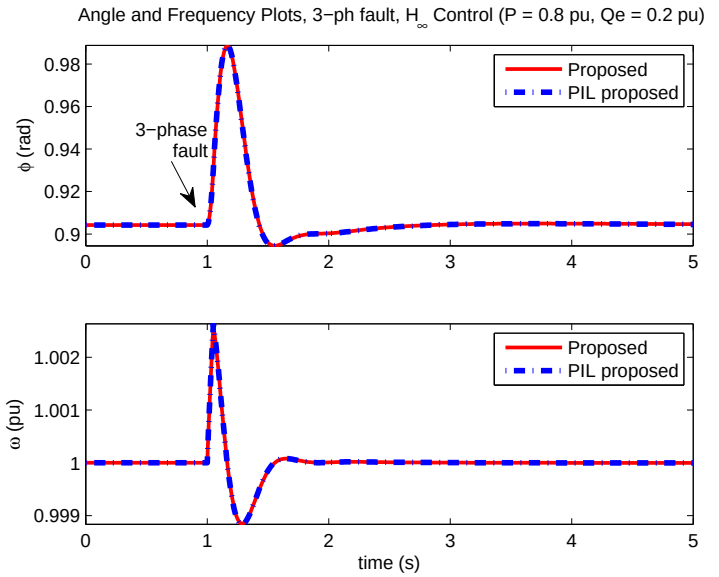

Figure 2.11: Rotor angle and angular frequency plots with the $\mathcal{H}_\infty$ controller under nominal loading, 3-phase fault for three cycles

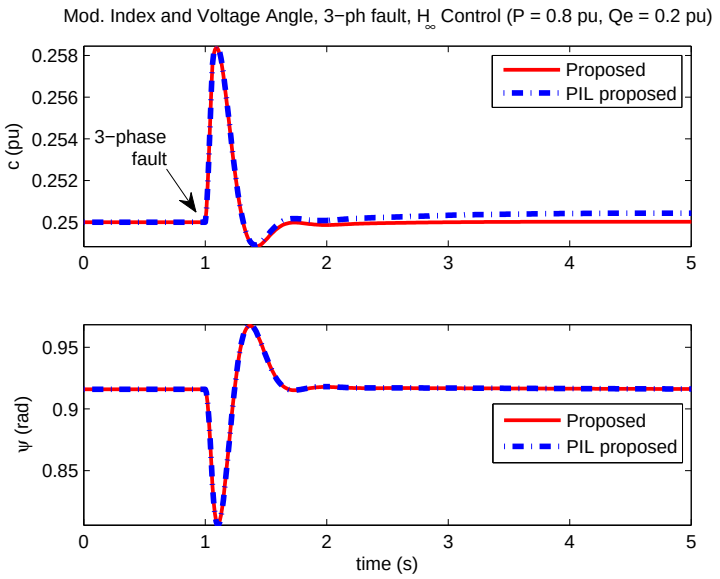

Figure 2.12: Modulation index and STATCOM output voltage angle plots with the $\mathcal{H}_\infty$ controller under nominal loading, 3-phase fault for three cycles

2.4 Discussion

From the results in fig. 2.2 and fig. 2.3, it can be seen that the with proposed robust $\mathcal{H}_\infty$ controller, the actual speed of the BLDC motor tracks the set-point speed in the presence of uncertainties and unknown load torque disturbance with no steady state error under different operating conditions. This demonstrates that the proposed controller resolves the robustness issue by fast tracking of the set-point speed. The proposed controller shows a faster response than the SOF based $\mathcal{H}_\infty$ controller of [145] under polytopic uncertainties.

The plots in fig. 2.5 to fig. 2.12 indicate that the robust controller successfully damps out the low frequency oscillations in the rotor angle and frequency and readily stabilizes the system's operating point, under an unknown mechanical step disturbance and a 3-phase fault in the presence of uncertainties in the model parameters under different operating conditions. This demonstrates that the proposed controller resolves the robustness issue by fast stabilization of the equilibrium point. Furthermore, the infeasibility of the SOF based LMIs of [145] for this problem indicate that the proposed LMIs are less conservative.

For both applications, the controller shows robustness in performance under adverse conditions i.e., without the perfect knowledge of uncertain parameters or the disturbance. The response of the closed loop system under the proposed observer-based controller can be further improved by imposing pole-placement constraints in LMI regions to control other performance goals like rise-time, oscillations, percentage overshoot, etc.

From the figs. 2.2 and 2.3 for the BLDC motor and figs. 2.5, 2.6, 2.7, 2.8, 2.9, 2.10, 2.11 and 2.12 for STATCOM based power system, it can be further observed that there is a close agreement between the closed loop responses of both systems in simulation and PIL modes, indicating the proper functioning of the controller in digital implementation. The steady state offset between the simulation and PIL results is less than 0.2%. The slight differences in the responses are mainly due to controller discretization introducing some inaccuracies, a limited sampling rate in the digital implementation, fixed-point data type conversion inaccuracies and choice of the numerical integration method.

CHAPTER 3

ROBUST OBSERVER-BASED CONTROL OF UNCERTAIN LINEAR SYSTEMS WITH MIXED $\mathcal{H}_2/\mathcal{H}_\infty$ PERFORMANCE

In this chapter, convex optimization based solution for the robust observer based mixed $\mathcal{H}_2/\mathcal{H}_\infty$ controller design is presented for the same class of uncertain linear systems with polytopic uncertainties and unknown disturbance as in Chapter 2. The proposed LMIs yield controller and observer gains in a single step without having to resort to multistep or iterative solutions. Equality constraints and nonconvex parameter dependencies as in [2, 13, 34, 78] are avoided altogether in the interest of reducing conservatism and restrictiveness. An approach similar to [14] is adopted to decouple the controller and observer designs into separate matrix inequalities, leading to sufficient

LMI design conditions. Free parameters, appearing in the development in a convex manner, are introduced to reduce restrictiveness and facilitate the development. No restrictions are placed on the uncertain parameters or their rate of change, except an upper and a lower bound. The effectiveness of the proposed results is demonstrated through a BLDC motor's speed control and stabilization of a STATCOM installed power system.

For the $\mathcal{H}_\infty$ performance constraint, much of the developmental steps are the same as the $\mathcal{L}_2$-gain development in Chapter 2. New results are derived for the $\mathcal{H}_2$ performance constraint. The mixed performance control structure also uses a full-order Luenberger type observer [142] as the $\mathcal{L}_2$-gain controller in the Chapter 2. Some new definitions are introduced that are used in this development.

3.1 Definitions

The following definitions will be used in this chapter and throughout the thesis [143, 144]:

Definition 3.1. *The convex hull of a set C is defined as the set of all convex combinations of points in C i.e.,*

$$\mathbf{conv}\ C = \{\theta_1 x_1 + \cdots + \theta_k x_k \mid x_i \in C,\ \theta_i \geq 0,\ i = 1, \ldots, k,\ \theta_1 + \cdots + \theta_k = 1\}\,. \tag{3.1}$$

The convex hull is always convex.

Definition 3.2. *The state-space representation of a finite dimensional linear time invariant (LTI) system is defined as*

$$\begin{aligned} \dot{x}(t) &= Ax(t) + Bu(t), \\ y(t) &= Cx(t) + Du(t), \end{aligned} \tag{3.2}$$

where $x \in \mathbb{R}^{n_x}$ is the state vector, $u \in \mathbb{R}^{n_u}$ in the input vector, $y \in \mathbb{R}^{n_y}$ is the output vector, and matrices A, B, C and D are the state, input, output and direct feedthrough matrices, respectively.

Definition 3.3. *The Laplace transform of a given signal $u(t)$ is defined as*

$$U(s) = \int_0^\infty u(t)e^{-st}dt. \tag{3.3}$$

Definition 3.4. *The transfer matrix of a finite dimensional LTI system is defined as*

$$G(s) = C(sI - A)^{-1}B + D. \tag{3.4}$$

It represents the Laplace transform of the input to the output impulse matrix.

Definition 3.5. *For a stable, strictly proper transfer matrix, we have:*

$$\|G(s)\|_2^2 = Trace(B^T G_o B), \tag{3.5}$$

where $\|G(s)\|_2$ is denotes the $\mathcal{H}_2$-norm of the transfer matrix $G(s)$ and the observability

Gramian G_o is the solution to the Lyapunov equation

$$A^T G_o + G_o A + C^T C = 0. \tag{3.6}$$

Alternatively, we can also have

$$\|G(s)\|_2^2 = Trace(CG_cC^T), \tag{3.7}$$

where the controllability Gramian G_c is the solution to the Lyapunov equation

$$AG_c + G_cA^T + BB^T = 0. \tag{3.8}$$

Definition 3.6. *The $\mathcal{H}_\infty$-norm of a transfer matrix $G(s)$ is defined as the ratio of $\mathcal{L}_2$-norm of the output to the $\mathcal{L}_2$-norm of the input i.e.,*

$$\|G\|_\infty = \frac{\|Gu\|_{\mathcal{L}_2}}{\|u\|_{\mathcal{L}_2}}. \tag{3.9}$$

3.2 Problem Statement and Main Results

Consider the uncertain linear system:

$$\begin{aligned} \dot{x}(t) &= A(\theta)x(t) + Bu(t) + D\xi(t) \\ y(t) &= Cx(t) \end{aligned} \tag{3.10}$$

where $x(t) \in \mathbb{R}^n$ is the state vector, $u(t) \in \mathbb{R}^m$ is the control input vector, $\xi(t) \in \mathbb{R}^d$ is the unknown disturbance input vector and $y(t) \in \mathbb{R}^p$ is the system output vector. The matrices $B \in \mathbb{R}^{n\times m}$, $D \in \mathbb{R}^{n\times d}$ and $C \in \mathbb{R}^{p\times n}$ are the input, disturbance and output matrices, respectively. The matrix $A(\theta)$ is given by:

$$A(\theta) \in \text{Convex Hull}\{A_1, A_2, \ldots, A_\mu\} \triangleq \mathbf{conv}\ A \tag{3.11}$$

that is

$$A(\theta) = \sum_{i=1}^{\mu} \zeta_i A_i, \qquad \zeta_i > 0\ \forall i, \qquad \sum_{i=1}^{\mu} \zeta_i = 1. \tag{3.12}$$

It is assumed that the pairs (A_i, B) and (A_i, C) are controllable and observable, respectively for all $i = 1, 2, \cdots, \mu$. Let $\hat{x}(t)$ represents the state vector of the following observer:

$$\dot{\hat{x}}(t) = A_o\hat{x}(t) + Bu + P_2Y_2(C\hat{x}(t) - y(t)) \tag{3.13}$$

where A_o is the observer state matrix to be determined. Let $T_i(s)$ be the i^{th} transfer matrix from the observation error $C\hat{x}(t) - y(t)$ to the disturbance input $\xi(t)$ for a constant A_i in (3.11). Our objective is to find a stabilizing observer-based controller $u(t) = Y_1P_1\hat{x}(t)$ such that the system (3.10) is globally asymptotically stable when $\xi(t) = 0$, and satisfy the following mixed $\mathcal{H}_2/\mathcal{H}_\infty$ performance objective when $\xi(t) \neq 0$:

$$\begin{aligned} &\|T_i(s)\|_\infty < \gamma_\infty, \\ &\|T_i(s)\|_2 < \gamma_2, \qquad \forall\ i = 1, 2, \ldots, \mu. \end{aligned} \tag{3.14}$$

where γ_∞ and γ_2 are certain positive performance scalers, and $\|.\|_2$ and $\|.\|_\infty$ represent the $\mathcal{H}_2$ and $\mathcal{H}_\infty$-norms, respectively. The symmetric and positive definite matrices $P_1 \in \mathbb{R}^{n\times n}$, $P_2 \in \mathbb{R}^{n\times n}$, and $Y_1 \in \mathbb{R}^{m\times n}$ and $Y_2 \in \mathbb{R}^{n\times p}$ are arbitrary real matrices to be determined. The design of the controller and observer gains is summarized in the following theorem:

Theorem 3.1. *Consider the system (3.10) and observer (3.13). Then if there exist four symmetric and positive definite matrices $X_1 \in \mathbb{R}^{n\times n}$, $X_2 \in \mathbb{R}^{n\times n}$, $Z_1 \in \mathbb{R}^{d\times d}$ and $Z_2 \in \mathbb{R}^{d\times d}$, three real matrices $Y_1 \in \mathbb{R}^{m\times n}$, $Y_2 \in \mathbb{R}^{n\times p}$, $Z \in \mathbb{R}^{n\times n}$ and six strictly positive constants α, β, δ, λ_i, $1 \leq i \leq 3$ such that the following convex optimization problem is solvable for $0 < \lambda_1 < 1$:*

$$\text{minimize } \eta_1,\ \eta_2 \text{ s.t.}$$

$$\begin{bmatrix} -X_1 & I \\ I & -(2\beta-\alpha)I \end{bmatrix} < 0 \tag{3.15}$$

$$\begin{bmatrix} \Phi_{1i} & X_1 & -BY_1 & D \\ * & -(2-\lambda_1)I & \mathbf{0} & \mathbf{0} \\ * & * & -\alpha I & \mathbf{0} \\ * & * & * & -\delta I \end{bmatrix} < 0 \qquad \forall\, i = 1, 2, \cdots, \mu. \tag{3.16}$$

$$\Phi_{1i} = X_1 A_i^T + A_i X_1 + Y_1^T B^T + B Y_1$$

$$\begin{bmatrix} \Phi_2 & \beta I & X_2 D \\ * & -X_1 & \mathbf{0} \\ * & * & -(\eta_1 - \lambda_3 - \delta) I \end{bmatrix} < 0 \tag{3.17}$$

$$\Phi_2 = Y_2 C + C^T Y_2^T + C^T C + Z^T + Z + \lambda_2 I$$

$$\begin{bmatrix} -\lambda_1 I & A_i^T X_2 - Z^T & \mathbf{0} \\ * & -\lambda_2 I & \mathbf{0} \\ * & * & -\lambda_3 I \end{bmatrix} < 0 \qquad \forall\, i = 1, 2, \cdots, \mu. \tag{3.18}$$

$$Tr(Z_1) + Tr(Z_2) < \eta_2 \tag{3.19}$$

$$\begin{bmatrix} Z_1 & D^T \\ D & X_1 \end{bmatrix} > 0 \tag{3.20}$$

$$Z_2 - D^T X_2 D > 0 \tag{3.21}$$

with $X_1 = P_1^{-1}$, $X_2 = P_2^{-1}$, $\eta_1 = \gamma_\infty^2$ and $\eta_2 = \gamma_2^2$, then the observer based controller with $u(t) = Y_1 P_1 \hat{x}(t)$ and $A_o = X_2^{-1} Z = P_2 Z$, is a stabilizing controller for system (3.10) verifying (3.14).

Proof. Let $e(t) = x(t) - \hat{x}(t)$ be the observer error. Then we can write the original system (3.10), with $u(t) = Y_1 P_1 \hat{x}(t)$ in terms of observer error as:

$$\dot{x}(t) = (A(\theta) + B Y_1 P_1) x(t) - B Y_1 P_1 e(t) + D\xi(t). \tag{3.22}$$

The observer dynamics (3.13) can be written in terms of $x(t)$ and $e(t)$ as:

$$\dot{\hat{x}}(t) = (A_o + BY_1P_1)x(t) - (A_o + BY_1P_1 + P_2Y_2C)e(t). \tag{3.23}$$

Since $\dot{e}(t) = \dot{x}(t) - \dot{\hat{x}}(t)$, the observer error dynamics are written as:

$$\dot{e}(t) = (A(\theta) - A_o)x(t) + (A_o + P_2Y_2C)e(t) + D\xi(t). \tag{3.24}$$

Combining (3.22) and (3.24), we can write the dynamics of the states and observer error in matrix form as:

$$\begin{bmatrix} \dot{x}(t) \\ \dot{e}(t) \end{bmatrix} = \begin{bmatrix} A(\theta) + BY_1P_1 & -BY_1P_1 \\ A(\theta) - A_o & A_o + P_2Y_2C \end{bmatrix} \begin{bmatrix} x(t) \\ e(t) \end{bmatrix} + \begin{bmatrix} D \\ D \end{bmatrix} \xi(t). \tag{3.25}$$

Defining the new state $x_e(t) = \begin{bmatrix} x(t) & e(t) \end{bmatrix}^T$, we can rewrite (3.25) as

$$\begin{aligned} \dot{x}_e(t) &= A_e(\theta)x_e(t) + D_e\xi(t), \\ z(t) &= C_e x_e(t), \end{aligned} \tag{3.26}$$

where

$$\begin{aligned} A_e(\theta) &= \begin{bmatrix} A(\theta) + BY_1P_1 & -BY_1P_1 \\ A(\theta) - A_o & A_o + P_2Y_2C \end{bmatrix}, \; D_e = \begin{bmatrix} D \\ D \end{bmatrix}, \\ C_e &= \begin{bmatrix} \mathbf{0} & C \end{bmatrix}. \end{aligned} \tag{3.27}$$

The matrix $A_e(\theta)$ also belongs to the convex hull of matrices

$$A_e(\theta) \in \text{Convex Hull}\{A_{e,1}, A_{e,2}, \ldots, A_{e,\mu}\} \triangleq \text{Co } A_e, \tag{3.28}$$

that is

$$A_e(\theta) = \sum_{i=1}^{\mu} \zeta_i A_{ei}, \qquad \zeta_i > 0 \; \forall i, \qquad \sum_{i=1}^{\mu} \zeta_i = 1. \tag{3.29}$$

Define the Lyapunov candidate function $V = x_e^T P x_e$ as

$$V(x(t), e(t)) = \begin{bmatrix} x(t) \\ e(t) \end{bmatrix}^T \underbrace{\begin{bmatrix} P_1 & \mathbf{0} \\ \mathbf{0} & P_2^{-1} \end{bmatrix}}_{P} \begin{bmatrix} x(t) \\ e(t) \end{bmatrix} \tag{3.30}$$

Then, by differentiating (3.30) we get:

$$\dot{V}(x(t), e(t)) = \begin{bmatrix} x(t) \\ e(t) \\ \xi(t) \end{bmatrix}^T \begin{bmatrix} \mathcal{M}_{11} & \mathcal{M}_{12} & P_1 D \\ \mathcal{M}_{12}^T & \mathcal{M}_{22} & P_2^{-1} D \\ D^T P_1 & D^T P_2^{-1} & \mathbf{0} \end{bmatrix} \begin{bmatrix} x(t) \\ e(t) \\ \xi(t) \end{bmatrix} \tag{3.31}$$

where,

$$\begin{aligned} \mathcal{M}_{11} &= A(\theta)^T P_1 + P_1 A(\theta) + P_1 (Y_1^T B^T + B Y_1) P_1, \\ \mathcal{M}_{12} &= -P_1 B Y_1 P_1 + (A(\theta) - A_o)^T P_2^{-1}, \\ \mathcal{M}_{22} &= A_o^T P_2^{-1} + P_2^{-1} A_o + C^T Y_2^T + Y_2 C. \end{aligned} \tag{3.32}$$

For a system of the form (3.26) the $\mathcal{L}_2$ gain from output $z(t)$ to input $\xi(t)$ is less than

γ_∞ i.e.,

$$\sup_{\|w\|_2 \neq 0} \frac{\|z(t)\|_2}{\|\xi(t)\|_2} < \gamma_\infty \tag{3.33}$$

if the following inequality holds with zero initial conditions:

$$z(t)^T z(t) - \gamma_\infty^2 \xi(t)^T \xi(t) + \dot{V}(x_e(t)) < 0. \tag{3.34}$$

Substituting the value of $z(t)$ from (3.26) in (3.34) we get

$$(e(t)^T C^T C e(t) - \gamma_\infty^2 \xi(t)^T \xi(t) + \dot{V}(x(t), e(t)) < 0. \tag{3.35}$$

Substituting (3.31) in (3.35), we get the matrix inequality

$$\begin{bmatrix} x(t) \\ e(t) \\ \xi(t) \end{bmatrix}^T \begin{bmatrix} \mathcal{M}_{11} & \mathcal{M}_{12} & P_1 D \\ \mathcal{M}_{12}^T & \mathcal{M}_{22} + C^T C & P_2^{-1} D \\ D^T P_1 & D^T P_2^{-1} & -\gamma_\infty^2 I \end{bmatrix} \begin{bmatrix} x(t) \\ e(t) \\ \xi(t) \end{bmatrix} < 0, \tag{3.36}$$

where $\mathcal{M}_{ii}$ are defined in (3.32). A sufficient condition for the matrix inequality (3.36) to hold is

$$\begin{bmatrix} \mathcal{M}_{11} & \mathcal{M}_{12} & P_1 D \\ \mathcal{M}_{12}^T & \mathcal{M}_{22} + C^T C & P_2^{-1} D \\ D^T P_1 & D^T P_2^{-1} & -\gamma_\infty^2 I \end{bmatrix} < 0 \tag{3.37}$$

Inequality (3.37) can be written as a sum of matrix inequalities as follows:

$$\begin{bmatrix} \mathcal{M}_{11}+\lambda_1 I & -P_1 B Y_1 P_1 & P_1 D \\ -P_1 Y_1^T B^T P_1 & \mathcal{M}_{22}+C^T C+\lambda_2 I & P_2^{-1} D \\ D^T P_1 & D^T P_2^{-1} & -(\gamma_\infty^2-\lambda_3) I \end{bmatrix} + \begin{bmatrix} -\lambda_1 I & (A(\theta)-A_o)^T P_2^{-1} & \mathbf{0} \\ P_2^{-1}(A(\theta)-A_o) & -\lambda_2 I & \mathbf{0} \\ \mathbf{0} & \mathbf{0} & -\lambda_3 I \end{bmatrix} < 0 \tag{3.38}$$

for some positive scalers λ_1, λ_2 and λ_3. Then, sufficient conditions for satisfying (3.38) are met if the following two matrix inequalities hold:

$$\begin{bmatrix} \mathcal{M}_{11}+\lambda_1 I & -P_1 B Y_1 P_1 & P_1 D \\ -P_1 Y_1^T B^T P_1 & \mathcal{M}_{22}+C^T C+\lambda_2 I & P_2^{-1} D \\ D^T P_1 & D^T P_2^{-1} & -(\gamma_\infty^2-\lambda_3) I \end{bmatrix} < 0 \tag{3.39}$$

and

$$\begin{bmatrix} -\lambda_1 I & (A(\theta)-A_o)^T P_2^{-1} & \mathbf{0} \\ P_2^{-1}(A(\theta)-A_o) & -\lambda_2 I & \mathbf{0} \\ \mathbf{0} & \mathbf{0} & -\lambda_3 I \end{bmatrix} < 0. \tag{3.40}$$

Now, multiplying (3.39) on both sides by the matrix $\begin{bmatrix} P_1^{-1} & \mathbf{0} & \mathbf{0} \\ \mathbf{0} & I & \mathbf{0} \\ \mathbf{0} & \mathbf{0} & I \end{bmatrix}$ we get

$$\begin{bmatrix} P_1^{-1}\mathcal{M}_{11}P_1^{-1} + \lambda_1 P_1^{-1}P_1^{-1} & -BY_1P_1 & D \\ -P_1Y_1^TB^T & \mathcal{M}_{22} + C^TC + \lambda_2 I & P_2^{-1}D \\ D^T & D^TP_2^{-1} & -(\gamma_\infty^2 - \lambda_3)I \end{bmatrix} < 0. \quad (3.41)$$

Let

$$\begin{aligned} \mathcal{G}_{11} &= P_1^{-1}\mathcal{M}_{11}P_1^{-1} + \lambda_1 P_1^{-1}P_1^{-1} \\ \mathcal{G}_{22} &= \mathcal{M}_{22} + C^TC + \lambda_2 I \end{aligned} \quad (3.42)$$

Inequality (3.41) can be rewritten as

$$\begin{bmatrix} I & \mathbf{0} & \mathbf{0} & -\frac{D}{\sqrt{\delta}} & \mathbf{0} \\ \mathbf{0} & P_1 & I & \mathbf{0} & \mathbf{0} \\ \mathbf{0} & \mathbf{0} & \mathbf{0} & \sqrt{\delta}I & I \end{bmatrix} \begin{bmatrix} \mathcal{G}_{11}+\delta^{-1}DD^T & -BY_1 & \mathbf{0} & \mathbf{0} & \mathbf{0} \\ -Y_1^TB^T & -\alpha I & \mathbf{0} & \mathbf{0} & \mathbf{0} \\ \mathbf{0} & \mathbf{0} & \mathcal{G}_{22}+\alpha P_1P_1 & \mathbf{0} & P_2^{-1}D \\ \mathbf{0} & \mathbf{0} & \mathbf{0} & -I & \mathbf{0} \\ \mathbf{0} & \mathbf{0} & D^TP_2^{-1} & \mathbf{0} & -(\gamma_\infty^2-\lambda_3-\delta)I \end{bmatrix} \begin{bmatrix} I & \mathbf{0} & \mathbf{0} \\ \mathbf{0} & P_1 & \mathbf{0} \\ \mathbf{0} & I & \mathbf{0} \\ -\frac{D^T}{\sqrt{\delta}} & \mathbf{0} & \sqrt{\delta}I \\ \mathbf{0} & \mathbf{0} & I \end{bmatrix} < 0 \quad (3.43)$$

for some positive scalers δ and α. Therefore a sufficient condition for (3.43) to hold is

$$\begin{bmatrix} \mathcal{G}_{11}+\delta^{-1}DD^T & -BY_1 & \mathbf{0} & \mathbf{0} & \mathbf{0} \\ -Y_1^TB^T & -\alpha I & \mathbf{0} & \mathbf{0} & \mathbf{0} \\ \mathbf{0} & \mathbf{0} & \mathcal{G}_{22}+\alpha P_1P_1 & \mathbf{0} & P_2^{-1}D \\ \mathbf{0} & \mathbf{0} & \mathbf{0} & -I & \mathbf{0} \\ \mathbf{0} & \mathbf{0} & D^TP_2^{-1} & \mathbf{0} & -(\gamma_\infty^2-\lambda_3-\delta)I \end{bmatrix} < 0. \tag{3.44}$$

Due to its decoupled structure (3.44) can be written as the following individual matrix inequalities:

$$\begin{bmatrix} \mathcal{G}_{11}+\delta^{-1}DD^T & -BY_1 \\ -Y_1^TB^T & -\alpha I \end{bmatrix} < 0 \tag{3.45}$$

$$\begin{bmatrix} \mathcal{G}_{22}+\alpha P_1P_1 & \mathbf{0} & P_2^{-1}D \\ \mathbf{0} & -I & \mathbf{0} \\ D^TP_2^{-1} & \mathbf{0} & -(\gamma_\infty^2-\lambda_3-\delta)I \end{bmatrix} < 0. \tag{3.46}$$

Expanding (3.45) by Schur's complement, we get

$$\mathcal{G}_{11}+\alpha^{-1}BY_1Y_1^TB^T < 0. \tag{3.47}$$

Let $X_1 = P_1^{-1}$. Then by substituting the value of $\mathcal{G}_{11}$ from (3.42) and the value of $\mathcal{M}_{11}$ from (3.32) into (3.47), the matrix inequality (3.47) becomes

$$\begin{aligned} &X_1A(\theta)^T + A(\theta)X_1 + Y_1^TB^T + BY_1 \\ &\quad +\lambda_1X_1X_1 + \delta^{-1}DD^T + \alpha^{-1}BY_1Y_1^TB^T < 0. \end{aligned} \tag{3.48}$$

Since $A(\theta) = \sum_{i=1}^{\mu} \zeta_i A_i$, (3.48) can be written as

$$\begin{aligned} X_1 \sum_{i=1}^{\mu} \zeta_i A_i^T + \sum_{i=1}^{\mu} \zeta_i A_i X_1 + Y_1^T B^T + BY_1 \\ +\lambda_1 X_1 X_1 + \delta^{-1} DD^T + \alpha^{-1} BY_1 Y_1^T B^T < 0. \end{aligned} \tag{3.49}$$

Since and $\sum_{i=1}^{\mu} \zeta_i = 1$, we can write (3.49) as,

$$\begin{aligned} X_1 \sum_{i=1}^{\mu} \zeta_i A_i^T + \sum_{i=1}^{\mu} \zeta_i A_i X_1 + \sum_{i=1}^{\mu} \zeta_i (Y_1^T B^T + BY_1 \\ +\lambda_1 X_1 X_1 + \delta^{-1} DD^T + \alpha^{-1} BY_1 Y_1^T B^T) < 0 \end{aligned} \tag{3.50}$$

which is equivalent to

$$\begin{aligned} \sum_{i=1}^{\mu} \zeta_i (X_1 A_i^T + A_i X_1 + Y_1^T B^T + BY_1 \\ +\lambda_1 X_1 X_1 + \delta^{-1} DD^T + \alpha^{-1} BY_1 Y_1^T B^T) < 0. \end{aligned} \tag{3.51}$$

Therefore a sufficient condition for (3.51) to hold is

$$\begin{aligned} X_1 A_i^T + A_i X_1 + Y_1^T B^T + BY_1 \\ +\lambda_1 X_1 X_1 + \delta^{-1} DD^T + \alpha^{-1} BY_1 Y_1^T B^T < 0 \end{aligned} \tag{3.52}$$

for all $i = 1, 2, \cdots, \mu$. Inequality (3.52) is equivalent by Schur's complement to

$$\begin{bmatrix} \Phi_{1i} & X_1 & D & -BY_1 \\ * & -\lambda_1^{-1} I & \mathbf{0} & \mathbf{0} \\ * & * & -\delta I & \mathbf{0} \\ * & * & * & -\alpha I \end{bmatrix} < 0 \qquad \forall\, i = 1, 2, \cdots, \mu, \tag{3.53}$$

with $\Phi_{1i} = X_1 A_i^T + A_i X_1 + Y_1^T B^T + B Y_1$. If λ_1 is chosen such that $0 < \lambda_1 < 1$, then we always have $-\lambda_1^{-1} I \leq -(2 - \lambda_1) I$. Therefore, (3.39) is satisfied if the following linear matrix inequality holds:

$$\begin{bmatrix} \Phi_{1i} & X_1 & D & -BY_1 \\ * & -(2-\lambda_1) I & \mathbf{0} & \mathbf{0} \\ * & * & -\delta I & \mathbf{0} \\ * & * & * & -\alpha I \end{bmatrix} < 0 \qquad \forall\, i = 1, 2, \cdots, \mu \tag{3.54}$$

which proves (3.16) in Theorem 3.1. Now, (3.46) can be written by Schur's complement as

$$\begin{bmatrix} \mathcal{G}_{22} + \alpha P_1 P_1 & \mathbf{0} \\ \mathbf{0} & -I \end{bmatrix} + \begin{bmatrix} X_2 D \\ \mathbf{0} \end{bmatrix} \begin{bmatrix} \chi^{-1} I \end{bmatrix} \begin{bmatrix} D^T X_2 & \mathbf{0} \end{bmatrix} < 0. \tag{3.55}$$

where $X_2 = P_2^{-1}$, $\eta_1 = \gamma_\infty^2$ and $\chi = \eta_1 - \lambda_3 - \delta$. Simplifying (3.55), we get

$$\begin{bmatrix} \mathcal{G}_{22} + \alpha P_1 P_1 + \chi^{-1} X_2 D D^T X_2 & \mathbf{0} \\ \mathbf{0} & -I \end{bmatrix} < 0. \tag{3.56}$$

It is clear that a sufficient condition for (3.56) to hold is

$$\mathcal{G}_{22} + \alpha P_1 P_1 + \chi^{-1} X_2 D D^T X_2 < 0. \tag{3.57}$$

Substituting the value of $\mathcal{G}_{22}$ from (3.42) and the value of $\mathcal{M}_{22}$ from (3.32), (3.57) becomes

$$\begin{aligned} A_o^T X_2 + X_2 A_o + C^T Y_2^T + Y_2 C + \\ C^T C + \alpha P_1 P_1 + \chi^{-1} X_2 D D^T X_2 + \lambda_2 I < 0. \end{aligned} \tag{3.58}$$

Using lemma 4 in [14], if the following LMI holds

$$\begin{bmatrix} -P_1^{-1} & I \\ I & -(2\beta - \alpha) I \end{bmatrix} < 0 \tag{3.59}$$

for some positive scaler β, then $\alpha P_1 P_1 < \beta P_1$. Therefore (3.58) holds if the following holds

$$\begin{aligned} A_o^T X_2 + X_2 A_o + C^T Y_2^T + Y_2 C + \\ C^T C + \beta^2 P_1 + \chi^{-1} X_2 D D^T X_2 + \lambda_2 I < 0. \end{aligned} \tag{3.60}$$

By letting $Z = X_2 A_o$, and using Schur's complement lemma (3.60) can be written as the following matrix inequality

$$\begin{bmatrix} \Phi_2 & \beta I & X_2 D \\ \beta I & -P_1^{-1} & \mathbf{0} \\ D^T X_2 & \mathbf{0} & -(\eta_1 - \lambda_3 - \delta) I \end{bmatrix} < 0, \tag{3.61}$$

where $\Phi_2 = Z^T + Z + C^T Y_2^T + Y_2 C + C^T C + \lambda_2 I$. Using $X_1 = P_1^{-1}$, (3.61) can be written as the LMI

$$\begin{bmatrix} \Phi_2 & \beta I & X_2 D \\ * & -X_1 & \mathbf{0} \\ * & * & -(\eta_1 - \lambda_3 - \delta) I \end{bmatrix} < 0 \tag{3.62}$$

which proves (3.17) in Theorem 3.1. By replacing P_1^{-1} in (3.59) with X_1 we get (3.15) in Theorem 3.1. Now from (3.40), since $A(\theta) = \sum_{i=1}^{\mu} \zeta_i A_i$, we can write

$$\begin{bmatrix} -\lambda_1 I & (\sum_{i=1}^{\mu} \zeta_i A_i - A_o)^T X_2 & \mathbf{0} \\ X_2(\sum_{i=1}^{\mu} \zeta_i A_i - A_o) & -\lambda_2 I & \mathbf{0} \\ \mathbf{0} & \mathbf{0} & -\lambda_3 I \end{bmatrix} < 0. \tag{3.63}$$

Since $\sum_{i=1}^{\mu} \zeta_i = 1$, we can write (3.63) as

$$\sum_{i=1}^{\mu} \zeta_i \begin{bmatrix} -\lambda_1 I & (A_i - A_o)^T X_2 & \mathbf{0} \\ X_2(A_i - A_o) & -\lambda_2 I & \mathbf{0} \\ \mathbf{0} & \mathbf{0} & -\lambda_3 I \end{bmatrix} < 0. \tag{3.64}$$

By substituting $Z = X_2 A_o$, and writing the sufficient condition for (3.64), we obtain the following LMI

$$\begin{bmatrix} -\lambda_1 I & A_i^T X_2 - Z^T & \mathbf{0} \\ X_2 A_i - Z & -\lambda_2 I & \mathbf{0} \\ \mathbf{0} & \mathbf{0} & -\lambda_3 I \end{bmatrix} < 0 \qquad \forall i = 1, 2, \cdots, \mu, \tag{3.65}$$

which proves (3.18) in Theorem 3.1. Now, for the system (3.26), if there exists a symmetric positive definite matrix P of appropriate dimensions such that

$$Tr(D_e^T P D_e) < \gamma_2^2, \tag{3.66}$$

$$A_{e,i}^T P + P A_{e,i} + C_e^T C_e < 0, \qquad \forall\, i = 1, 2, \ldots, \mu, \tag{3.67}$$

then the $\mathcal{H}_2$-norm of the transfer matrix $T_i(s) = C_e(sI - A_{e,i})^{-1} D_e$ is less than γ_2 for all $i = 1, 2, \ldots, \mu$ [144]. Choosing the Lyapunov variable P as in (3.30) and substituting (3.27) in (3.67), we get

$$\begin{bmatrix} \mathcal{M}_{11} & \mathcal{M}_{12} \\ \mathcal{M}_{12}^T & \mathcal{M}_{22} \end{bmatrix} + \begin{bmatrix} \mathbf{0} & \mathbf{0} \\ \mathbf{0} & C^T C \end{bmatrix} < 0, \tag{3.68}$$

where $\mathcal{M}_{ii}$ are defined in (3.32). Inequality (3.68) can be rewritten as

$$\begin{bmatrix} \mathcal{M}_{11} + \lambda_1 I & -P_1 B Y_1 P_1 \\ -P_1 Y_1^T B^T P_1 & \mathcal{M}_{22} + C^T C + \lambda_2 I \end{bmatrix} + \begin{bmatrix} -\lambda_1 I & (A(\theta) - A_o) P_2^{-1} \\ P_2^{-1}(A(\theta) - A_o) & -\lambda_2 I \end{bmatrix} < 0. \tag{3.69}$$

Clearly, (3.69) is satisfied if the following two matrix inequalities are satisfied;

$$\begin{bmatrix} \mathcal{M}_{11} + \lambda_1 I & -P_1 B Y_1 P_1 \\ -P_1 Y_1^T B^T P_1 & \mathcal{M}_{22} + C^T C + \lambda_2 I \end{bmatrix} < 0, \tag{3.70}$$

$$\begin{bmatrix} -\lambda_1 I & (A(\theta) - A_o) P_2^{-1} \\ P_2^{-1}(A(\theta) - A_o) & -\lambda_2 I \end{bmatrix} < 0. \tag{3.71}$$

The development herein is almost identical to the development from (3.39) onward. Now, multiplying (3.70) on both sides by the matrix $\begin{bmatrix} P_1^{-1} & \mathbf{0} \\ \mathbf{0} & I \end{bmatrix}$ we get

$$\begin{bmatrix} P_1^{-1}\mathcal{M}_{11}P_1^{-1} + \lambda_1 P_1^{-1}P_1^{-1} & -BY_1P_1 \\ -P_1Y_1^TB^T & \mathcal{M}_{22} + C^TC + \lambda_2 I \end{bmatrix} < 0. \tag{3.72}$$

Let

$$\begin{aligned} \mathcal{E}_{11} &= P_1^{-1}\mathcal{M}_{11}P_1^{-1} + \lambda_1 P_1^{-1}P_1^{-1}, \\ \mathcal{E}_{22} &= \mathcal{M}_{22} + C^TC + \lambda_2 I. \end{aligned} \tag{3.73}$$

Inequality (3.72)can be rewritten as

$$\begin{bmatrix} I & \mathbf{0} & \mathbf{0} \\ \mathbf{0} & P_1 & I \end{bmatrix} \begin{bmatrix} \mathcal{E}_{11} & -BY_1 & \mathbf{0} \\ -Y_1^TB^T & -\alpha I & \mathbf{0} \\ \mathbf{0} & \mathbf{0} & \mathcal{E}_{22} + \alpha P_1P_1 \end{bmatrix} \begin{bmatrix} I & \mathbf{0} \\ \mathbf{0} & P_1 \\ \mathbf{0} & I \end{bmatrix} < 0 \tag{3.74}$$

for any positive scaler α. Therefore a sufficient condition for (3.74) to hold is

$$\begin{bmatrix} \mathcal{E}_{11} & -BY_1 & \mathbf{0} \\ -Y_1^TB^T & -\alpha I & \mathbf{0} \\ \mathbf{0} & \mathbf{0} & \mathcal{E}_{22} + \alpha P_1P_1 \end{bmatrix} < 0. \tag{3.75}$$

Due to its decoupled structure (3.75) can be written as the following individual matrix

inequalities:

$$\begin{bmatrix} \mathcal{E}_{11} & -BY_1 \\ -Y_1^T B^T & -\alpha I \end{bmatrix} < 0, \tag{3.76}$$

$$\mathcal{E}_{22} + \alpha P_1 P_1 < 0. \tag{3.77}$$

Expanding (3.76) by Schur's complement, we get

$$\mathcal{E}_{11} + \alpha^{-1} BY_1 Y_1^T B^T < 0. \tag{3.78}$$

Recalling $X_1 = P_1^{-1}$, and substituting the value of $\mathcal{E}_{11}$ from (3.73) and the value of $\mathcal{M}_{11}$ from (3.32) into (3.78), the matrix inequality (3.78) becomes

$$\begin{aligned} X_1 A(\theta)^T + A(\theta) X_1 + Y_1^T B^T + BY_1 \\ + \lambda_1 X_1 X_1 + \alpha^{-1} BY_1 Y_1^T B^T < 0. \end{aligned} \tag{3.79}$$

From hereon forward, following the same developmental steps as before, a sufficient condition for (3.79) to hold can be derived as

$$\begin{aligned} X_1 A_i + A_i X_1 + Y_1^T B^T + BY_1 \\ + \lambda_1 X_1 X_1 + \delta^{-1} DD^T + \alpha^{-1} BY_1 Y_1^T B^T < 0, \end{aligned} \tag{3.80}$$

for all $i = 1, 2, \cdots, \mu$. Inequality (3.80) is equivalent by Schur's complement to

$$\begin{bmatrix} \Phi_{1i} & X_1 & -BY_1 \\ * & -\lambda_1^{-1} I & \mathbf{0} \\ * & * & -\alpha I \end{bmatrix} < 0, \qquad \forall\, i = 1, 2, \cdots, \mu \tag{3.81}$$

with $\Phi_{1i} = X_1 A_i^T + A_i X_1 + Y_1^T B^T + BY_1$. If λ_1 is chosen such that $0 < \lambda_1 < 1$, then we always have $-\lambda_1^{-1} I \leq -(2 - \lambda_1) I$. Therefore, (3.81) is satisfied if the following linear matrix inequality holds:

$$\begin{bmatrix} \Phi_{1i} & X_1 & -BY_1 \\ * & -(2 - \lambda_1) I & \mathbf{0} \\ * & * & -\alpha I \end{bmatrix} < 0, \qquad \forall\, i = 1, 2, \cdots, \mu \tag{3.82}$$

which are guaranteed to hold if (3.54) holds, by the definition of positive/negative definiteness [149]. Now, expansion and development of (3.77) in an identical fashion to (3.57) leads us to the LMI

$$\begin{bmatrix} \Phi_2 & \beta I \\ * & -X_1 \end{bmatrix} < 0, \tag{3.83}$$

where $\Phi_2 = Z^T + Z + C^T Y_2^T + Y_2 C + C^T C + \lambda_2 I$. LMI (3.83) holds if (3.61) holds, by the definition of positive/negative definiteness. Now developing (3.71) identical to (3.40) we get

$$\begin{bmatrix} -\lambda_1 I & A_i^T X_2 - Z^T \\ X_2 A_i - Z & -\lambda_2 I \end{bmatrix} < 0, \qquad \forall i = 1, 2, \cdots, \mu \tag{3.84}$$

which is equivalent to (3.65). The developmental steps for (3.83) and (3.84) are omitted since they are identical to the ones for (3.57) and (3.40), respectively. Expanding the left hand side (3.66) and replacing γ_2^2 by η_2 yields

$$Tr(D^T P_1 D + D^T P_2^{-1} D) < \eta_2, \tag{3.85}$$

or equivalently,

$$Tr(D^T P_1 D) + Tr(D^T P_2^{-1} D) < \eta_2. \tag{3.86}$$

Introducing two new positive definite matrices $Z_1 \in \mathbb{R}^{d\times d}$ and $Z_2 \in \mathbb{R}^{d\times d}$ such that the following inequalities hold:

$$Tr(Z_1) + Tr(Z_2) < \eta_2, \tag{3.87}$$

$$Z_1 - D^T P_1 D > 0, \tag{3.88}$$

$$Z_2 - D^T P_2^{-1} D > 0, \tag{3.89}$$

the sufficient conditions for satisfying (3.86) are met. Inequality (3.87) is (3.19) in Theorem 3.1. By Schur's complement, (3.88) can be written as

$$\begin{bmatrix} Z_1 & D^T \\ D & P_1^{-1} \end{bmatrix} > 0. \tag{3.90}$$

Now, with $P_1^{-1} = X_1$ and $P_2^{-1} = X_2$ already defined, inequalities (3.90) and (3.89)

can be written as the LMIs

$$\begin{bmatrix} Z_1 & D^T \\ D & X_1 \end{bmatrix} > 0 \tag{3.91}$$

$$Z_2 - D^T X_2 D > 0 \tag{3.92}$$

which are (3.20) and (3.21) in Theorem 3.1, respectively. This completes the proof. ■

Remark 3.1. *The fact that LMI conditions of Theorem 3.1 are met ensures that the performance constraint (3.14) is met for all the constant matrices A_i in $\mathrm{Co}\ A$.*

Remark 3.2. *The transition from inequality (3.41) to sufficient conditions (3.45) and (3.46) comes at the cost of a certain conservatism. However, the degree of conservatism is relieved by introduction of positive parameters α and β. Note that no restrictive assumptions are made on the choice of these parameters, allowing for more degree of freedom to impose other optimality constraints [14]. These parameters also facilitate the decomposition of observer-controller problem into two decoupled matrix inequalities; one related to the existence of a controller and the other related to the existence of the observer.*

3.3 Application of Results

The results of Theorem 3.1 are applied to practical systems to demonstrate their effectiveness. The results are shown for robust speed control of the BLDC motor drive and robust stabilization of STATCOM based power system. The results are novel among

their kind and a similar formulation for comparing their performance could not be found in the literature.

3.3.1 Speed Control of the BLDC Motor Drive

The dynamic model of the BLDC motor drive is given in subsection 2.3.1 in (2.57) and was reformulated as (2.64) to apply the results of Theorem 2.1. The form of (2.64) is also suitable for the application of Theorem 3.1 results. This form will be used in this chapter.

Numerical Solution

Using the YALMIP toolbox [146] of MATLAB® [147], the convex optimization problem in Theorem 3.1 is solved for the system (2.64) with the uncertainty limits of (2.65). The following numerical solution is obtained for the mixed $\mathcal{H}_2/\mathcal{H}_\infty$ controller:

$$X_1 = \begin{bmatrix} 0.40615 & -0.37615 & -0.079495 & -0.47471 \\ -0.37615 & 210.35 & -17.466 & 0.90451 \\ -0.079495 & -17.466 & 10.414 & -0.12435 \\ -0.47471 & 0.90451 & -0.12435 & 1.2293 \end{bmatrix} \tag{3.93}$$

$$X_2 = \begin{bmatrix} 3024.5 & -0.00026816 & -0.0010513 & 0.048642 \\ -0.00026816 & 9.0325\times10^{-6} & -0.00013755 & -4.1942\times10^{-6} \\ -0.0010513 & -0.00013755 & 0.0020949 & -1.6157\times10^{-5} \\ 0.048642 & -4.1942\times10^{-6} & -1.6157\times10^{-5} & 2054.8 \end{bmatrix} \tag{3.94}$$

$$Y_1 = \begin{bmatrix} -0.604 & -0.015741 & -0.061746 & -2.2226 \end{bmatrix}, \tag{3.95}$$

$$Y_2 = \begin{bmatrix} -1619.2 \\ -3024.7 \\ -0.82638 \\ -25.634 \end{bmatrix} \tag{3.96}$$

$$Z = \begin{bmatrix} -1.7505\times10^{-10} & 3024.6 & -0.11922 & -0.11357 \\ -1.0646\times10^{-12} & -0.23134 & 0.065448 & -0.0084916 \\ 1.0989\times10^{-12} & -0.19797 & -0.99675 & 0.12941 \\ 3.3375\times10^{-10} & 0.05004 & -0.0019667 & -2054.8 \end{bmatrix} \tag{3.97}$$

$$Z_1 = \begin{bmatrix} 0.0055432 \end{bmatrix}, \; Z_2 = \begin{bmatrix} 9.0332 \end{bmatrix} \times 10^{-6}, \tag{3.98}$$

$$\begin{aligned} &\alpha = 2.2226, \; \beta = 3.7743, \; \delta = 0.0005472, \; \gamma_2 = 0.074513, \; \gamma_\infty = 0.023454, \\ &\lambda_1 = 0.1821, \; \lambda_2 = 0.38368, \lambda_3 = 2.1786 \times 10^{-8}. \end{aligned} \tag{3.99}$$

Time-Domain Simulation Results

The designed observer-controller is tested for the speed control of a $1\ kW$ BLDC motor, whose parameters are given in Table A.2. The same test cases are run for time domain simulation as in subsection 2.3.1 under identical operating conditions. The performance of the controller in PIL is also validated against the simulation. The results of speed regulation and tracking test cases along with control voltage plots are shown in are shown in fig. 3.1 and fig. 3.2. The plots of comparison between the $\mathcal{L}_2$-gain and the mixed $\mathcal{H}_2/\mathcal{H}_\infty$ controllers are shown in figs. 3.3 and 3.4.

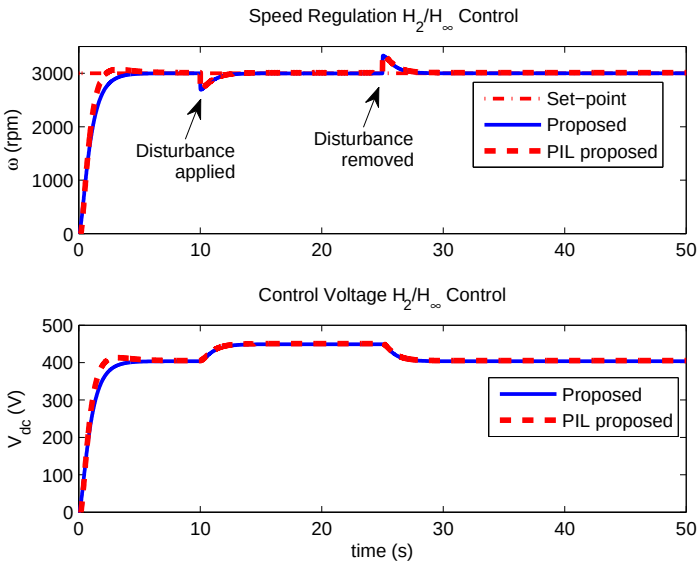

Figure 3.1: Speed regulation results for the mixed $\mathcal{H}_2/\mathcal{H}_\infty$ controller under rated load application

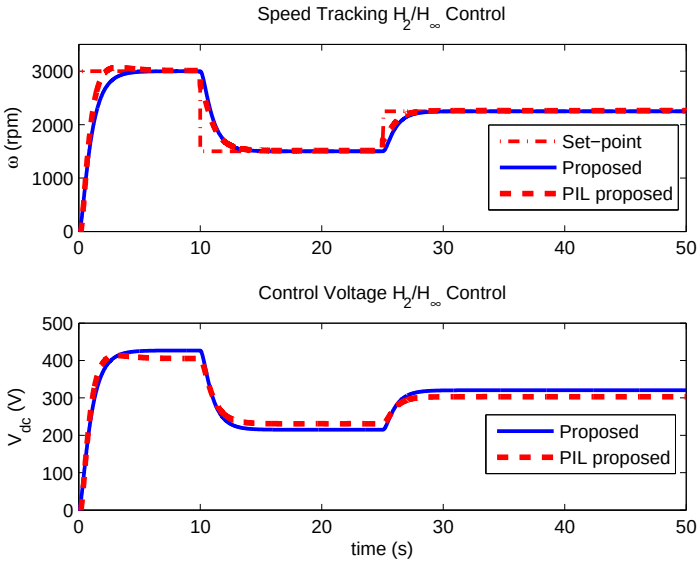

Figure 3.2: Speed tracking results for the mixed $\mathcal{H}_2/\mathcal{H}_\infty$ controller under 50% rated load application

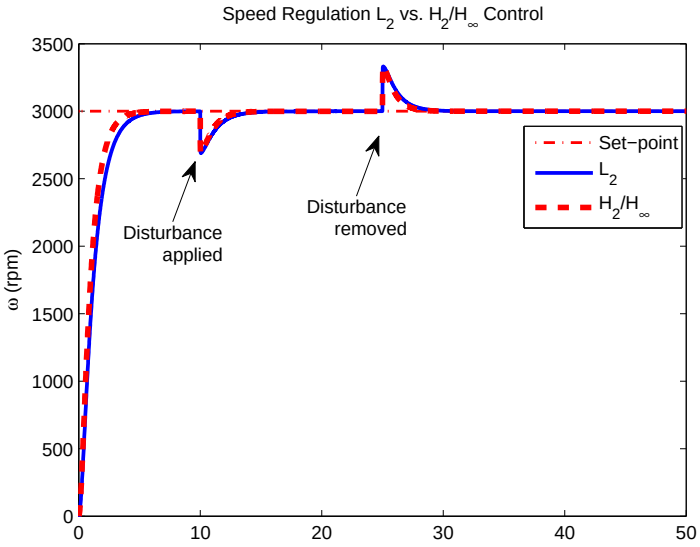

Figure 3.3: Speed regulation comparison between the $\mathcal{L}_2$-gain and the mixed $\mathcal{H}_2/\mathcal{H}_\infty$ controllers under rated load application

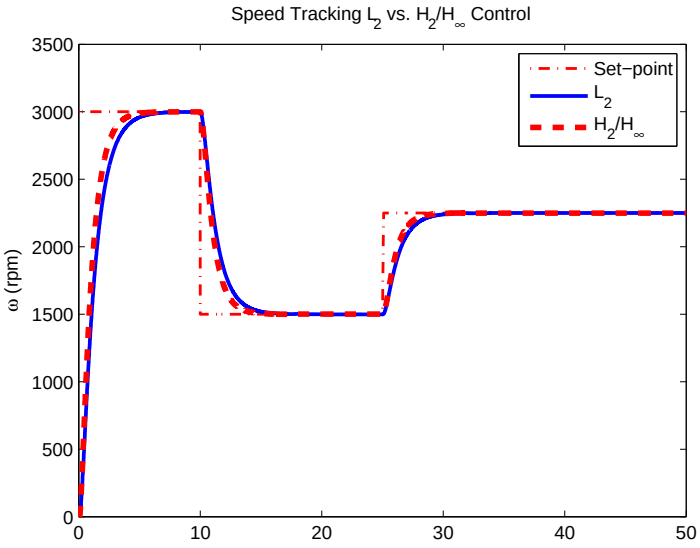

Figure 3.4: Speed tracking comparison between the $\mathcal{L}_2$-gain and the mixed $\mathcal{H}_2/\mathcal{H}_\infty$ controllers 50% rated load application

3.3.2 Power System Stabilization using STATCOM

The results of Theorem 3.1 are applied to the reformulated model (2.77) of the STATCOM based power system and the numerical and time domain simulation results are reported in this section.

Numerical Solution

At the heavy loading operating point $(P, Q) = (1.2, 0.4)\ pu$, using the YALMIP toolbox [146] of MATLAB® and the uncertainty limits (2.79) the numerical solution to the convex optimization problem of Theorem 3.1 is

$$X_1 = \begin{bmatrix} 9.9666 & -0.0796 & -0.4085 & -0.7663 & 1.0706 & 0.9213 & -1.4301 \\ -0.0796 & 0.0033 & 0.0089 & 0.0715 & -0.0061 & 0.0032 & -0.0846 \\ -0.4085 & 0.0089 & 1.6070 & -0.3656 & -0.2112 & -0.6623 & 0.1920 \\ -0.7663 & 0.0715 & -0.3656 & 450.5917 & 0.0101 & 11.5809 & 2.3537 \\ 1.0706 & -0.0061 & -0.2112 & 0.0101 & 0.8344 & 0.1054 & 0.2679 \\ 0.9213 & 0.0032 & -0.6623 & 11.5809 & 0.1054 & 2.6676 & -0.8171 \\ -1.4301 & -0.0846 & 0.1920 & 2.3537 & 0.2679 & -0.8171 & 15.9627 \end{bmatrix}, \tag{3.100}$$

$$X_2 = \begin{bmatrix} 0.3669 & -0.0000 & 0.0020 & 0.0002 & 0.0000 & -0.0001 & -0.0002 \\ -0.0000 & 0.0000 & -0.0000 & 0.0000 & -0.0000 & 0.0000 & -0.0000 \\ 0.0020 & -0.0000 & 0.0774 & 0.0016 & -0.0000 & 0.1498 & -0.0515 \\ 0.0002 & 0.0000 & 0.0016 & 0.0004 & 0.0000 & -0.0064 & -0.0004 \\ 0.0000 & -0.0000 & -0.0000 & 0.0000 & 0.0000 & 0.0000 & -0.0000 \\ -0.0001 & 0.0000 & 0.1498 & -0.0064 & 0.0000 & 8.5449 & 0.5386 \\ -0.0002 & -0.0000 & -0.0515 & -0.0004 & -0.0000 & 0.5386 & 0.3285 \end{bmatrix} \times 10^6, \tag{3.101}$$

$$Y_1 = \begin{bmatrix} -7.2194 & 0.2433 & -0.5923 & 12.8041 & -0.7268 & -173.5203 & 0.0031 \\ 62.4650 & -1.6212 & -2.7941 & 1.8026 & 8.4976 & -0.0076 & -173.4734 \end{bmatrix}, \tag{3.102}$$

$$Y_2 = \begin{bmatrix} -0.0043 & 0.0000 & 0.0000 \\ -1.3891 & -0.2827 & 0.0000 \\ -0.0008 & 0.0002 & -0.0005 \\ -0.0002 & 0.0003 & 0.0000 \\ 0.0000 & 0.0041 & -0.0036 \\ 0.0073 & -0.0001 & -0.0049 \\ 0.0007 & -0.0023 & 0.0001 \end{bmatrix} \times 10^8, \tag{3.103}$$

$$Z = \begin{bmatrix} 0.0002 & 1.3833 & -0.0009 & -0.0002 & -0.0001 & -0.0021 & -0.0001 \\ 0.0000 & -0.0000 & -0.0000 & -0.0000 & -0.0000 & -0.0001 & -0.0000 \\ 0.0015 & 0.0075 & -0.0084 & -0.0015 & -0.0013 & -0.0207 & -0.0006 \\ 0.0003 & 0.0007 & -0.0018 & -0.0004 & -0.0003 & -0.0042 & -0.0002 \\ 0.0000 & 0.0000 & -0.0000 & -0.0000 & -0.0000 & -0.0000 & -0.0000 \\ -0.0062 & -0.0004 & 0.0312 & 0.0067 & 0.0050 & -0.0093 & -0.0008 \\ -0.0003 & -0.0009 & 0.0021 & 0.0003 & 0.0003 & -0.0011 & -0.0031 \end{bmatrix} \times 10^8, \tag{3.104}$$

$$Z_1 = \begin{bmatrix} 0.002 \end{bmatrix},\ Z_2 = \begin{bmatrix} 0.0045 \end{bmatrix}, \tag{3.105}$$

$$\begin{aligned} &\alpha = 173.4754,\ \beta = 336.1731,\ \delta = 0.002,\ \gamma_2 = 0.0808,\ \gamma_\infty = 0.0653, \\ &\lambda_1 = 0.066,\ \lambda_2 = 298.8490, \lambda_3 = 1.0138 \times 10^{-5}. \end{aligned} \tag{3.106}$$

Time-Domain Simulation

Time domain simulations in MATLAB®/Simulink are run on the nonlinear power system model installed with STATCOM at two different operating points to validate the performance of the designed observer based controller. The operating points are $(P, Q) = (1.2, 0.4)$ and $(P, Q) = (0.8, 0.2)$ for heavy and nominal loading, respectively. The performance of the controller in PIL is also validated against the simulation. Numerical results for the nominal operating point are omitted for conciseness. The parameters M and C_{DC} are set to M^{min} and C_{DC}^{max}, and simulations are run for $t = 5\ s$ with a 15% step torque disturbance and a 3-phase fault at the infinite bus, applied at $t = 1\ s$ instant, lasting three cycles [122]. The results of the simulations under torque

disturbance are shown in figs. 3.5, 3.6, 3.7, 3.8 and 3.9, while under 3-phase fault are shown in fig. 3.10, 3.11, 3.12 and 3.13. The plots of comparison between the $\mathcal{L}_2$-gain and the mixed $\mathcal{H}_2/\mathcal{H}_\infty$ controllers are shown in figs. 3.14 and 3.15. The results of instability under torque fault are depicted in fig. 3.5 only for the heavy loading operating point under torque fault, for conciseness.

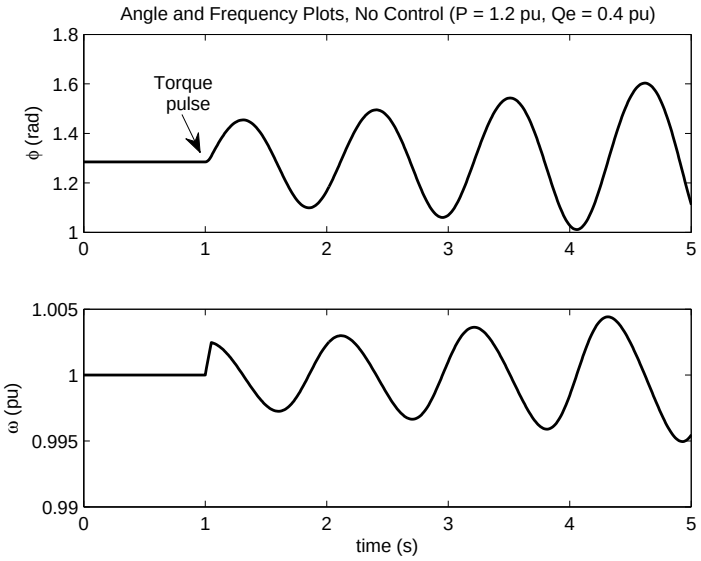

Figure 3.5: Rotor angle and angular frequency plots with no controller under heavy loading, 15% torque disturbance

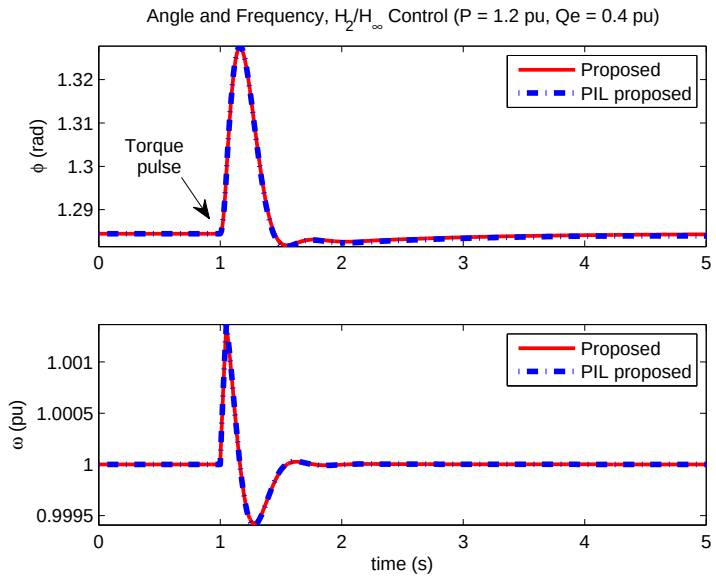

Figure 3.6: Rotor angle and angular frequency plots with the mixed $\mathcal{H}_2/\mathcal{H}_\infty$ controller under heavy loading, 15% torque disturbance

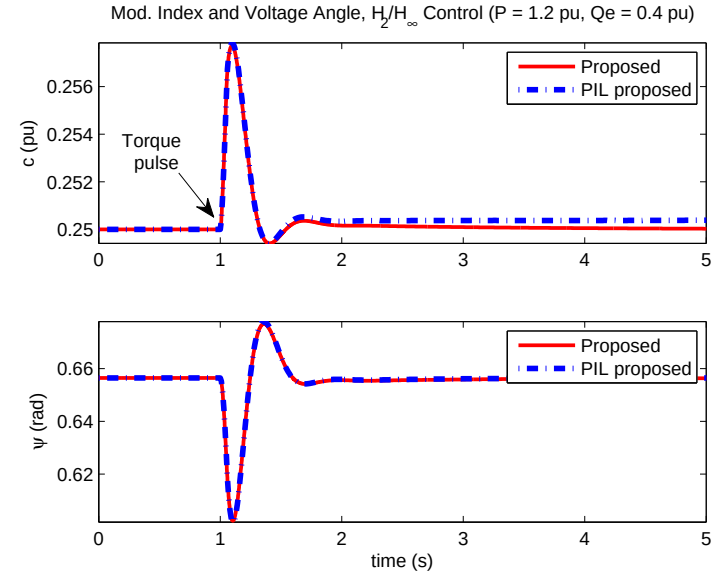

Figure 3.7: Modulation index and STATCOM output voltage angle plots with the mixed $\mathcal{H}_2/\mathcal{H}_\infty$ controller under heavy loading, 15% torque disturbance

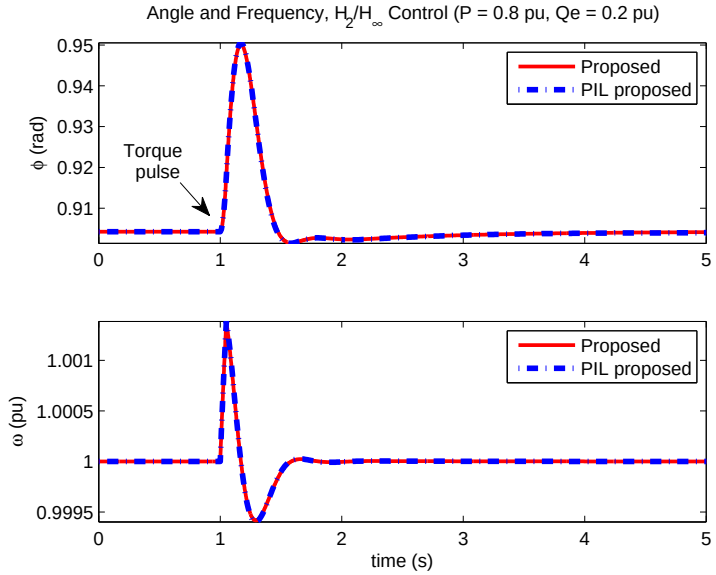

Figure 3.8: Rotor angle and angular frequency plots with the mixed $\mathcal{H}_2/\mathcal{H}_\infty$ controller under nominal loading, 15% torque disturbance for three cycles

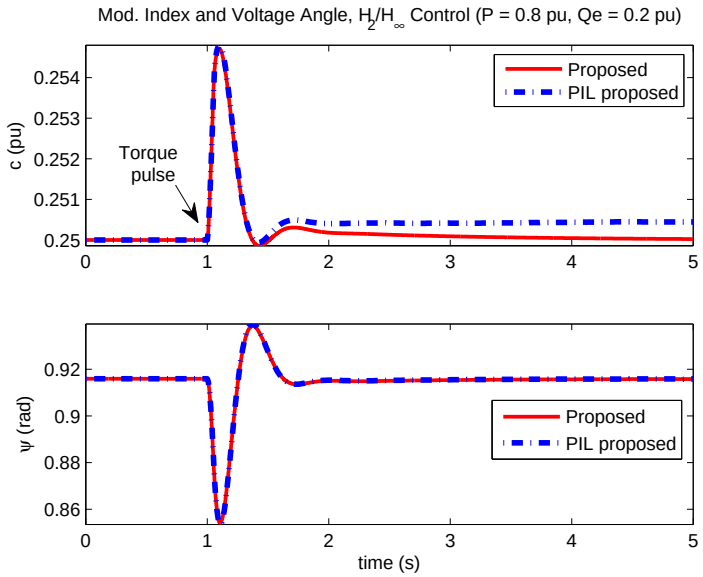

Figure 3.9: Modulation index and STATCOM output voltage angle plots under the with $\mathcal{H}_2/\mathcal{H}_\infty$ controller under nominal loading, 15% torque disturbance

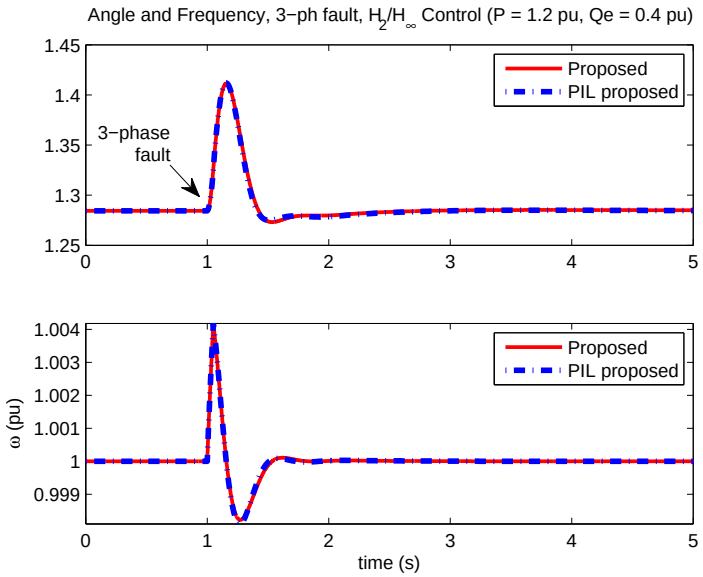

Figure 3.10: Rotor angle and angular frequency plots with the mixed $\mathcal{H}_2/\mathcal{H}_\infty$ controller under heavy loading, 3-phase fault for three cycles

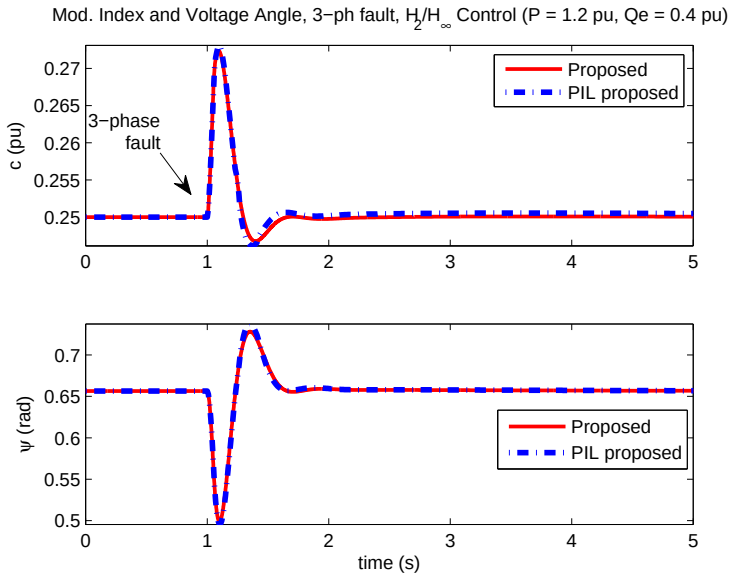

Figure 3.11: Modulation index and STATCOM output voltage angle plots with the mixed $\mathcal{H}_2/\mathcal{H}_\infty$ controller under heavy loading, 3-phase fault for three cycles

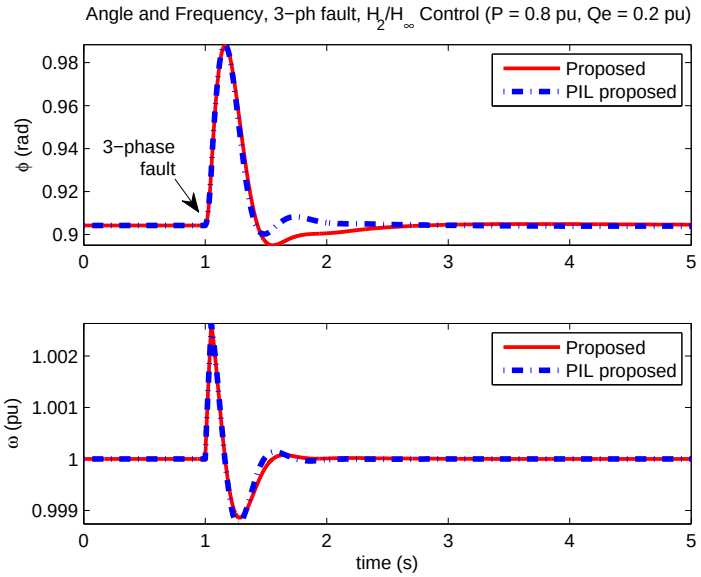

Figure 3.12: Rotor angle and angular frequency plots with the mixed $\mathcal{H}_2/\mathcal{H}_\infty$ controller under nominal loading, 3-phase fault for three cycles

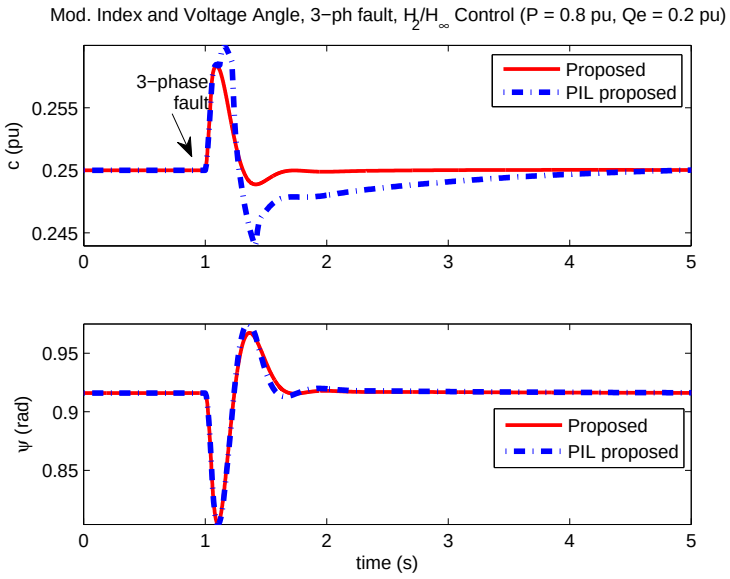

Figure 3.13: Modulation index and STATCOM output voltage angle plots with the mixed $\mathcal{H}_2/\mathcal{H}_\infty$ controller under nominal loading, 3-phase fault for three cycles

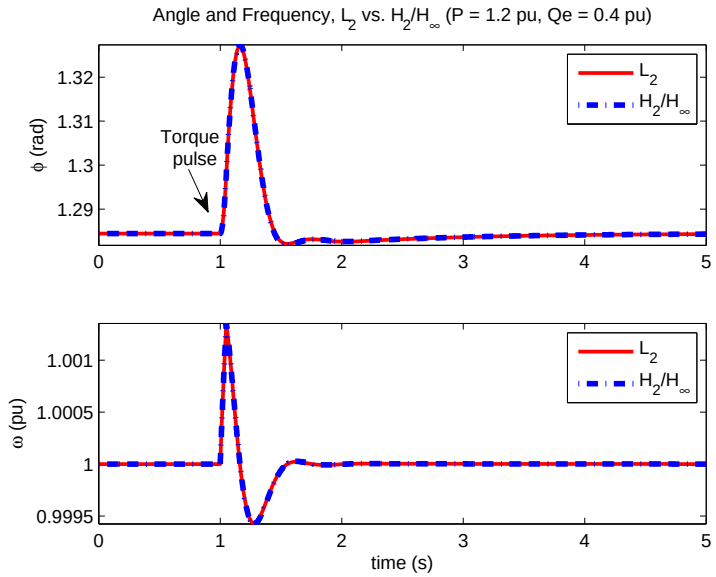

Figure 3.14: Comparison between the $\mathcal{L}_2$-gain and the mixed $\mathcal{H}_2/\mathcal{H}_\infty$ controllers under heavy loading, 15% torque disturbance for three cycles

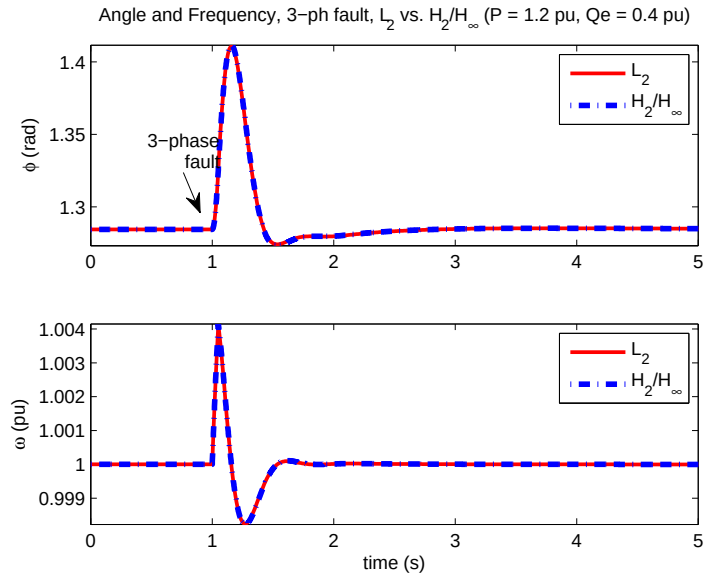

Figure 3.15: Comparison between the $\mathcal{L}_2$-gain and the mixed $\mathcal{H}_2/\mathcal{H}_\infty$ controllers under heavy loading, 3-phase fault for three cycles

3.4 Discussion

The results in fig. 3.1 and fig. 3.2 show that with the proposed robust $\mathcal{H}_2/\mathcal{H}_\infty$ controller, the actual speed of the BLDC motor successfully tracks the set-point speed in the presence of uncertainties and unknown load torque disturbance with no steady state error under different operating conditions.

The plots in fig. 3.6 to fig. 3.9 indicate that the robust controller successfully damps out the low frequency oscillations in the rotor angle and frequency and readily stabilizes the system's operating point, under a mechanical step disturbance and a 3-phase fault in the presence of uncertainties in the model parameters under different operating conditions.

The close agreement between the responses of the $\mathcal{H}_\infty$ and the mixed $\mathcal{H}_2/\mathcal{H}_\infty$ controllers in figs. 3.3, 3.4, 3.14 and 3.15 is primarily due to the disturbance type. As previously mentioned in Chapter 1, the $\mathcal{H}_2$ performance is useful when the input is of white noise type. For both our applications, the disturbances are not of the white noise type. Their effects are successfully mitigated by the $\mathcal{L}_2/\mathcal{H}_\infty$ performance and its behavior dominates the system responses. The effect of the $\mathcal{H}_2$ performance will be more pronounced once the disturbance has white noise components, for which the $\mathcal{L}_2/\mathcal{H}_\infty$ performance is known to have limits [80].

For both applications, the controller resolves the robustness issue by fast tracking of the set-point speed and stabilization of the equilibrium point under adverse conditions. The response of the closed loop system under the proposed observer-based controller can be further improved by imposing pole-placement constraints in LMI regions.

Results of the test cases run in PIL configuration, depicted in figs. 3.1 and 3.2 for

the BLDC motor and in figs. 3.6, 3.8, 3.8, 3.9, 3.10, 3.11, 3.12 and 3.13 for the STATCOM based power system, show close agreement with the simulated results. This indicates that the controller functions as expected in digital implementation. The difference between the steady state values in simulation and PIL modes is less than 0.2%. The differences in the responses are mainly due to controller discretization introducing some inaccuracies, a limited sampling rate in the controller's digital implementation, fixed-point data type conversion inaccuracies and choice of the numerical integration method.

CHAPTER 4

A NOVEL AND SIMPLE HYBRID FUZZY/PI CONTROLLER: DESIGN AND APPLICATION

A novel controller is designed using a combination of fuzzy logic and PI control. A very simple fuzzy logic control structure is employed using only three rules; based on the input being either in the positive, negative or zero regions. A unique supervisory scheme based on the variance of the input is implemented to appropriately select the controller best suited to the operating conditions. The design procedure for the controller and the supervisory switching scheme are detailed. The generality of the controller is demonstrated through its application to robust speed control of BLDC motor drive and robust stabilization of STATCOM installed power system.

4.1 Proposed Fuzzy/PI Controller Design

4.1.1 Fuzzy Logic Design Steps

The general design process of a fuzzy logic controller can be summarized in the following steps [53, 150]:

1. *Define inputs, outputs and the universe of discourse*

   As a first step in the design process, the inputs, outputs and the universe of discourse are defined. A range of all the possible values taken by the input (output) is called the universe of discourse of the input (output).

2. *Fuzzification*

   Fuzzification is the process of converting crisp inputs into fuzzy inputs. A set of membership functions are chosen that quantify the degree to which each of the crisp inputs belong to a given fuzzy set. The degree of membership is then mapped on to the unit interval [0,1].

3. *Fuzzy Rules Definition*

   The fuzzified information is then linguistically represented in terms of a list of '*if-then* 'statements, defining the input-output relationship. This representation is also called *if–then rule–based form* or the *deductive form*. These rules form the core of the fuzzy inference process.

4. *Defuzzification*

   The process of converting the fuzzy output of the inference process to a crisp

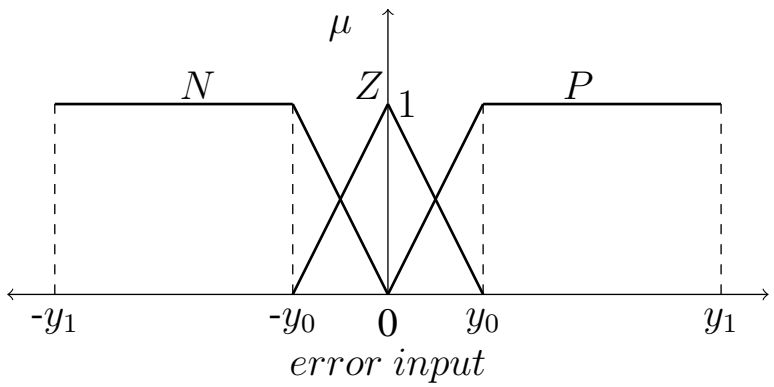

Figure 4.1: Error input membership functions (not to scale)

output is called defuzzification. The defuzzification method can be chosen from a wide variety of methods reported in the literature namely the max membership principle, centroid method, weighted average and mean max principle.

4.1.2 Fuzzy logic design guidelines

For the fuzzy logic controller, the Mamdani system structure is chosen, that is most common in practice [150]. According to the aforementioned design process in subsection 4.1.1, the first step is to specify the inputs, outputs and their universe of discourse. The input to the controller is selected to be the error between the actual signal and its reference, termed as regulation or tracking error. The output is chosen as the control signal to be applied to the plant.

For the fuzzification process, membership functions are assigned to the input and output. Each of the input and output are characterized by three membership functions namely *negative (N)* , *zero (Z)* and *positive (P)*. Triangular and trapezoidal membership functions are assigned to both the input and the output, as shown in fig. 4.1 and fig. 4.2.

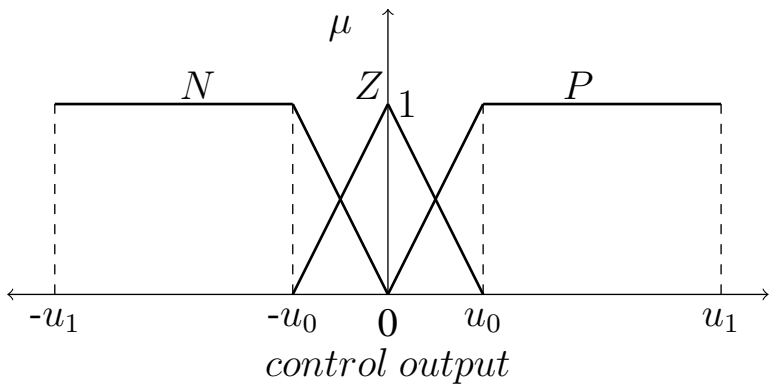

Figure 4.2: Control output membership functions (not to scale)

The limits y_i and u_i of the input and output membership functions are chosen based on the application and knowledge of the designer. Next the input-output relationship is established through fuzzy rules. The key guidelines that are followed in controller design are as follows:

1. *If the error input is positive, then control output value is positive*

2. *If the error input is negative, then control output value is negative*

3. *If the error input is zero, the control output value is zero*

This rule-base outputs a control signal proportional to the error input. The physical limits on the terms *'positive'*, *'negative'* and *'zero'* are subjective choices and depend upon the designer's expertise and knowledge of the target application.

Finally, the defuzzification process can be chosen from a variety methods mentioned in subsection 4.1.1 that best suits the application. For the proposed design, the centroid method is selected. The simplified block diagram of the fuzzy logic controller is shown in fig. 4.3.

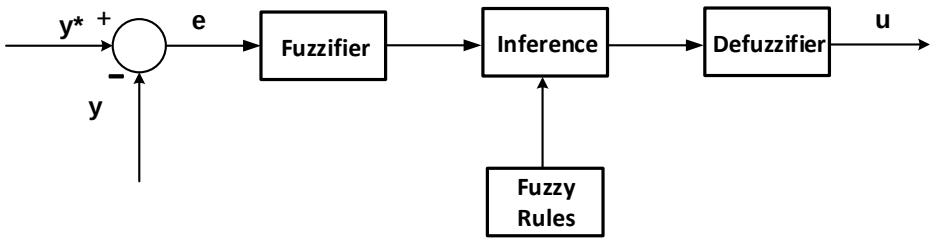

Figure 4.3: Fuzzy controller block diagram; y^* : reference input, y : actual input, e : error, u : controller output

Remark 4.1. *The membership functions of fig. 4.1, fig. 4.2 and the rule-base in subsection 4.1.2 lead to a proportional controller with saturation. The proportional gain can be adjusted by tuning the slopes of the input and output membership functions. Using steep slopes will result in an 'aggressive' controller, while decreasing the slopes will yield a 'milder' controller behavior. Due to proportional action alone and lack of an integral action, elimination of steady state error under this type of control alone can not be guaranteed.*

4.1.3 Hybrid control and supervisory switching scheme

In general, a fuzzy logic controller can give an oscillation-free transient response, but the response may be slow and have a finite steady state error. A conventional PI controller performs well in providing offset free tracking. However, a controller tuned for certain operating conditions may exhibit unsatisfactory performance when those conditions vary. In some cases, a PI controller can also yield oscillatory response [49]. In the proposed hybrid control scheme the fuzzy logic and PI controllers are combined to fully utilize their merits and overcome their limitations. The scheme uses fuzzy logic

controller in the transient state and PI controller in the steady state. Consequently, the transient and steady states must be characterized and a mechanism is required to identify them.

A novel idea using the variance of the error input is employed to identify the transient and steady states of the system. The transient state is defined as the stage when the error input is increasing or decreasing. The steady state is defined as the condition when the error is constant. Accordingly, in the transient state, variance of the error will be nonzero, while in the steady state under constant error, it will ideally be zero. Using this fact, the current state of the system can be identified from the error input's variance. The controller to use can be selected by a supervisory mechanism. The switching rule is described as:

$$Control = \begin{cases} Fuzzy, & e_v > threshold\ (transient\ state) \\ PI, & e_v <= threshold\ (steady\ state) \end{cases} \tag{4.1}$$

where e_v stands for the error variance. The threshold value for error variance can be identified by running the closed loop system under the fuzzy logic controller alone. When the closed loop system is run, under the proportional action of the fuzzy controller the error will decay and eventually reach its steady state value. At this point, a threshold value can be chosen slightly above the peak value of error variance. The gains for the PI controller can be selected by trial and error or systematic tuning. The simplified block diagram of a generalized closed loop system under the hybrid controller is shown in fig. 4.4.

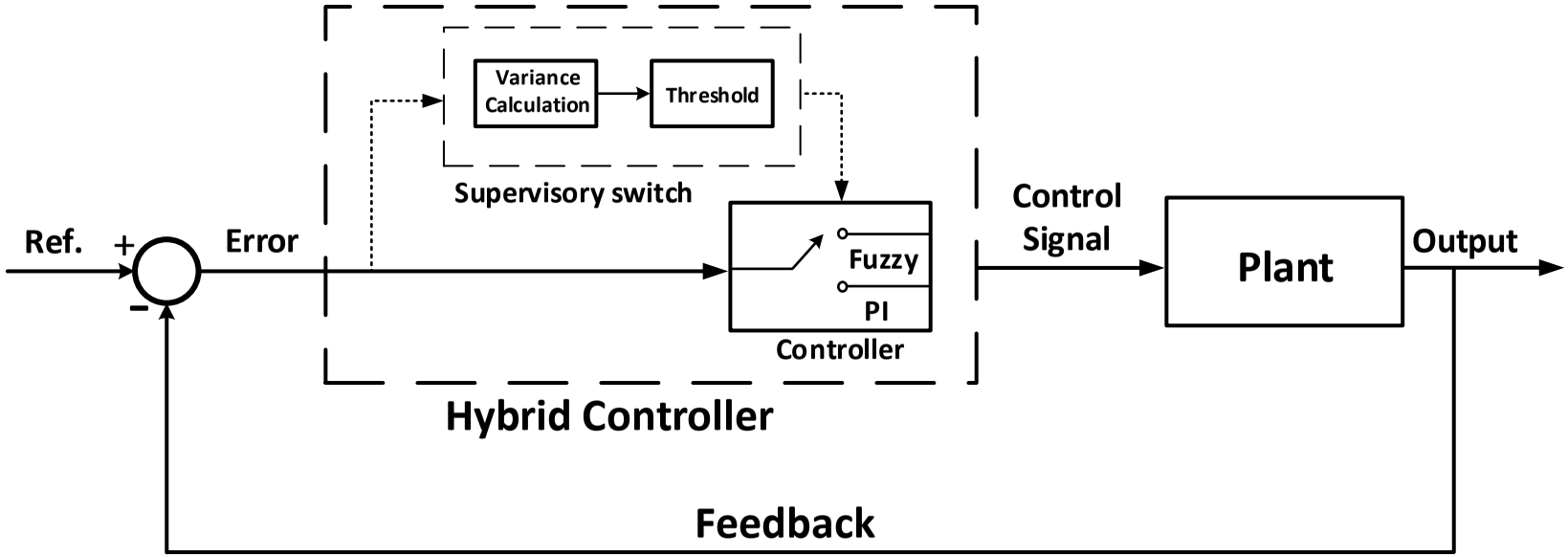

Figure 4.4: Simplified block diagram of the generalized closed loop system with the hybrid controller

4.2 Controller Applications

4.2.1 Speed Control of BLDC Motor Drive

The hybrid fuzzy/PI controller is designed using the guidelines in Section 4.1 for speed control of BLDC motor drive. The controller is designed for two different wye-connected 3-phase motors labeled M1 (rated $1\ kW$, $3000\ rpm$, $3\ N.m$), and M2 (rated $0.75\ kW$, $3000\ rpm$, $1.91\ N.m$). The motor model, drive schematic and commutation logic table are given in Appendix A section A.1. The parameters of motors M1 and M2 are given in Table A.6 in Appendix A. The design details for motor M1 are discussed.

Controller Design

As the first step, input to the fuzzy logic controller is chosen as the speed error e_ω defined as $\omega_r - \omega$, with ω_r and ω denoting speed set-point and actual speed, respectively. The output is taken as the current command I^* to be applied to the PWM controller. Based on ratings of the motor M1, the universe of discourse of input is chosen to be between $-3200\ rpm$ to $3200\ rpm$ while for the output it is chosen as $-11\ A$ to $11\ A$. These values do not represent the actual limits on the error input or the current output, but are chosen so that the defuzzification process yields a desired value for a particular input range. More explanation on this appears later in this section.

Next, membership functions are defined for the process of fuzzification. Three linguistic terms are defined for the fuzzy variable e_ω namely *Negative (N)*, *Zero (Z)* and *Positive (P)*. The linguistic terms for output are defined the same way. Triangular and trapezoidal membership functions are chosen for both e_ω and I^*, depicted in fig. 4.5

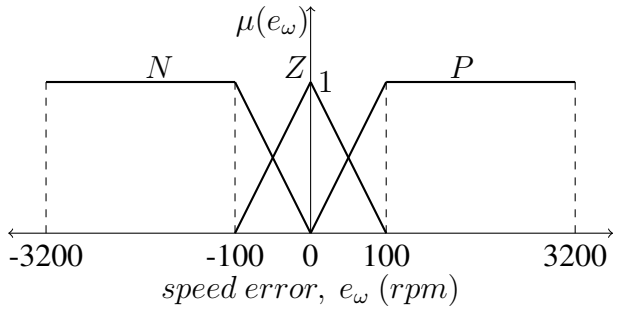

Figure 4.5: Input e_ω membership functions, motor M1 (not to scale)

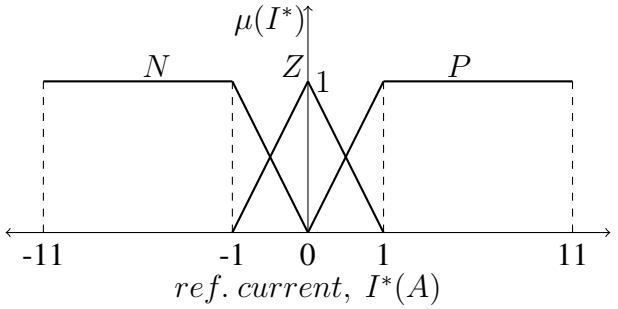

Figure 4.6: Output I^* membership functions motor M1 (not to scale)

and 4.6, where $\mu(e_\omega)$ and $\mu(I^*)$ represent the degree of membership of the speed error e_ω and reference current I^* in their corresponding fuzzy sets.

In the next step, decision making rules in the form of '*if-then* 'statements are defined to specify the control action. A total of three rules are defined as follows:

1. If e_ω is negative then I^* is negative

2. If e_ω is zero then I^* is zero

3. If e_ω is positive then I^* is positive

Similar design rules are followed in the design of fuzzy controller for motor M2. The membership function ranges are adjusted according to M2 ratings. They are depicted in figures 4.7 and 4.8.

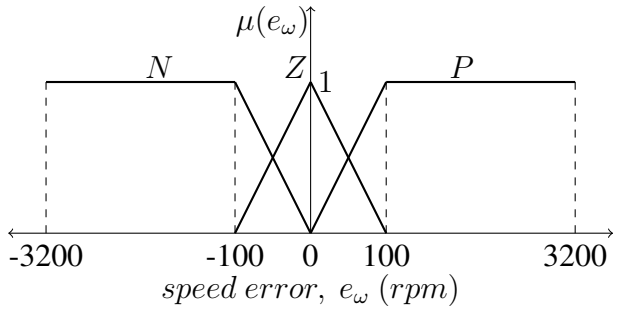

Figure 4.7: Input e_ω membership functions, motor M2 (not to scale)

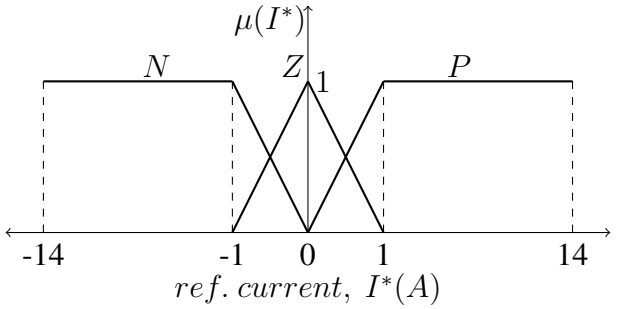

Figure 4.8: Output I^* membership functions motor M2 (not to scale)

With the chosen membership functions and rules, the following input-output relationship is obtained using the centroid method:

$$\begin{aligned} I^* &\cong 2I_r, && if\ \ e_\omega \geq 100\ rpm \\ I^* &\cong -2I_r, && if\ \ e_\omega \leq -100\ rpm \\ -2I_r &\leq I^* \leq 2I_r, && if\ \ 0 \leq |e_\omega| \leq 100\ rpm \end{aligned} \tag{4.2}$$

Here I_r stands for the motor's continuous rated current. Although the motor under consideration could withstand up to $4I_r$ for a short time, here the maximum current output of the controller is limited for safety. The rated value of current required by M1 under full load to maintain rated speed is $3.3\ A$ while for M2 it is $4.4\ A$.

The fuzzy output of the membership functions for each input must be combined

corresponding to the rules. With the chosen rule-base, each input's degree of membership corresponding to a fuzzy number, is directly mapped on to the output fuzzy set called the consequent, through the process of implication. Finally, the resultant fuzzy set is defuzzified. The truncation and centroid methods are used for implication and defuzzification, respectively [89].

From (4.2), it can be seen that the control law leads to an equivalent of a proportional type controller with saturation. Within the saturation limits, the fuzzy logic controller would behave like an 'aggressive' proportional controller. Therefore, a finite steady state error is to be expected under this type of control, an inherent feature of proportional type controllers. Increasing the slopes of membership functions as shown in fig. 4.9 for M1, is equivalent to increasing the proportional gain. This would increase the rate of transient response and reduce steady state error. However, it would also increase the amount of steady state torque and speed ripples. On the other hand, decreasing the slopes of membership functions as shown in fig. 4.10 would cause lesser steady state torque and speed ripple, but slow down the response and increase steady state error.

For instance, for M1 to maintain rated speed at rated load, using the membership functions of Fig. 4.9 would give the required current of $3.3\ A$ at a speed error of $e_\omega = 5\ rpm$, if the same output membership functions of fig. 4.6 are used. If those in fig. 4.10 are used, the required current would be output at $e_\omega = 15\ rpm$. Hence, the average steady state errors under rated conditions using membership functions of Fig. 4.9 and 4.10 would be close to $5\ rpm$ and $15\ rpm$, respectively. Their respective 'aggressive' and 'gentle' slopes would lead to a higher and lower amount of steady state

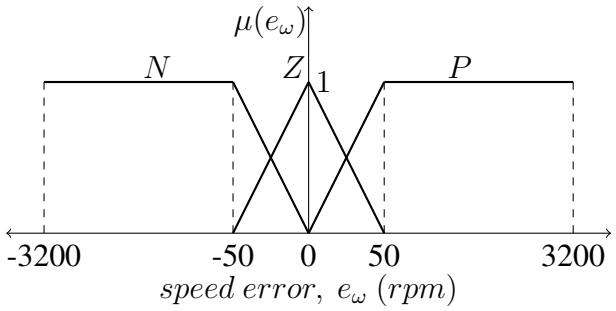

Figure 4.9: Modified Input e_ω membership functions, motor M1 (not to scale) with increased slopes

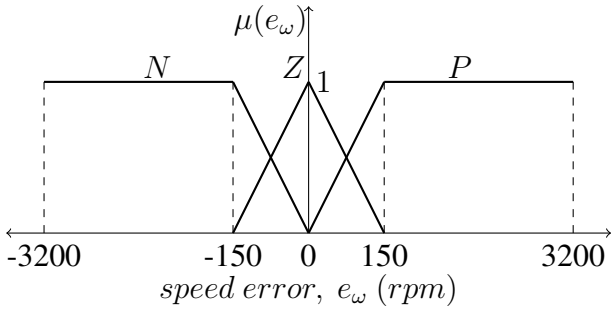

Figure 4.10: Modified Input e_ω membership functions, motor M1 (not to scale) with reduced slopes

torque and speed ripples in the response.

The input-output calculation process of the fuzzy logic controller under no-load and load conditions is depicted in fig. 4.11. The third fuzzy input set *Negative (N)* is not shown since its membership value is zero and does not contribute to the output.

This fuzzy control scheme alone can be employed in applications where lower computational complexity is required and small steady state error is acceptable. For the hybrid controller, the PI controller's gains are tuned by systematic Zieglar-Nichols and trial and error methods. The trial and the error method yields better results for this particular application, and is hence chosen for the design. The variance threshold is identified by running the closed loop simulation under fuzzy controller alone. The

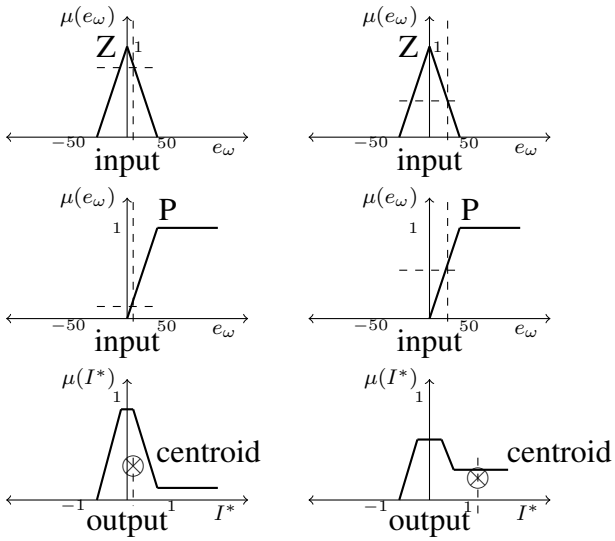

(a) No Load (b) Full Load

Figure 4.11: Input fuzzy sets (top and middle rows), output fuzzy sets (bottom row) and centroid locations under no–load and full load at rated speed (not to scale)

gains and threshold values are also reported in Appendix A section A.4. The block diagram of drive system under the composite control scheme is shown in Fig. 4.12. The simulation results of drive performance under the fuzzy logic controller alone and the proposed hybrid fuzzy/PI controller are given next.

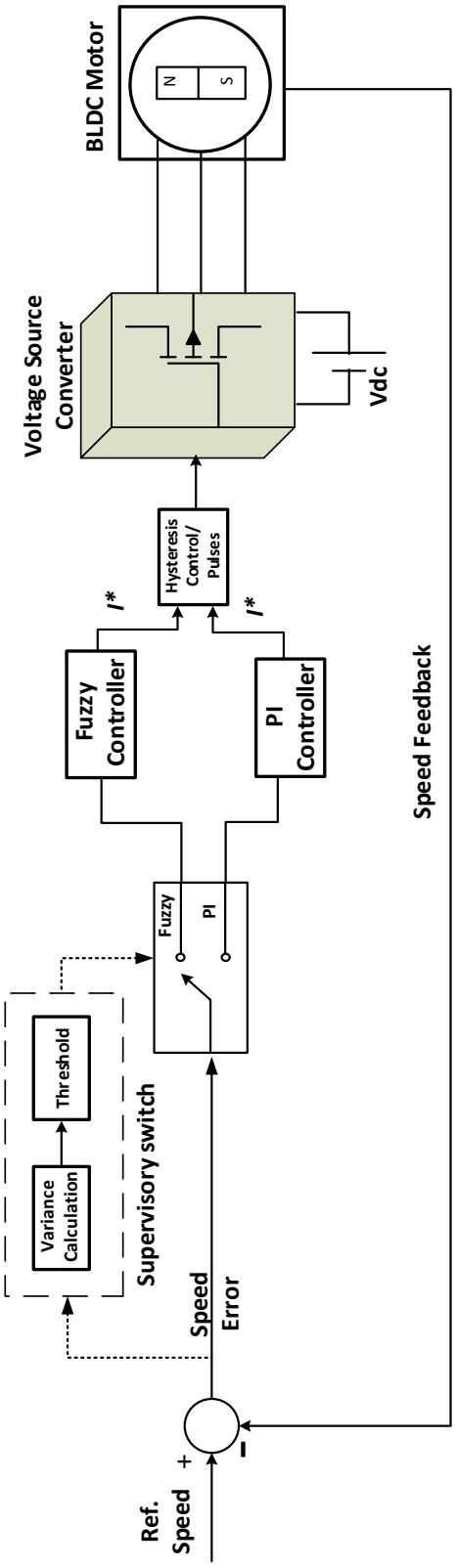

Figure 4.12: Simplified block diagram of the drive system under proposed control

Simulation Results

Simulation studies are carried out using MATLAB®/Simulink's SimPowerSystems toolbox and Fuzzy Logic toolbox. The motors' resistances, inductances and friction coefficients are off from their nominal values by 30%. Speed regulation response of the fuzzy logic controller under rated load for motors M1 and M2 is shown in fig. 4.13. For comparison, the plot of speed regulation under proposed control is shown in fig. 4.14. Error plots under speed regulation and zoomed view of speed regulation responses under rated conditions are shown in fig. 4.15 and 4.16. For this test case, a set-point speed of $3000\ rpm$ is selected while rated loads of $3\ N.m$ and $1.91\ N.m$ are applied to the motors M1 and M2 respectively at $t = 0.25\ s$.

Speed tracking responses of the fuzzy and proposed controllers under fixed load are shown in fig. 4.17 and 4.18. The speed error comparison plots are shown in fig. 4.19. For this test case, speed reference is changed periodically in steps from rated to fractions of rated speed under constant loading. The speed set-point is sequentially changed as $3000\ rpm$, $500\ rpm$, $2000\ rpm$, $2500\ rpm$ and $1000\ rpm$ at regular intervals. The load for M1 and M2 is kept constant at $1.5\ N.m$ and $1\ N.m$ respectively.

Speed regulation and tracking performance for M1 under the proposed hybrid controller is compared with three other benchmark controllers namely (1) a simple PI controller, (2) PI based variable dc-link voltage controller and (3) a sliding mode (SM) variable dc-link voltage controller for motor M1. Gains for the PI based controllers are designed by trial and error to achieve the best trade-off between transient response, overshoot and oscillations. These gains are given in Table A.4 in Appendix A. The slid-

ing mode controller is designed using the model (2.57) and choosing a sliding surface $\mathcal{S}$ as:

$$\mathcal{S} = c_1 z_1 + z_2 \tag{4.3}$$

where $z_1 = \omega_r - \omega$, $z_2 = \dot{z_1}$, and c_1 is a weight chosen by design to obtain the best dynamic response (see Appendix A, Table A.5). A control law is derived satisfying the reachability $\mathcal{S}\dot{\mathcal{S}}$ and stability conditions [151]. Plots comparing the speed regulation performance are shown in fig. 4.20. Speed tracking comparison plots are shown in fig. 4.21. Rated loading is applied for regulation test case at $0.25\ s$ while constant loading of $1.5\ N.m$ is applied for the tracking case. A step changing speed set-point is applied in tracking test case and sequentially changed as $3000\ rpm$, $500\ rpm$, $2000\ rpm$, $2500\ rpm$ and $1000\ rpm$ at regular intervals. Figure 4.22 shows the phase A currents of M1 and M2 for proposed controller under speed regulation. Figure 4.23 shows the reference current outputs of the fuzzy alone, PI and hybrid controllers for motors M1 and M2.

Processor-in-the-Loop Results

The designed fuzzy/PI controller is implemented in PIL configuration on the dsPIC33EP256MC502 16-bit DSP, running at a sampling time of $1\ ms$. The results of speed regulation and tracking test cases for both M1 and M2 are shown in figs. 4.24 and 4.25, respectively.

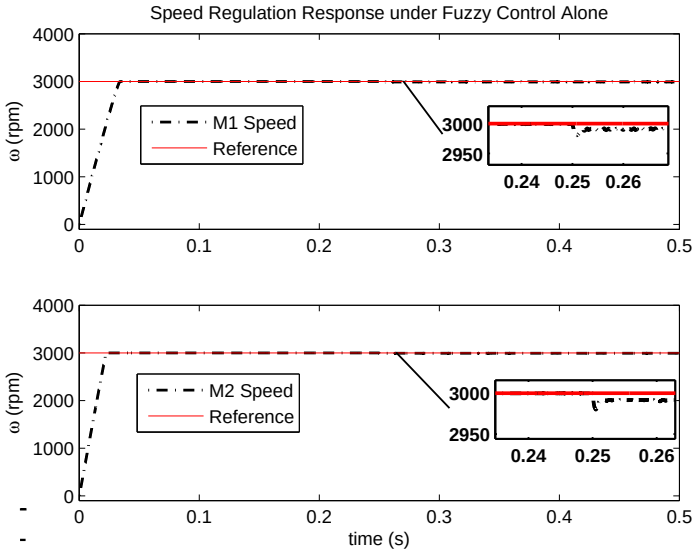

Figure 4.13: Speed regulation response with fuzzy logic controller alone for M1 and M2 under $\omega_r = 3000\ rpm$ and rated load applied at $t = 0.25\ s$

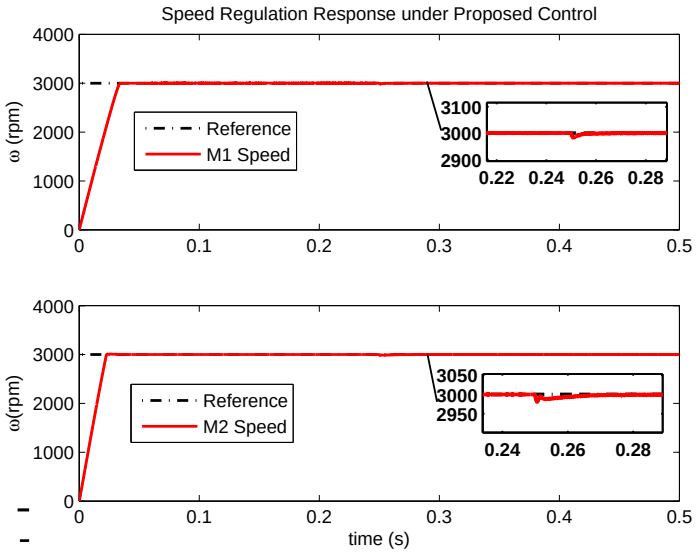

Figure 4.14: Speed regulation response with proposed controller for M1 and M2 under $\omega_r = 3000\ rpm$ and rated load applied at $t = 0.25\ s$

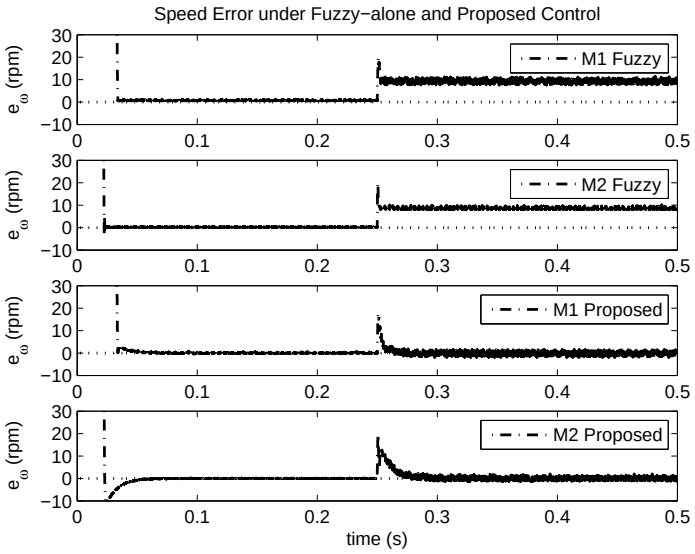

Figure 4.15: Speed regulation error comparison between fuzzy and proposed controllers under $\omega_r = 3000\ rpm$ and rated load applied at $t = 0.25\ s$

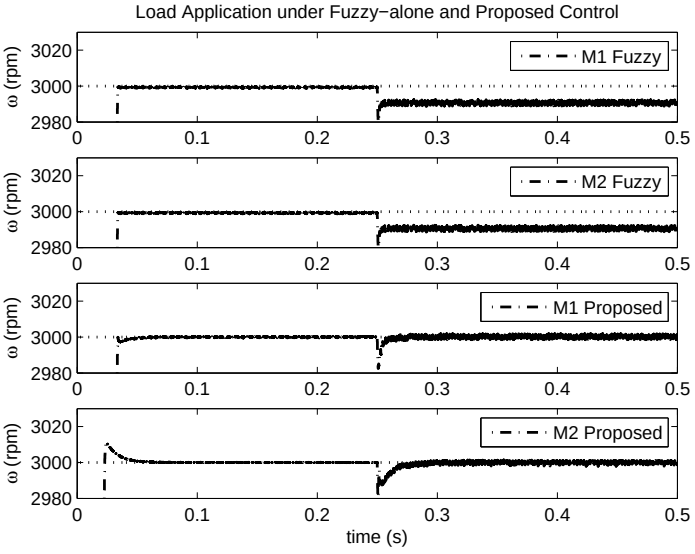

Figure 4.16: Speed regulation comparison (zoomed view) between fuzzy and proposed controllers under $\omega_r = 3000\ rpm$ and rated load applied at $t = 0.25\ s$

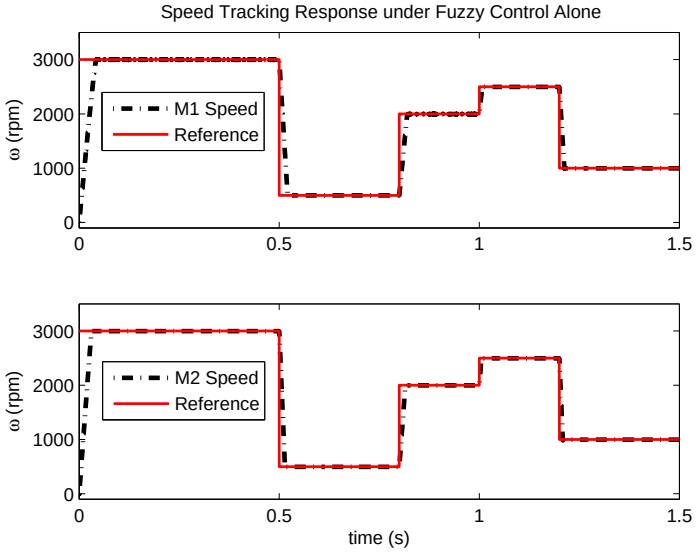

Figure 4.17: Speed tracking response of fuzzy logic controller alone, for M1 and M2 under a constant 50% rated load

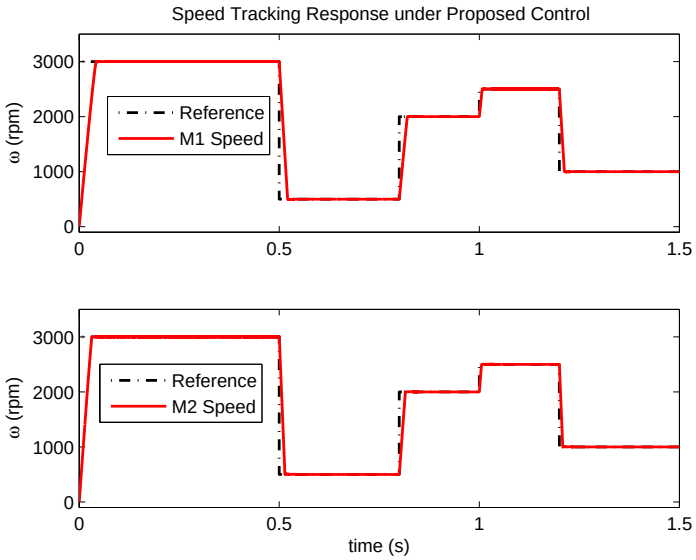

Figure 4.18: Speed tracking response of proposed controller, for M1 and M2 under a constant 50% rated load

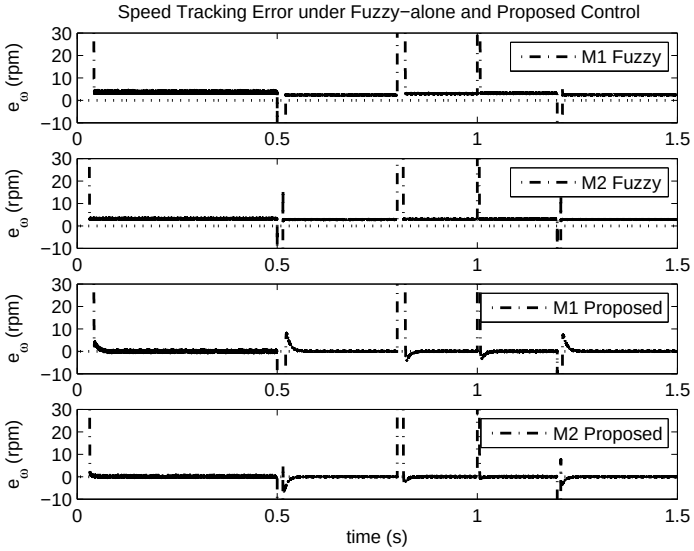

Figure 4.19: Speed tracking error comparison between fuzzy and proposed controllers for M1 and M2 under a constant 50% rated load

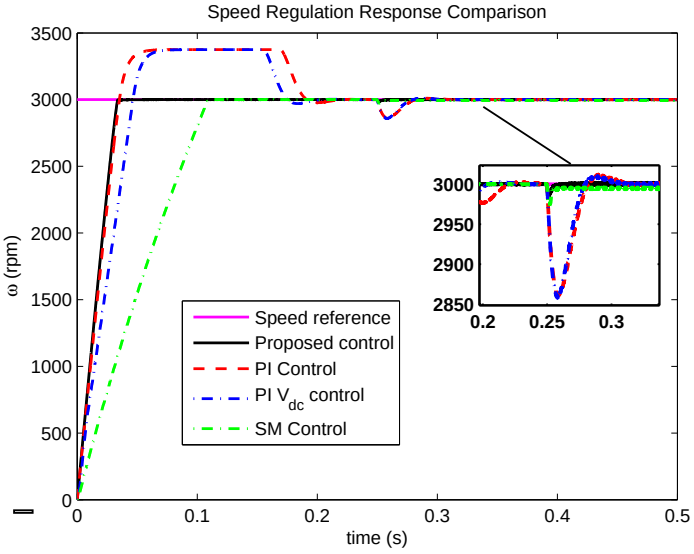

Figure 4.20: Speed regulation comparison of the proposed, PI and SM controllers at $\omega_r = 3000\ rpm$, $T_{load} = 3\ N.m$ applied at $0.25\ s$, motor M1

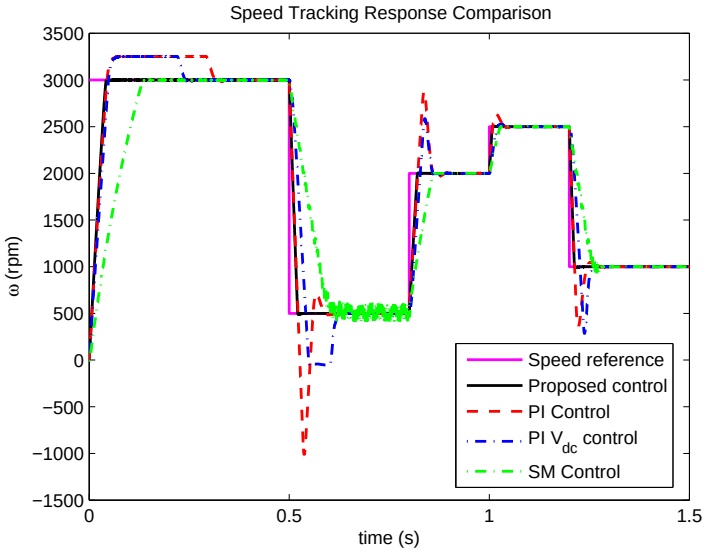

Figure 4.21: Speed tracking comparison of the proposed, PI and SM controllers under constant $T_{load} = 1.5\ N.m$, motor M1

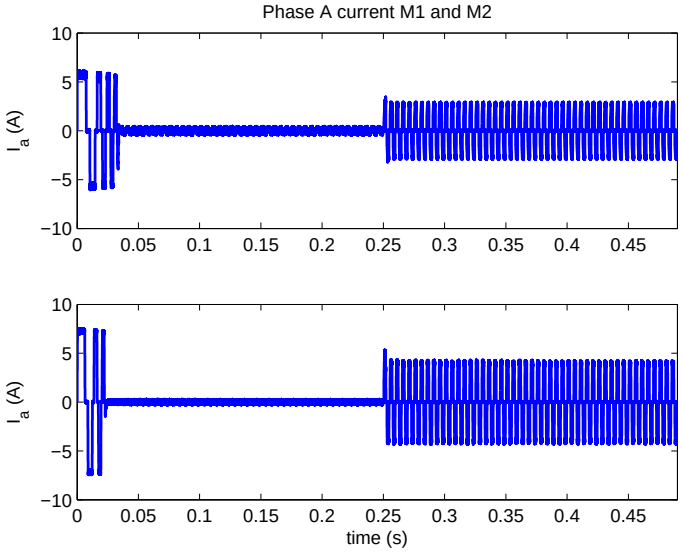

Figure 4.22: Phase A currents of M1 and M2 under proposed scheme for a set-point speed of $3000\ rpm$, $T_{load} = 3\ N.m$ for M1 and $T_{load} = 1.91\ N.m$ for M2 applied at $0.25\ s$

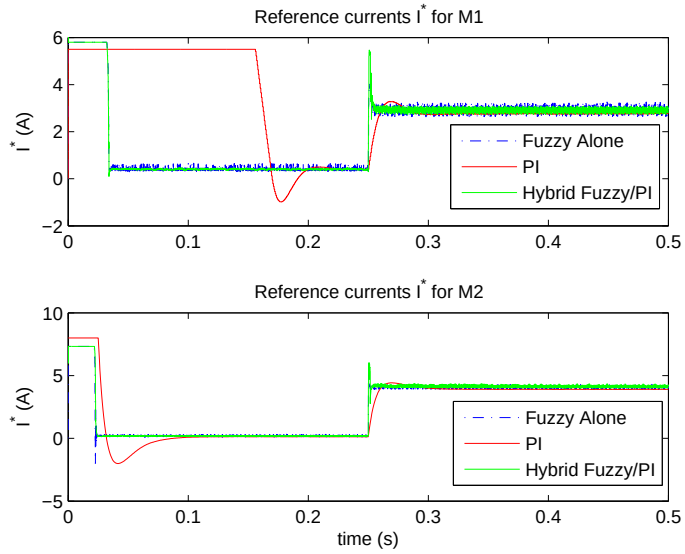

Figure 4.23: Reference current I^* for M1 and M2 under the fuzzy alone, PI and the proposed control schemes at rated speed of $3000\ rpm$ and rated load applied at $0.25\ s$

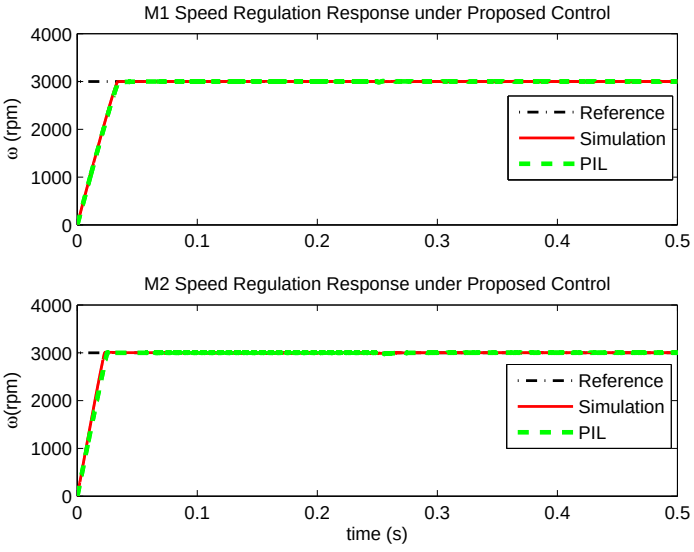

Figure 4.24: Speed regulation response comparison with proposed controller in simulation and PIL modes, for M1 and M2 under $\omega_r = 3000\ rpm$ and rated load applied at $t = 0.25\ s$

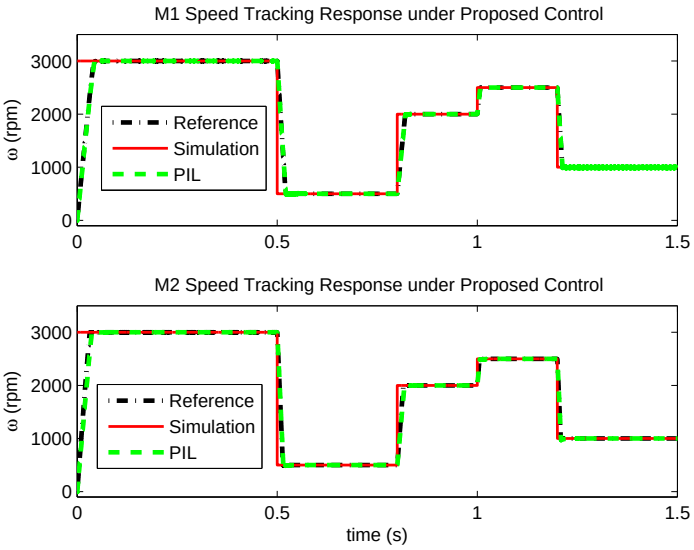

Figure 4.25: Speed tracking response comparison of proposed controller in simulation and PIL modes, for M1 and M2 under a constant 50% rated load

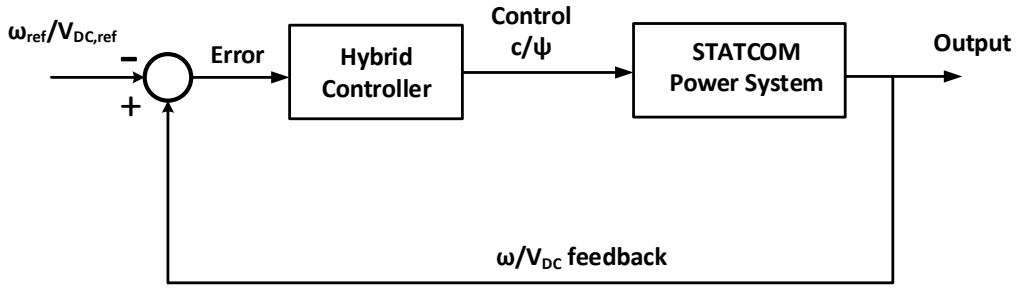

Figure 4.26: Closed loop block diagram for the STATCOM based power system under hybrid fuzzy/PI control

4.2.2 Power System Stabilization using STATCOM

The hybrid fuzzy/PI controller is used in stabilizing a STATCOM based power system whose parameters are given in the Appendix A in Section A.3. The controller design and comparative study results with a simple PI controller are presented.

Controller Design

The fuzzy logic part of the hybrid controller is designed following the guidelines in subsection 4.1.2 and based on the system ratings. The controller is employed in the angular frequency and the dc-link voltage loops. For the angular frequency loop, the controller output is the modulation index c while for the dc-link voltage loop the controller output is the voltage angle ψ, as shown in fig. 4.26. Identical membership functions are chosen for both the loops according to the guidelines as depicted in fig. 4.27 and 4.28. The same one-to-one mapping as in the case of BLDC motor drive is chosen for the fuzzy rule-set and the centroid defuzzification method is used. The gains for the PI controller are chosen by trial and error; they yield better performance for this application in comparison to using the Zieglar-Nichols tuning method. The error variance thresholds for

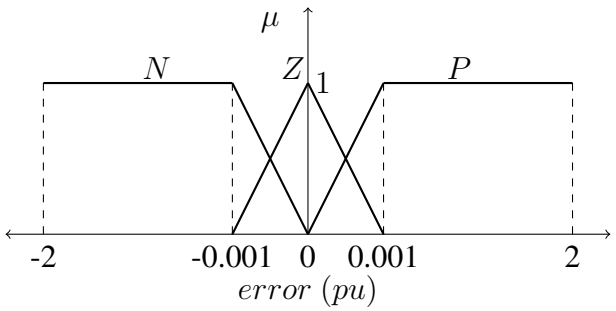

Figure 4.27: Input membership functions, identical for both the ω and V_{DC} loops

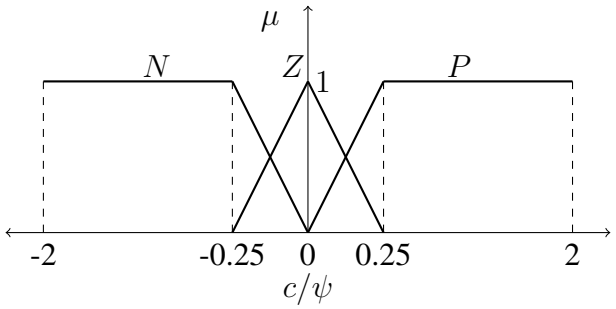

Figure 4.28: Out membership functions, identical for both the ω and V_{DC} loops

the two loops are selected by running the simulation under fuzzy logic controller alone. They are given in Appendix A in section A.4, Tables A.7 and A.8.

Simulation Results

Time domain simulations of the closed loop system under the hybrid and simple PI controller are run in MATLAB®/Simulink on the nonlinear system at two different operating points of $(P, Q) = (1.2, 0.4)$ and $(P, Q) = (0.8, 0.2)$ representing heavy and nominal loading, respectively. The parameters M and C_{DC} are each 50% off from their nominal values given in the Appendix A. PIL results are also compared with the simulations. Simulations are run for $t = 5\ s$ with a 15% step torque disturbance and a 3-phase fault at the infinite bus applied at $t = 1\ s$ instant, lasting three cycles [122].

The results under torque disturbance are shown in figs. 4.29, 4.30, 4.31, 4.32 and 4.33, while under 3-phase fault are shown in figs. 4.34, 4.35, 4.36 and 4.37. Instability under torque disturbance alone is shown in fig. 4.29 for conciseness.

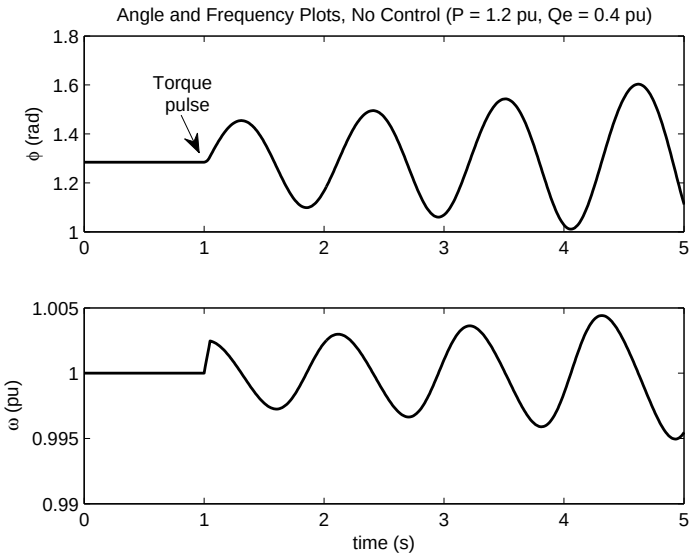

Figure 4.29: Rotor angle and angular frequency plots with no controller under heavy loading, 15% torque disturbance

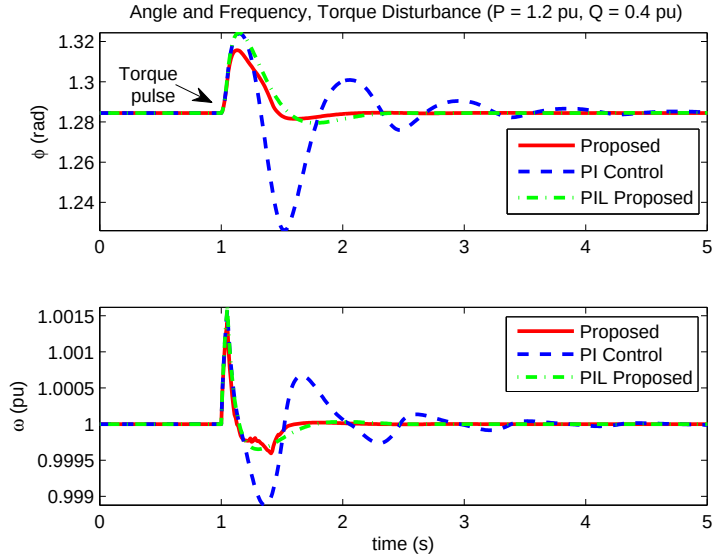

Figure 4.30: Rotor angle and angular frequency plots under the hybrid and PI alone controllers under heavy loading, 15% torque disturbance

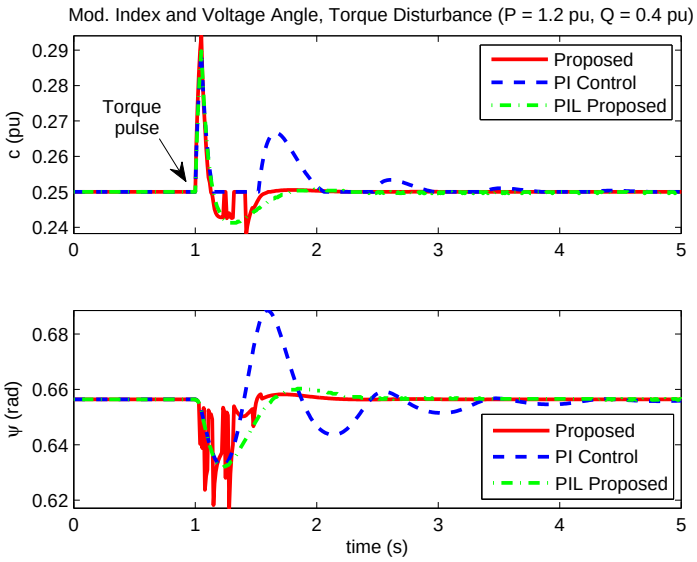

Figure 4.31: Modulation index and STATCOM output voltage angle plots under the hybrid and PI alone controllers under heavy loading, 15% torque disturbance

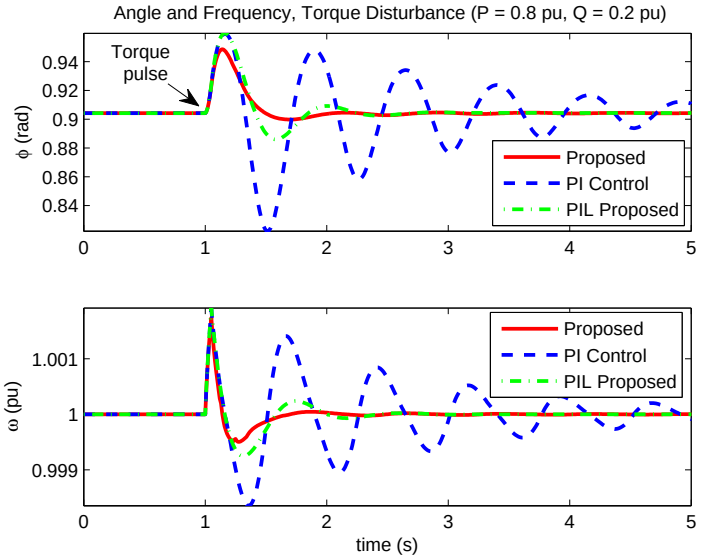

Figure 4.32: Rotor angle and angular frequency plots under the hybrid and PI alone controllers under nominal loading, 15% torque disturbance

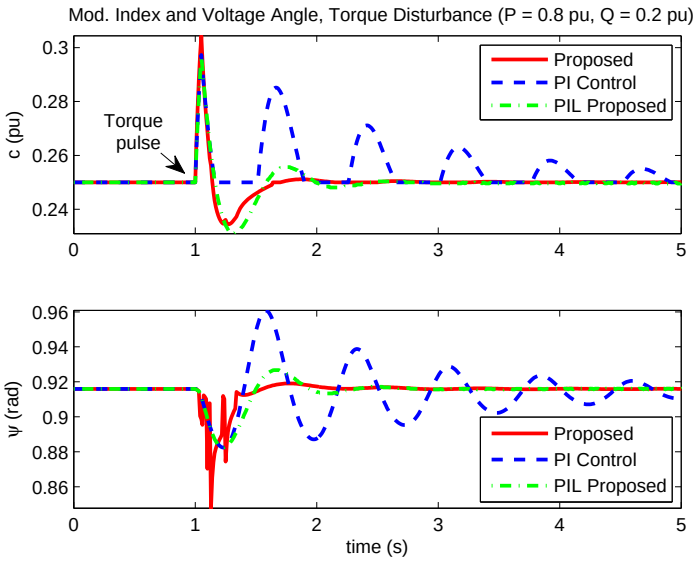

Figure 4.33: Modulation index and STATCOM output voltage angle plots under the hybrid and PI alone controllers under nominal loading, 15% torque disturbance

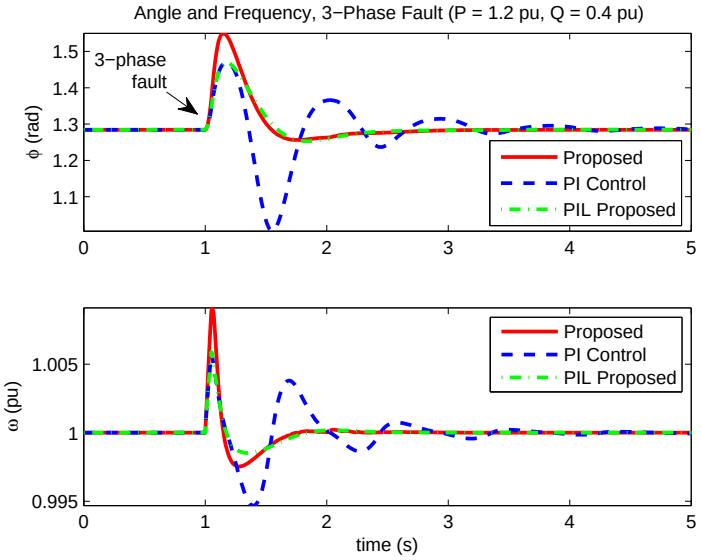

Figure 4.34: Rotor angle and angular frequency plots under the hybrid and PI alone controllers under heavy loading, 3-phase fault for three cycles

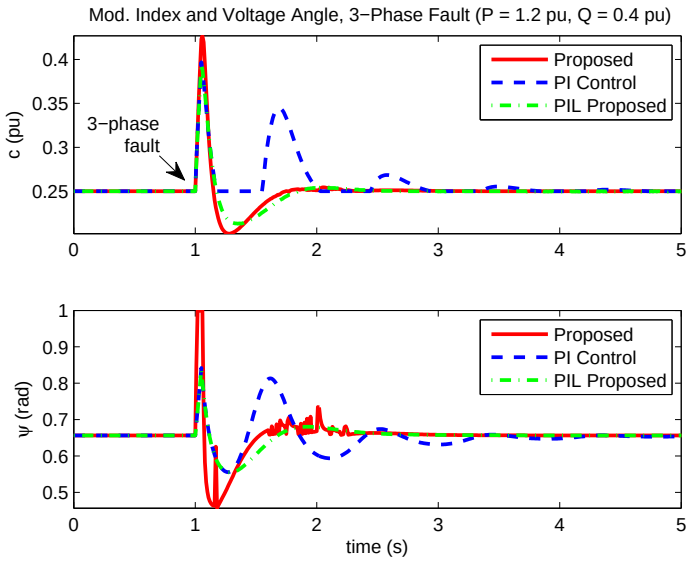

Figure 4.35: Modulation index and STATCOM output voltage angle plots under the hybrid and PI alone controllers under heavy loading, 3-phase fault for three cycles

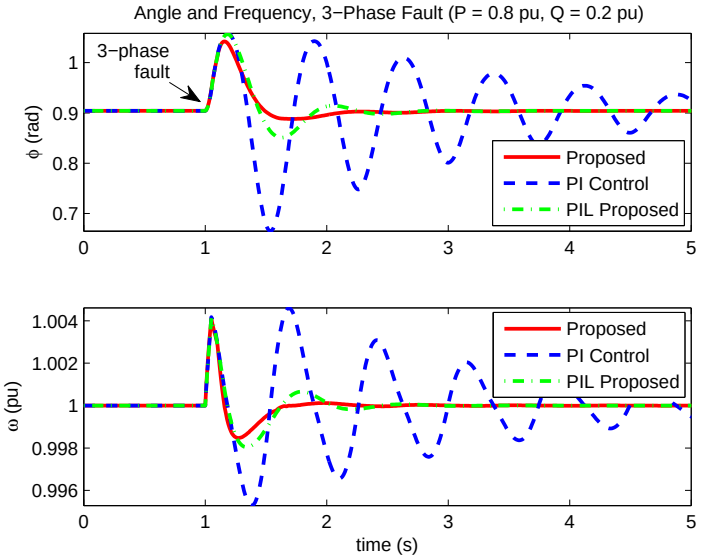

Figure 4.36: Rotor angle and angular frequency plots under the hybrid and PI alone controllers under nominal loading, 3-phase fault for three cycles

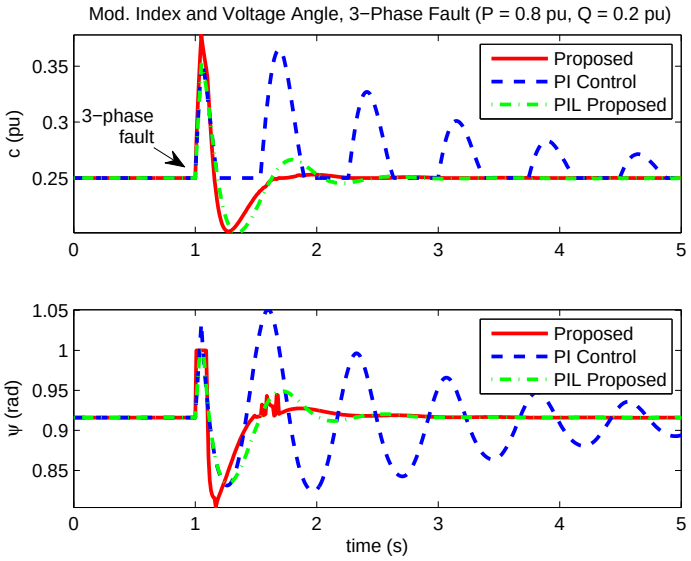

Figure 4.37: Modulation index and STATCOM output voltage angle plots under the hybrid and PI alone controllers under nominal loading, 3-phase fault for three cycles

4.3 Discussion

From the speed regulation responses in figs. 4.13 and 4.14 it can be observed that the speed reaches its set-point within $0.035\ s$ for M1 and $0.025\ s$ for M2, with no overshoot. However, in case of fuzzy controller alone, there is a finite steady state error under rated load as expected, shown in figs. 4.15 and 4.16. It is approximately $10\ rpm$ for M1 and $9\ rpm$ for M2. This is the worst case steady state error that occurs under rated conditions, and is less than 1% for both M1 and M2.

From the speed tracking response in fig. 4.17, similar results are observed. The fuzzy logic controller quickly responds to a changing speed reference both under no load and load conditions with no overshoot, but with a finite steady state error under loading.

From the speed regulation response in fig. 4.20, it can be seen that the proposed hybrid controller exhibits a better speed regulation response than the PI and SM controllers. It allows the least amount of dip in the actual speed with sudden application of rated load at $t = 0.25\ s$, and quickly restores the speed to its set-point with no steady state error. In comparison, the responses of PI based controllers show a high amount of overshoot and speed dips under sudden load application. The response of SM based controller is slower and has a finite steady state error. From the speed tracking response in fig. 4.21 it can be seen that the proposed hybrid controller provides a fast, overshoot and offset free tracking for a step changing speed command under constant loading. The quick dynamic response of the drive system under transients (speed set-point changes, sudden loading, etc.) is achieved by the fuzzy logic controller through

fast reference current generation, driving the speed error to a small steady value. At this point, the supervisory switching control activates the PI controller, which drives the steady state offset to zero. The flat top responses in the overshoot region for simple PI based controllers in figs. 4.20 and 4.21 are due to rate limitation enforced to keep the motor current within the safety limits. The higher amount of ripple apparent in the reference current response of the fuzzy controller alone, especially under loaded conditions, can be seen from fig. 4.23. This causes a higher steady torque ripple due to reasons already discussed.

From the simulation results of STATCOM based power system in fig. 4.30 to fig. 4.37, it can be seen the proposed hybrid controller outperforms the simple PI controller in damping out low frequency oscillations. The controller stabilizes the power system with the same fuzzy controller and PI controller gains for both the heavy and nominal loading conditions under a step torque disturbance and 3-phase fault, with minimal oscillations and overshoot. In comparison, the simple PI controller shows excessive oscillations for the two different operating conditions. It can be concluded that the fuzzy logic controller in the proposed scheme enhances the performance of the PI controller in hybrid combination, in comparison to the PI controller acting alone. Thus, the ability of the proposed controller to effectively stabilize the system under a wide range of operating conditions without the additional tuning of gains, is effectively demonstrated.

For both applications, the controller shows robustness by fast tracking of the set-point speed and stabilization of the equilibrium point under adverse conditions.

Results of the test cases run in PIL configuration, depicted in figs. 4.24 and 4.25

for the BLDC motor and in figs. 4.30, 4.31. 4.32 and 4.33, 4.34, 4.35, 4.36 and 4.37 for the STATCOM based power system, show close agreement with the simulated results, indicating that the controller functions as expected in digital implementation. The differences in transient responses are primarily due to controller discretization introducing some inaccuracies, limitations on the sampling rate in the digital implementation, fixed-point data type conversion inaccuracies and choice of the numerical integration method.

CHAPTER 5

EXPERIMENTAL IMPLEMENTATION OF THE HYBRID FUZZY/PI CONTROLLER FOR BLDC MOTOR DRIVE

In this chapter, experimental results for the low complexity hybrid fuzzy/PI controller proposed in Chapter 4 are presented, for speed of the BLDC motor drive. For performance assessment, the proposed controller's response is experimentally compared to the responses of the conventional PI controller and a purely fuzzy logic based controller reported recently in [53] for different test cases. Results show that the hybrid scheme demonstrates better performance in comparison to the conventional PI and fuzzy logic controllers under various operating conditions. The experimental implementation and hardware testbench details are also described.

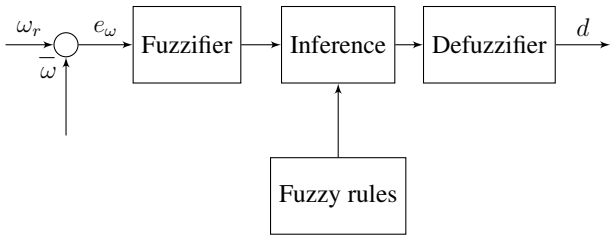

Figure 5.1: Fuzzy controller block diagram

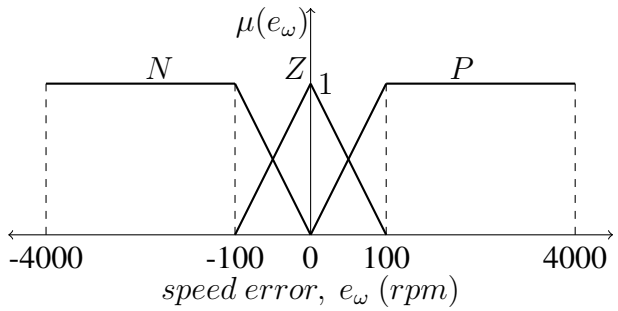

Figure 5.2: Input e_ω membership functions (not to scale)

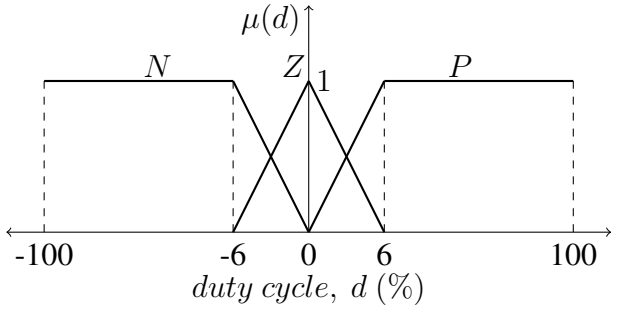

Figure 5.3: Output d membership functions (not to scale)

5.1 Fuzzy Logic Controller Design

The simplified block structure of the fuzzy logic controller for the BLDC motor drive is shown in fig. 5.1. It uses the Mamdani system structure that is most commonly used in practice [150]. Unlike the conventional fuzzy logic controllers that usually employ error and change in error as inputs [48–50, 52–54], the proposed fuzzy controller uses only a single error input. The input is chosen as the error e_ω between the set-point

speed ω_r and the actual speed ω_m. Unlike Chapter 4, instead of a reference current, the output is chosen as the duty cycle d for the PWM module. This eliminates the need for sensing any of the phase currents and makes the implementation simpler and more cost-effective. Based on ratings of the motor, the universe of discourse for the input is chosen to be from -4000 to 4000 in revolutions per minute (rpm), and that for the output from -100 to 100 in percent (%), to obtain a desired defuzzified output for a certain input using the centroid method. Triangular and trapezoidal membership functions are chosen for both the input and output as shown in fig. 5.2 and 5.3, namely *Negative (N)*, *Zero (Z)* and *Positive (P)*. The following rule-set is chosen to define the input-output relationship:

- *If the speed error is Negative, then duty cycle is Negative*
- *If the speed error is Zero, then duty cycle is Zero*
- *If the speed error is Positive, then duty cycle is Positive*

This rule-set yields a duty cycle proportional to the speed error. In reality, the duty cycle can not exceed 100% or go below 0%. A saturation function is used to ensure that the duty cycle stays between 0% and 100%. Consequently, in case of the actual speed being greater than the set-point speed, the saturated duty cycle output is either zero or a very low positive value thus, driving the actual speed toward its set-point. Next, the membership degree μ of each input to its corresponding fuzzy set is mapped to the output fuzzy sets; a process called implication. Finally, the resultant fuzzy sets are defuzzified using the centroid method [147, 150]. The entire fuzzy inference process under two different values of speed error is illustrated in figs. 5.4 and 5.5.

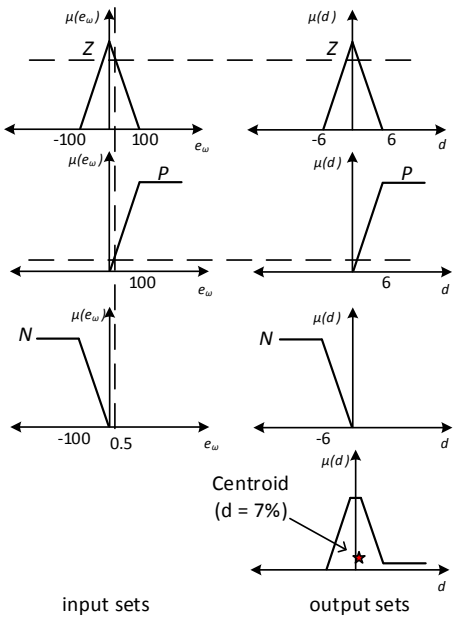

Figure 5.4: Fuzzy inference process for speed error of $0.5\ rpm$ (not to scale)

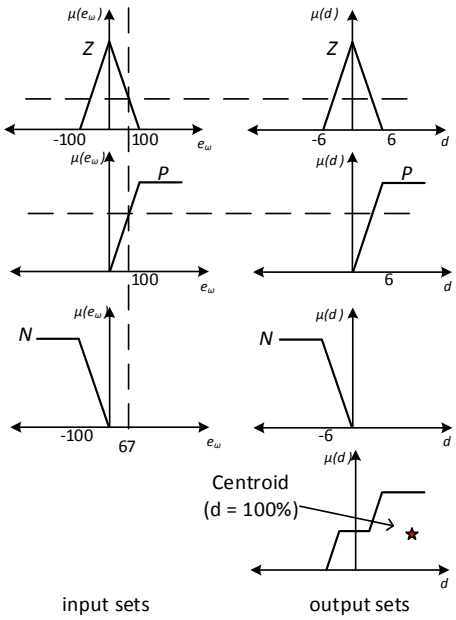

Figure 5.5: Fuzzy inference process for speed error of $67\ rpm$ (not to scale)

As previously mentioned in subsection 4.2.1, the fuzzy logic part of the designed controller behaves like an 'aggressive' proportional controller within the saturation limits of the duty cycle, as a result of the steep slopes of the input and output membership functions. The 'aggressive' nature of the fuzzy controller can be seen from the illustrations in figs. 5.4 and 5.5. The controller outputs 100% duty cycle at just $67\ rpm$ speed error. As previously specified in subsection 4.2.1 this 'aggressiveness' and a lack of integral action can cause ripples and finite error in the steady state speed response. Therefore, this controller can effectively be utilized only in the transient state e.g., startup from zero speed, a step change in set-point speed or sudden load application. A PI controller is better suited for steady state operation in eliminating the offset.

In case of changes to the system e.g., change in motor or equipment ratings, the fuzzy controller's design can be adjusted to the new ratings by accordingly modifying only the input's universe of discourse. Thus, little effort is required on the designer's part to adjust the controller's design to changing system specifications. This makes the controller adaptable to a wide range of ratings.

5.1.1 Supervisory Control and Variance Threshold

The active controller is selected based on identifying the transient and steady states from the speed error variance. The supervisory scheme utilizes the fuzzy controller for transient state and the PI controller for the steady state according to (4.1). The variance threshold value is identified by running the BLDC motor drive under fuzzy controller alone. The simplified block diagram of the complete system is shown in fig. 5.6.

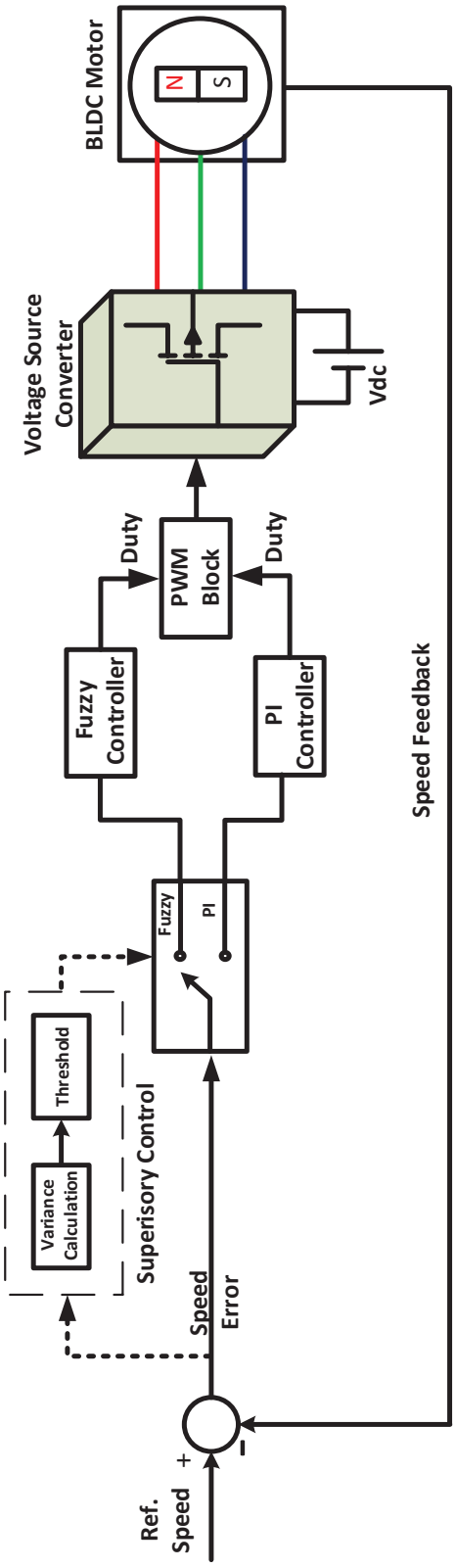

Figure 5.6: Simplified block diagram of the complete system

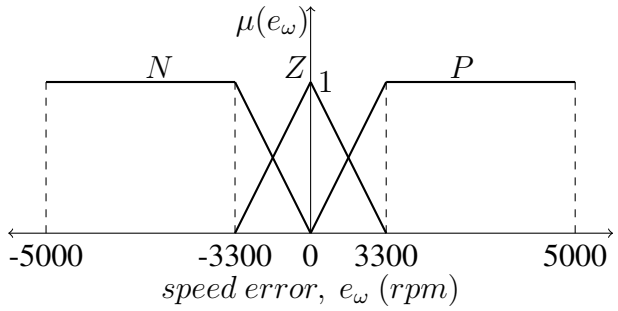

Figure 5.7: Input e_ω membership functions of the FL controller (not to scale)

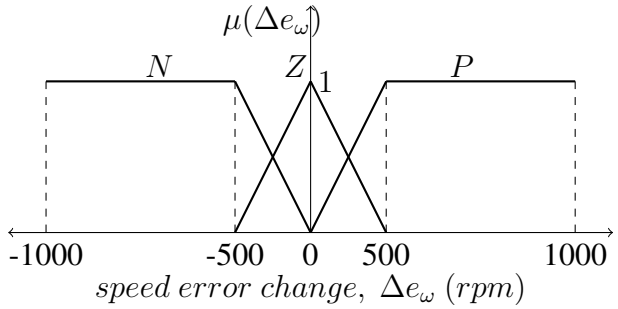

Figure 5.8: Input Δe_ω membership functions of the FL controller (not to scale)

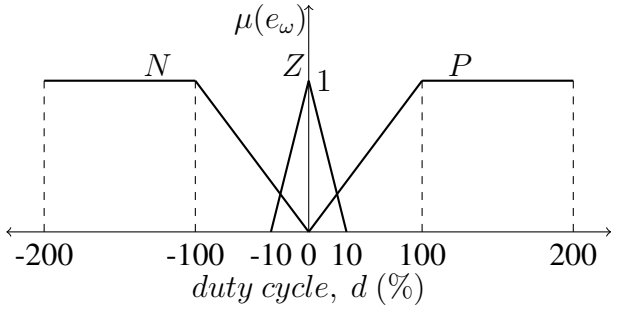

Figure 5.9: Output d membership functions of the FL controller (not to scale)

5.2 Comparison Models

The performance of the proposed controller is compared with two other benchmark controllers namely the conventional PI controller and the fuzzy logic (FL) controller reported in [53]. Gains for the PI controller are tuned by trial and error for reasons described in Section 4.2; achieving the best trade-off between oscillations, transient

response and steady state performance. The FL controller is designed using the method of [53] and adjusting the input and output ranges according the test system's ratings. The resultant input and output membership functions obtained are shown in figs. 5.7, 5.8 and 5.9. The same rule-set as in [53] is used.

5.3 Experimental Setup and Results

In this section, the experimental setup, implementation details and test case results for the proposed, PI and FL controllers are reported. Motor parameters and controller gains are given in Appendix A in Tables A.9 and A.10, respectively.

5.3.1 Hardware and Implementation Details

A simplified block diagram of the experimental setup is shown in fig. 5.10 while a snapshot of the experimental setup is shown in fig. 5.11. The controller and 3-phase power module are implemented on Microchip's MCLV-2 motor control board [152]. The board has a 16-bit dsPIC33EP256MC502 MCU with 256-Kbytes of program flash memory and 32-Kbytes of RAM. It also has a 3-legged, six switch power electronic converter that can handle ratings upto 48V, 15A and 720W. A 3-phase, Y-connected BLDC motor with Hall sensor feedback from Hurst [153] is used. The motor is loaded by coupling its shaft to another 3-phase Y-connected BLDC machine and connecting a 3-phase resistive load in Y-connection to its terminals. Commutation signal generation and speed calculation are carried out using Hall sensor feedback from the motor. A serial interface is used for communicating between the MCLV-2 and the host computer to

monitor the motor's speed and command signals in real-time and for data recording purposes. The data is recorded and monitored in real time using MATLAB®/Simulink's [147] built-in functions and serial data handling routines in the 16-bit device blocks toolbox from Microchip [154]. For the phase current and line voltage monitoring and recording, HIOKI 3197 power quality analyzer [155] is used. The MCU is programmed using Microchip's ICD-3 programmer/debugger [156] and the 16-bit device blocks toolbox in MATLAB®/Simulink environment on the host computer. A PWM frequency of $16\ kHz$ is used for all control schemes. A sampling time of $0.25\ ms$ is set to ensure compatibility between the sampling rates of MCU's analog-to-digital converter (ADC) and the Simulink blockset. A lower sampling rate and PWM frequency can also be chosen. However, they should both be sufficiently high since the mechanical time constant of the BLDC motor is also very small due to small inertia. A low PWM frequency and sampling rate may cause the switching harmonics to appear in the mechanical response. Fuzzy logic algorithms are implemented on the MCU using lookup tables to speed up calculations and avoid complex computations. A 1-D lookup table with 161 entries for the proposed controller and a 2-D lookup table with 2121 entries for the FL controller are used. Interested readers are referred to the fuzzy toolbox documentation [89] for details on generating lookup tables for fuzzy logic.

5.3.2 Results

Speed responses of the proposed hybrid and benchmark controllers are analyzed for two different scenarios under load and no-load conditions: (1) speed regulation and (2)

speed tracking. Two regulation test cases are run; the first regulation test case is run on all three controllers while the second regulation test case is run on the proposed and PI controllers only. In the first regulation test case, the motor is started from rest under no-load and a set-point speed of about 1.05% of the rated value i.e., $2170\ rpm$. Rated load torque is applied as a step disturbance at approximately $t = 4\ s$ time and removed shortly before $t = 7\ s$ time. For the second regulation test case, the motor is started from rest under no load at a set-point speed of $1450\ rpm$. A load of 75% the rated value is applied shortly before $t = 5\ s$ time and removed at approximately $t = 8\ s$ time. The speed regulation responses, duty cycle and error plots of the proposed hybrid, PI and FL controllers are shown in fig. 5.12, 5.13 and 5.14, respectively. Speed regulation comparison between the proposed controller and the simple PI controller at a set-point speed of $1450\ rpm$ is shown in fig. 5.15 while their duty cycle and error plots are shown in fig. 5.16. This test case is run to more clearly distinguish between the performances of the proposed and the conventional PI controllers at a different operating point.

For the tracking test case, a varying speed command is applied starting from the rated value and decreasing it in steps as 2170, 1800 and $1400\ rpm$ in sequence. The motor is started under no-load at a set-point speed of $2170\ rpm$. A load varying in proportion to the actual speed is applied to the motor starting with rated load applied at $t = 4\ s$. The tracking performance, duty cycle and error plots of the proposed, PI and FL controllers are depicted in figs. 5.17, 5.18 and 5.19, respectively. Waveforms of the phase A current and line AB voltage are depicted in figs. 5.20, 5.21, 5.22 and 5.23 under no-load and full-load conditions.

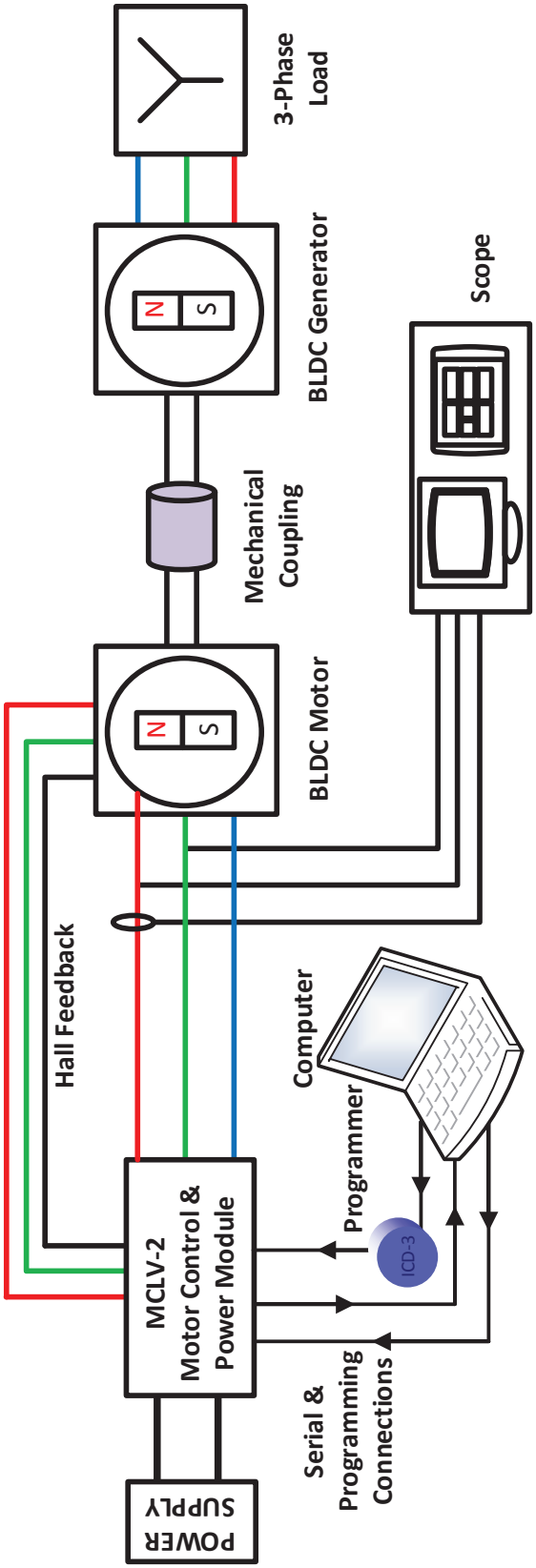

Figure 5.10: Block diagram of the experimental setup

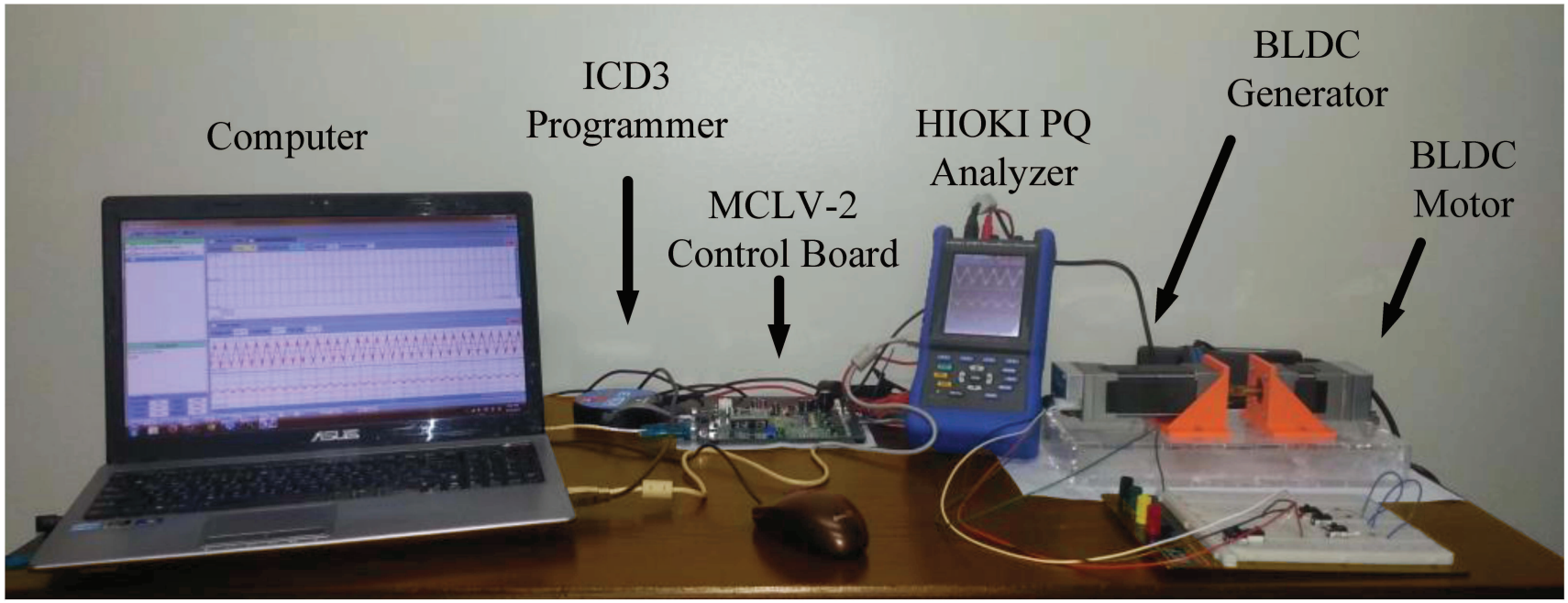

Figure 5.11: Experimental test bench

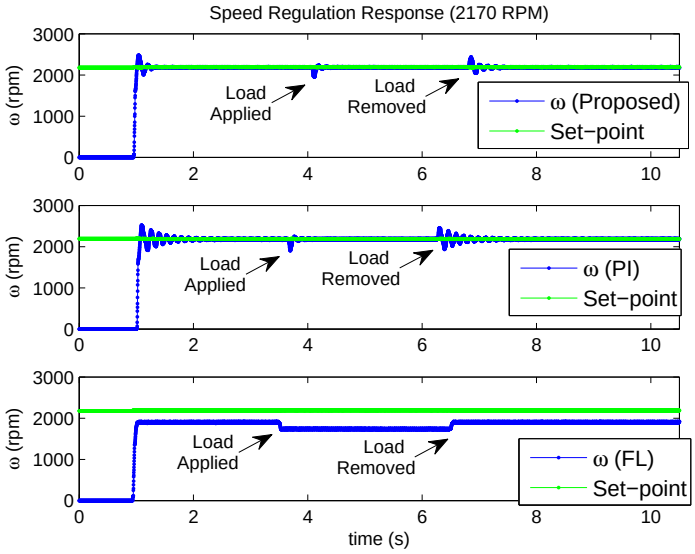

Figure 5.12: Speed regulation response at rated speed under no-load and full-load

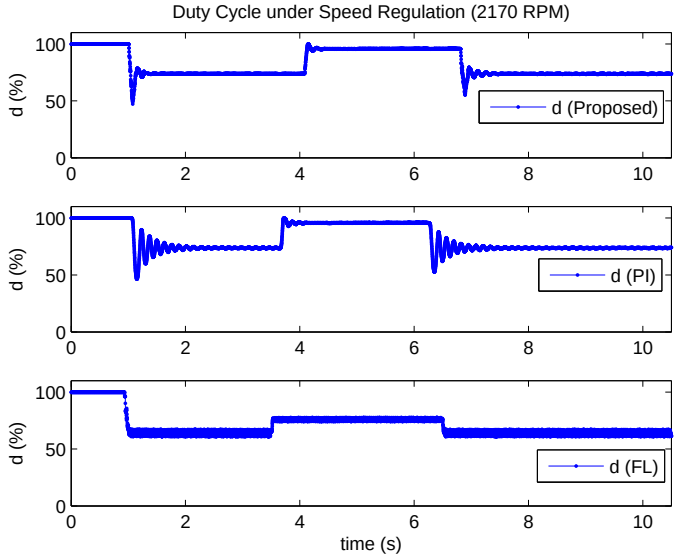

Figure 5.13: Duty cycle plots at rated speed under no-load and full-load

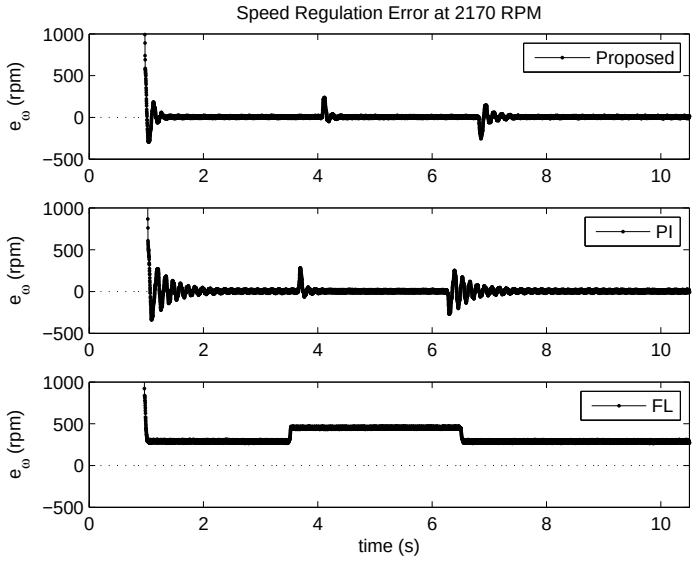

Figure 5.14: Speed regulation error at rated speed under no-load and full-load

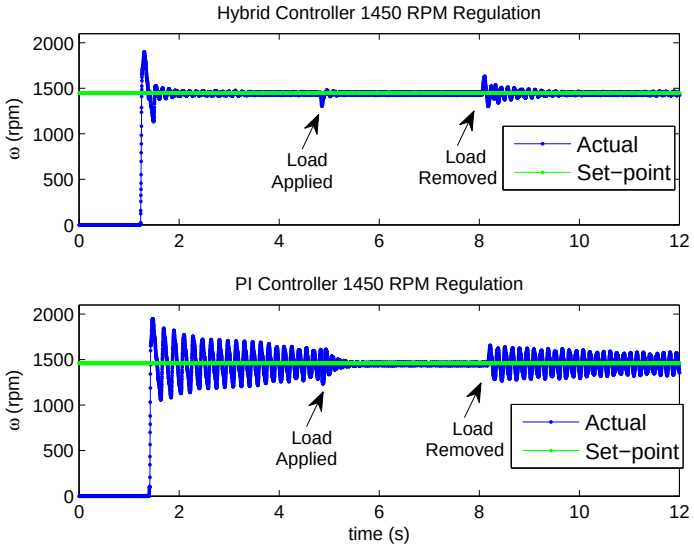

Figure 5.15: Speed regulation response at $1450\ rpm$ under no-load and 75% of rated load

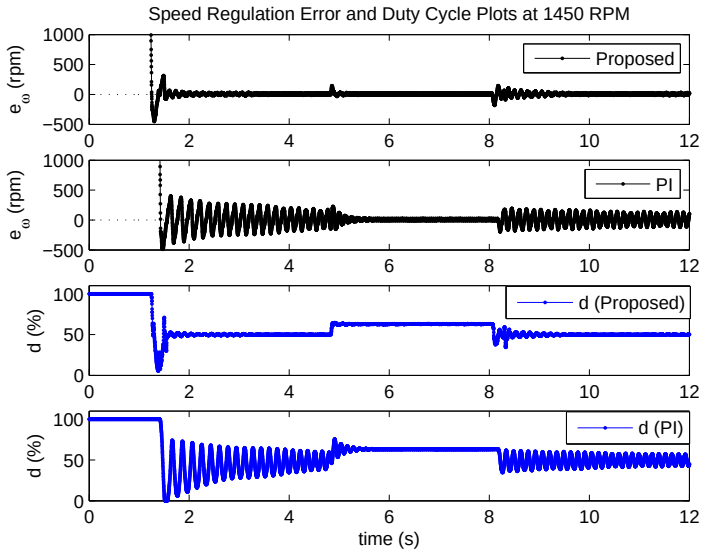

Figure 5.16: Speed regulation error and duty cycle plots at $1450\ rpm$ under no-load and 75% of rated load

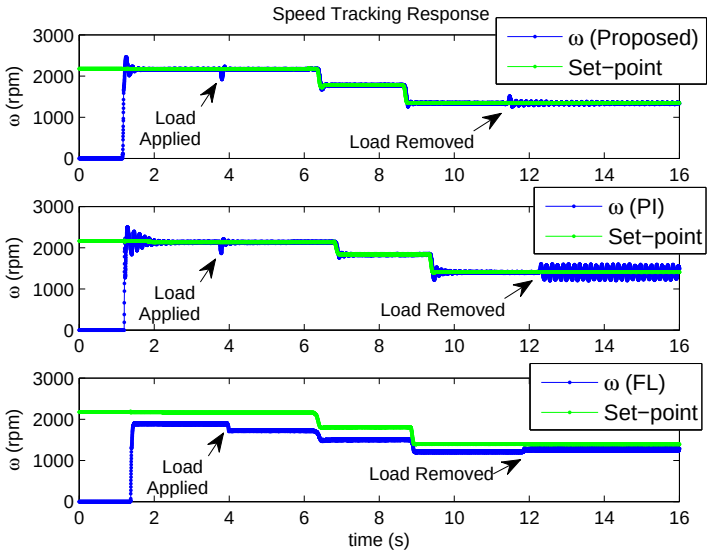

Figure 5.17: Speed tracking response under varying set-point speed and load

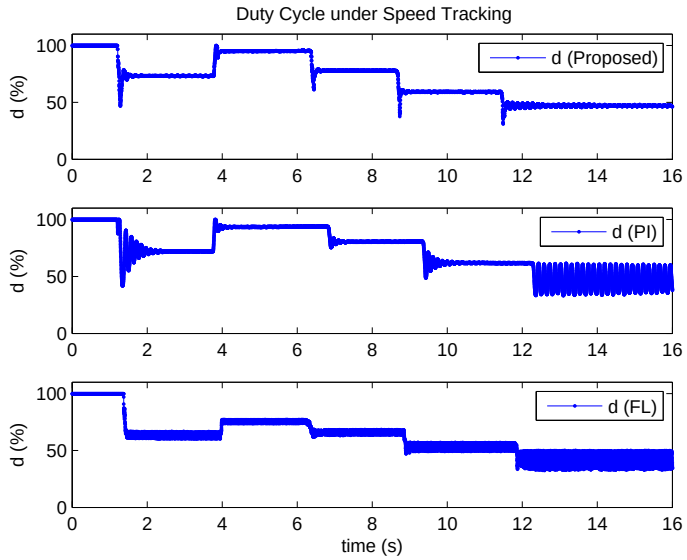

Figure 5.18: Duty cycle plots under varying set-point speed and load

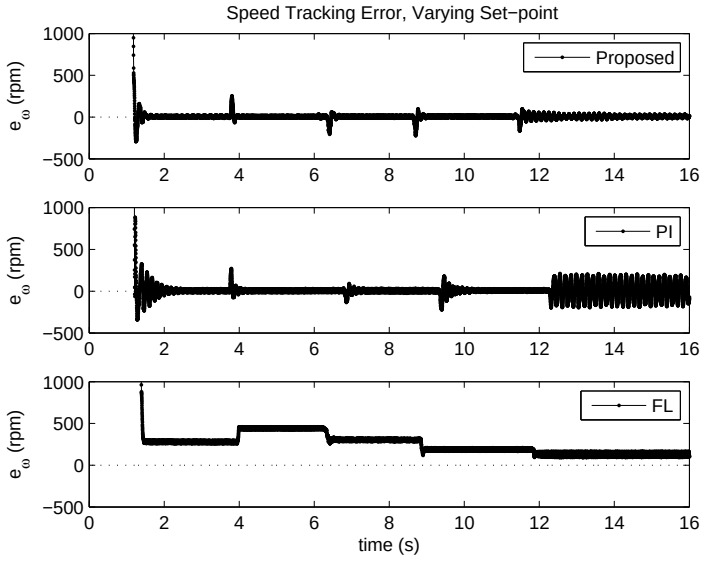

Figure 5.19: Tracking error under varying set-point speed and load

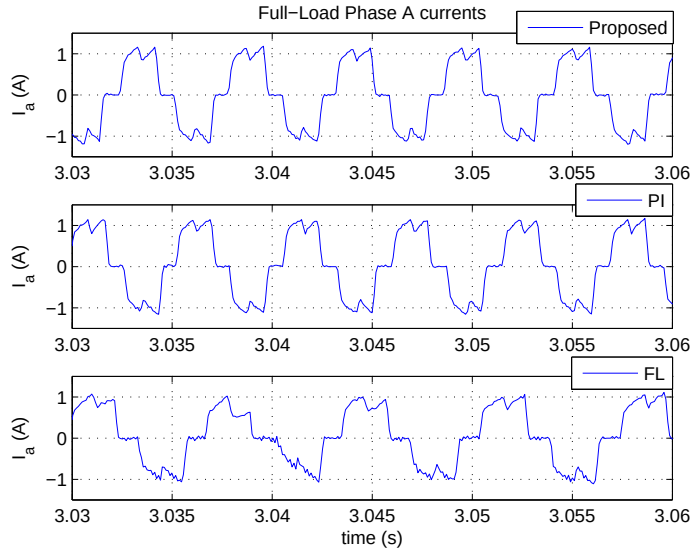

Figure 5.20: Full-load phase A current waveforms

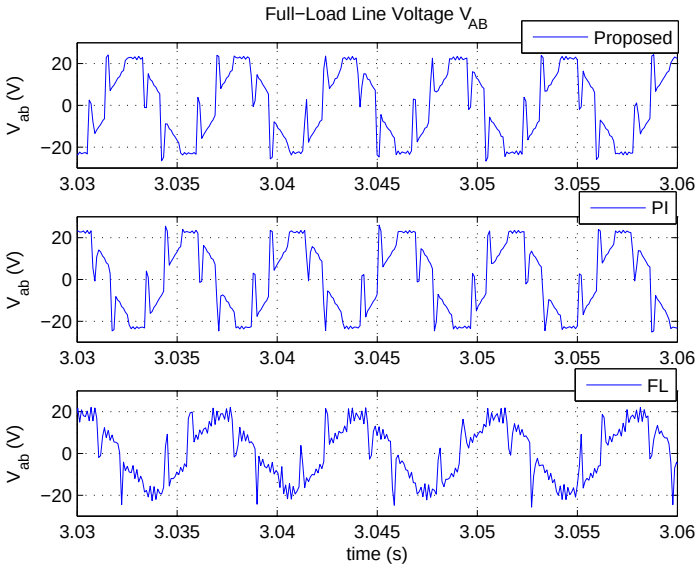

Figure 5.21: Full-load line AB voltage waveforms

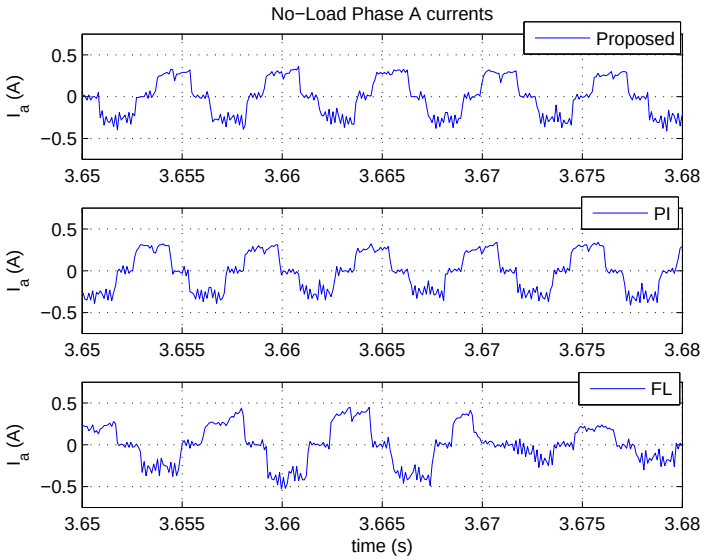

Figure 5.22: No-load phase A current waveforms

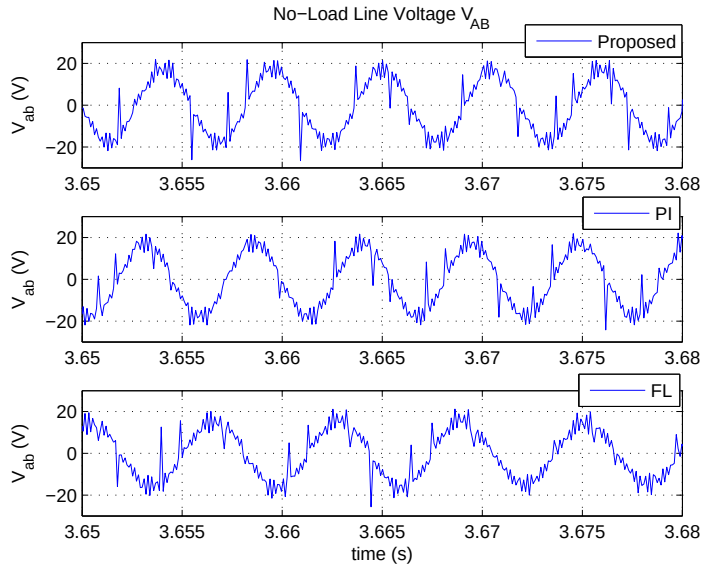

Figure 5.23: No-load line AB voltage waveforms

5.3.3 Discussion

From the speed regulation plot of fig. 5.12 it can be observed that the proposed controller has a good transient response. The set-point speed is attained with minimal oscillations and no steady state error. Transient response of the PI controller is comparable however, it shows oscillations at startup and load removal instances. The response of the FL controller exhibits a large steady state error. The characteristic responses of each of these controllers can also be seen from their corresponding duty cycle and error plots in figs. 5.13 and 5.14, reflecting the oscillations in the PI controller and large steady state offset in the FL controller.

Although there is a lesser degree of difference between the performance of the proposed hybrid and the PI controllers under rated speed regulation, the difference is more obvious at lower speeds as shown in fig. 5.15. At no-load startup, the PI controller's response shows large oscillations. It becomes stable with load application at nearly $t = 5\ s$ but the oscillations return as the motor is unloaded. In comparison, the proposed hybrid controller provides a stable startup and smooth response under step changes in operating conditions.

From the speed tracking response in fig. 5.17 it can be seen that the proposed controller shows a fast and stable transient response with low overshoot and tracks the reference without steady offset. The PI controller's response exhibits oscillations at startup, no-load and low speed conditions, similar to the regulation test case. The response of the FL controller, although smooth and overshoot free, suffers from large steady state error that further increases with load application.

The gains of the PI controller could be further tuned to improve the response and lessen the oscillations to a certain degree under specific operating conditions. However, the performance improvement is not guaranteed over the entire operating range. By combining the fuzzy logic and PI controllers in the proposed scheme, this shortcoming is overcome. The hybrid controller leads to a stable and satisfactory system operation over a much wider operating range using the same gains for the PI controller. The gains need not be tuned separately for different operating points or regions.

For the FL controller, a large steady state error (approximately $300\ rpm$) is seen that increases further under load application. The primary reason for this large error is the small number of rules and membership functions used. This leads to a coarsely tuned controller providing insufficient and inaccurate coverage of the system's operating range. Additional membership functions and rules are required to increase the controller's resolution and accuracy and to reduce the steady state error. However, more membership functions and a larger rule-set would also require a larger memory on the MCU, posing as a limitation in low cost hardware implementation. The current lookup table size of 2121 entries for the FL controller is approximately 13 times larger than the one for the proposed controller, with only 161 entries.

The total harmonic distortions in line voltages for the proposed, PI and FL controller are -18.7624, -19.2872 and -20.4679 in dBc, while those for the phase currents are -12.5025, -12.4101 and -13.5402 in dBc, respectively.

In summary, experimental results demonstrate that the proposed hybrid controller outperforms the conventional PI and FL controllers under various testing conditions. It

overcomes the drawbacks exhibited when each of the PI or FL controllers are employed in standalone. The drive system's dynamic response under the hybrid control scheme is fast, smooth and ripple-free with minimal oscillations and no steady state error. Having low computational complexity and minimal memory and sensing requirements, the controller can be conveniently implemented on low cost hardware. Due to its simple design rules and flexible structure, the control scheme is adoptable to a wide range of equipment and motor ratings. Moreover, the design does not rely on the system model or current sensing, making it robust in the presence of noise, model mismatches and parametric uncertainties.

CHAPTER 6

DISCUSSION, CONCLUSION AND FUTURE WORK

6.1 Comparison of the Proposed Control Schemes

Although the control design techniques presented in this research share the common goal of controlling uncertain systems, they possess both matching and differing features that may result in a varying degree of performance for different applications. A comparative analysis highlighting their common and contrasting features is presented in this section.

The primary classification used in this work to differentiate between control design techniques is their model-based and model-free nature. The first half of the thesis (Chapters 2 and 3) presents the design of a model-based robust controller for uncertain linear systems with single and multiobjective performance constraints using convex optimization. The second half of the thesis (Chapters 4 and 5) focuses on the design

and practical implementation of a model-free intelligent robust controller using hybrid fuzzy logic/PI control.

The observer-based $\mathcal{L}_2$-gain and mixed $\mathcal{H}_2/\mathcal{H}_\infty$, and the hybrid fuzzy/PI controllers both asymptotically stabilize the equilibrium point and track the set-point for their target applications. Both controllers exhibit robustness in their closed loop responses, to unknown disturbances and uncertain parameters. Finally, both the control schemes, having low computation and memory requirements, demonstrate convenient implementation on low-cost DSP.

For the observer-based control scheme, stability of the closed loop system is guaranteed with the fulfillment of Theorems 2.1 and 3.1. In comparison, establishing the proof of closed loop stability for the hybrid fuzzy/PI control scheme is not straightforward. This is primarily due to the fact that the closed loop system is an arbitrarily switched, two-structure system containing a combination of a linear and a nonlinear controller. Even with a reliable system model at hand, proving closed loop stability requires finding a common Lyapunov function for both closed loop structures (under fuzzy and PI controllers), which is a non-trivial task.

While the observer-based and the hybrid fuzzy/PI controllers exhibit comparable performance for the STATCOM based power system in terms of stabilization, convergence time and disturbance rejection, there is a significant difference in their performance for the BLDC motor system. All three controllers achieve error free reference tracking. However, the fuzzy/PI controller's convergence rate is much faster than those of the observer-based controllers. This is due to the fact that for the latter, it takes a

finite amount of time for the observer states to converge to their references. The rate at which the states of the closed loop system converge is limited by the rate of convergence of the observer states. Since no constraints are placed on the convergence rate, the design yields non-optimal controller and observer gains with respect to the rate of convergence. The faster convergence of the hybrid fuzzy/PI controller for the BLDC motor application is also due to the simplicity of the system. The system being a second order linear system, can easily be controlled by a simple control structure such as a PI controller or the proposed fuzzy/PI controller. For complex systems of higher order such as the STATCOM based power system, the convergence rates under the two different controllers are comparable. For the case of the fuzzy/PI controller, the convergence rate is dictated by the design of the fuzzy membership functions, as explained in Chapter 4. The convergence rates of the $\mathcal{L}_2$-gain and mixed $\mathcal{H}_2/\mathcal{H}_\infty$ controllers for different applications are controlled by imposing additional constraints on the design.

In contrast to the hybrid controller, state reconstruction in observer-based controllers provides a useful tool for identification of unknown system state information, fault analysis and performance monitoring. Using the hybrid controller, no new information is gained about the system.

The analytical design process involved in observer-based controllers allows the designer to impose single or multi-objective performance constraints on the system. In contrast, the design process of the hybrid fuzzy/PI controller is based on expert knowledge of the system, gained from the output. Imposing performance constraints on the design can not be done analytically due to the arbitrarily varying system structure.

Finally, the observer-based control scheme require a system model for the design, whereas the hybrid fuzzy/PI controller can be designed based on some a-priori expert knowledge of the system, without using the system model in the design process.

The results of the comparative analysis between the two different control schemes are summarized in Table 6.1 and Table 6.2. In Table 6.2, blue colored text represents strengths while red color represents limitations.

Control/Feature	**Observer-based Control**	**Fuzzy/PI Control**
Asymptotic Stability and Tracking	Yes; asymptotic stabilization and tracking for target systems	Yes; asymptotic stabilization and tracking for target systems
Robustness Features	Good; robust against parametric uncertainties and unknown disturbances	Good; robust against parametric uncertainties and unknown disturbances
DSP Implementation	Convenient; low computation and memory requirements	Convenient; low computation and memory requirements

Table 6.1: Comparison of control techniques: common features

Control/Feature	Observer-based Control	Fuzzy/PI Control
Performance and Optimality Constraints	Yes. Allow for imposing performance and optimality constraints on the design	No. Due to variable and arbitrarily switching structure
Proof of Closed Loop Stability	Guaranteed with the fulfillment of Theorems 2.1 and 3.1	Non-trivial; requires finding common Lyapunov function for different structures
State Reconstruction	Yes. Additional information gained, useful for fault analysis, performance monitoring	No additional information gained about the system
System Model	Required for design	Not required for design
Convergence Rate	Additional constraints required for controlling convergence rate	Convergence rate embedded in design

Table 6.2: Comparison of control techniques: contrasting features

6.2 Concluding Remarks

In this research, novel robust control techniques are developed using model-based and model-free approaches. The techniques are developed in a generalized framework thus making them applicable to a variety of practical systems.

New LMI results on robust observer based control for a class of uncertain linear systems subject to parametric uncertainties and unknown disturbances are presented. The proposed LMIs can be solved in a single step through any commercially available convex optimization software without having to resort to iterative or multistep solutions. The proposed results are shown to be less conservative than the existing results on output feedback problem. A number of existing solutions require having to separately search for certain parameters occurring in the formulation in a nonconvex manner, and treat them as constants to solve the problem as convex optimization. This may require a careful selection in a properly chosen search space for guaranteed convergence. It may also lead to a computationally intensive solution, as highlighted in the literature overview. In this regard, the proposed single-step solutions are computationally simpler and facilitate the controller synthesis by avoiding these additional steps.

A novel hybrid fuzzy/PI controller is proposed employing fewer design rules than the existing fuzzy logic based implementations. The key features of the control scheme are simple structure, fewer decision making rules and ease of design and implementation. A new supervisory switching mechanism based on error input's variance is employed to select the appropriate controller best suited to the operating conditions.

The generality of the proposed results is demonstrated through their application to

robust speed control of the BLDC motor drive and robust stabilization of STATCOM installed power system, through simulations and PIL results in the MATLAB®/Simulink environment. The results validate the effectiveness of the proposed techniques and highlight their potential for application to different practical systems.

The hybrid fuzzy/PI controller is practically implemented on low cost MCU for high performance speed control of the BLDC motor drive. It is shown that the lower rule count of the proposed controller leads to significant memory savings on the MCU in comparison to the conventional fuzzy logic schemes. The results are compared with the conventional PI controller and a recently proposed fuzzy logic controller, demonstrating the improved performance achieved by the proposed hybrid controller under various operating conditions. The details of the hardware and software tools employed are also given.

6.3 Summary of Contributions

The key contributions of this research work can be summarized as follows:

- Development of novel LMI conditions with a single-step solution for synthesis of robust $\mathcal{L}_2$-gain observer based controller for uncertain linear systems
- Development of novel LMI conditions with a single-step solution for synthesis of robust $\mathcal{H}_2/\mathcal{H}_\infty$ observer based controller for uncertain linear systems
- Design of a new high performance fuzzy logic based hybrid controller with lower computational complexity and memory requirements than the existing techniques

- Application of the proposed results to two different practical systems, demonstrating their validity, effectiveness and application potential
- Digital implementation of the proposed control techniques on a low cost DSP chip to demonstrate their hardware functionality
- Practical implementation of the proposed hybrid fuzzy/PI controller to speed control of the BLDC motor drive; experimental comparison with other techniques to demonstrate its performance gains

6.4 Future Work

The research presented in this thesis can be expanded in various directions. Some of the recommendations for future work are listed here:

- The response and performance of the closed loop system under the observer-based robust controller can be improved by adding additional constraints to the problem. Imposing a prescribed degree of stability and placing the poles of the closed loop system in specific LMI regions to improve its response time, oscillation and overshoot characteristics can lead to an interesting research problem.
- Convex optimization conditions for robust observer based controller synthesis under single and multiobjective performance constraints can be extended to discrete-time systems.
- The results presented in Chapter 2 and 3 can be experimentally implemented on hardware testbench to examine their performance. For the BLDC motor drive,

the proposed results of Theorem 2.1 and 3.1 can be tested on customized hardware with variable dc-link voltage capability. For the STATCOM installed power system, experimental validation can be carried out using hardware like RTDS.

- The observer-controller design using Theorem 2.1 and 3.1 for the STATCOM based power system is carried out using a linearized model around an operating point. The linearization approach is quite common in control literature (see for example [11, 16, 86, 157–159]). In order to extend the results to the entire operating range, the LMIs of Theorem 2.1 and 3.1 can be solved for various operating points and a gain-scheduling approach in the form of a lookup table can be implemented. The feasibility of the LMIs under extreme and nominal operating conditions has been established, serving as a foundation for the expansion of proposed results.

- Proof of stability of the closed loop system under the hybrid fuzzy/PI controller can be developed using the system model and finding a common Lyapunov function for the two-structure closed loop system.

- Simulations and experiments show that the proposed hybrid fuzzy/PI controller can offer a good alternative to the conventional PI controller for frequently changing operating points. Thus, the hybrid controller can be tested on other types of power electronic drives with nonlinear models such as induction motor drive or PMSM drive, or on large power systems with high penetration of renewable energy sources where changes in operating conditions are frequently encountered.

- The calculational complexity and performance of the hybrid fuzzy/PI controller can be compared with computationally intensive adaptive controllers in power and power electronic system applications to evaluate performance gains and computational resource efficiency.

APPENDIX A

PARAMTERS AND GAINS

A.1 Dynamic Model, Commutation Logic and Schematic of the BLDC Motor Drive used in Simulink

Mathematical Model

The mathematical model of a three phase wye-connected BLDC motor can be described by the following dynamic equations [92, 98]:

$$\begin{aligned}
\frac{di_a}{dt} &= \frac{1}{L_s}(-R_s i_a + v_{an} - e_{an}),\\
\frac{di_b}{dt} &= \frac{1}{L_s}(-R_s i_b + v_{bn} - e_{bn}),\\
\frac{di_c}{dt} &= \frac{1}{L_s}(-R_s i_c + v_{cn} - e_{cn}),\\
\frac{d\omega_m}{dt} &= \frac{1}{J}(T_e - T_{load} - B\omega_m),\\
\frac{d\theta_e}{dt} &= \frac{P}{2}\omega_m
\end{aligned} \tag{A.1}$$

Here v_{an}, v_{bn} and v_{cn} stand for the phase to neutral voltages in $[V]$; i_a, i_b and i_c represent phase currents in $[A]$, and e_{an}, e_{bn} and e_{cn} represent the back-emf in $[V]$, of each of the phases a, b and c respectively. J is the rotor inertia in $[kg.m^2]$, B is the friction coefficient in $[N.m.s]$, R_s is the stator resistance in $[\Omega]$, L_s is the winding inductance in $[H]$, T_e and T_{load} are the electromagnetic torque and the load torque in $[N.m]$, respectively, ω_m is the rotor mechanical speed in $[\frac{rad}{s}]$, θ_e is the rotor angle in electrical radians, and P is the number of machine poles. The back-emf of each of the phases, and the electromagnetic torque can be further expressed as:

$$\begin{aligned} e_{an} &= K_e \omega_m f(\theta_e), \\ e_{bn} &= K_e \omega_m f(\theta_e - \frac{2\pi}{3}), \\ e_{cn} &= K_e \omega_m f(\theta_e - \frac{4\pi}{3}), \\ T_e &= K_t(f_a(\theta_e) i_a + f_b(\theta_e) i_b + f_c(\theta_e) \end{aligned} \tag{A.2}$$

where K_e and K_t are the back-emf and torque constants, respectively. The electrical rotor angle θ_e is equal to the rotor angle θ_m times the number of pole-pairs $\frac{P}{2}$. Functions $f_a(\theta_e)$, $f_b(\theta_e)$ and $f_c(\theta_e)$ are the trapezoidal unit envelopes of the back-emf waveforms or phases a, b and c respectively. One full cycle of the $f_a(\theta_e)$ is given as:

$$f_a(\theta_e) = \begin{cases} 1, & 0 \leq \theta_e \leq \frac{2\pi}{3} \\ 1 - \frac{6}{\pi}(\theta_e - \frac{2\pi}{3}), & \frac{2\pi}{3} \leq \theta_e \leq \pi \\ -1, & \pi \leq \theta_e \leq \frac{5\pi}{3} \\ -1 + \frac{6}{\pi}(\theta_e - \frac{5\pi}{3}), & \frac{5\pi}{3} \leq \theta_e \leq 2\pi \end{cases} \tag{A.3}$$

The functions $f_b(\theta_e)$ and $f_c(\theta_e)$ in the fourth equation of (A.2) are given as:

$$f_b(\theta_e) = f_a(\theta_e - \frac{2\pi}{3}),$$
$$f_b(\theta_e) = f_a(\theta_e - \frac{4\pi}{3}) \tag{A.4}$$

Switching Logic Table

Switch Interval	Seq. number	Switch closed		Phase current A	B	C
0°–60°	0	S1	S6	+	off	-
60°–120°	1	S3	S6	off	+	-
120°–180°	2	S3	S2	-	+	off
180°–240°	3	S5	S2	-	off	+
240°–300°	4	S5	S4	off	-	+
300°–360°	5	S1	S4	+	-	off

Table A.1: Commutation logic for the BLDC motor drive used in Simulink

Drive Schematic

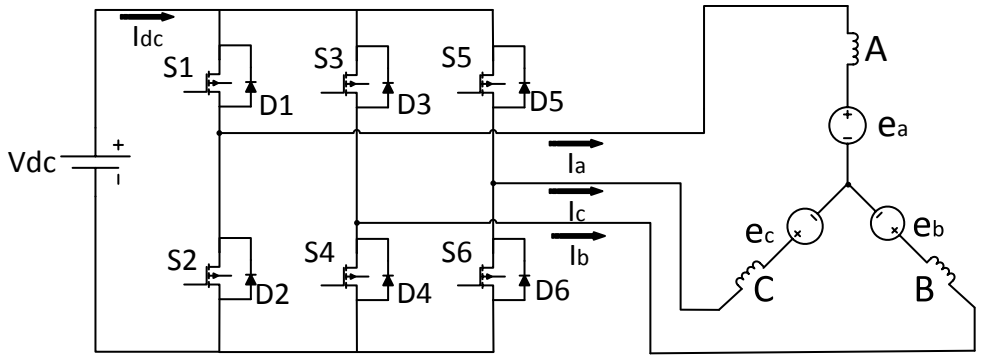

Figure A.1: Simplified schematic of the 3-phase wye-connected BLDC motor drive

A.2 Parameters of the BLDC Motor used in Chapters 2 & 3

Motor parameters	Values
Armature resistance, $\{R_a^{min}, R_a^{max}\}$	$\{5.175, 6.325\}\ \Omega$
Armature inductance, $\{L_a^{min}, L_a^{max}\}$	$\{0.015455, 0.018889\}\ H$
Friction coefficient, $\{b^{min}, b^{max}\}$	$\{0.0009, 0.0011\}\ N.m.s$
Motor constant, $\{K_m^{min}, K_m^{max}\}$	$\{1.26, 1.54\}\ \frac{V.s}{rad}$
Rotor inertia, J_m	$0.0008\ kg.m^2$

Table A.2: Motor parameters

A.3 STATCOM based Power System

Parameters

All the parameters are in per unit (pu) unless specified.

$M = 6$, $C_{DC} = 1$, $T'_{d0} = 5.044$, $K_E = 10$, $T_E = 0.01$, $\omega_b = 120\pi\ (rad/s)$, $x_{TL} = 0.3$,

$x_d = 1.0$, x'_d, $x_q = 0.6$, $x_{LB} = 0.3$, $x_{SDT} = 0.15$.

Power System Schematic

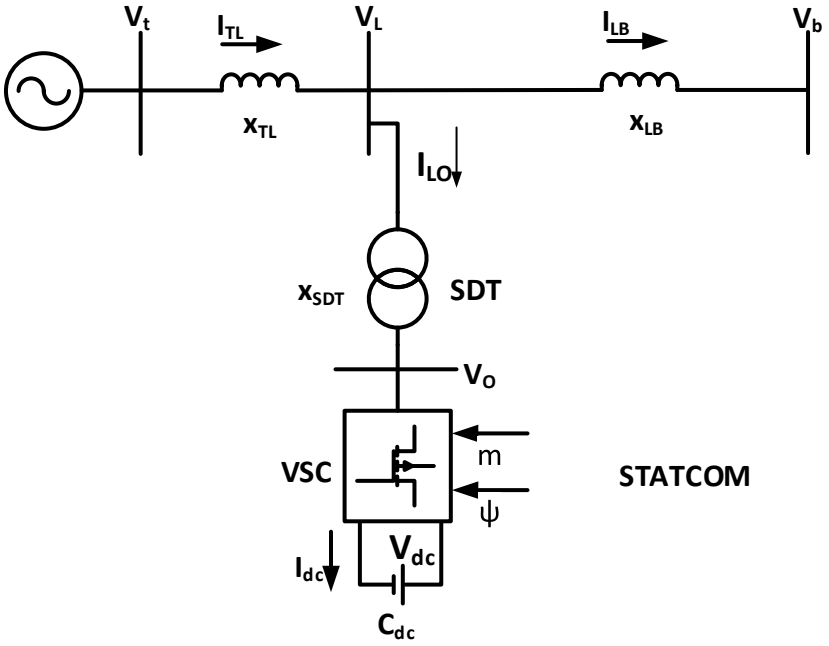

Figure A.2: Single-line diagram of single machine infinite bus system installed with STATCOM

A.4 Parameters and Gains used in Chapter 4

Variance Thresholds

Variance Threshold	Value
Motor M1	0.015
Motor M2	0.050

Table A.3: BLDC motor error variance threshold values

PI Gains

Parameter	Value
Proportional Gain (PWM based), K_p[a]	0.1
Integral Gain (PWM based), K_i[a]	10
Proportional Gain (Variable V_{dc}), K_p	0.013
Integral Gain (Variable V_{dc}), K_i	16.61

[a] Same for both M1 and M2 in both PI alone and hybrid controller modes

Table A.4: BLDC motor PI controller gains

SM Sufrace Weight

Parameter	Value
Surface weight c_1	1000

Table A.5: BLDC motor SM controller surface weight

Motor Parameters

Parameter	Motor M1	Motor M2	Units
$V_{rated,LL}$	500	320	V
I_{rated}	3.3	4.4	A
R_s	2.875	3.16	Ω
L_s	0.0085	0.0064	H
J	0.0008	0.000259	$kg.m^2$
B	0.001	0.00002865	$N.m.s$
K_e	1.4	0.5162	$\frac{V.s}{rad}$
P	4	4	–

Table A.6: Parameters of the motors M1 and M2

STATCOM Power System PI Gains

Parameter	Value
Proportional Gain, K_p[a]	25
Integral Gain, K_i[a]	1

[a] Same for both ω and V_{DC} loops in PI alone and hybrid controller modes

Table A.7: STATCOM based power system PI controller parameters

STATCOM Power System Variance Thresholds

Variance Threshold	Value
ω loop	3×10^{-10}
V_{DC} loop	1×10^{-9}

Table A.8: STATCOM based power system error variance threshold values

A.5 Parameters and Gains for the BLDC Motor Drive in Chapter 5

BLDC Motor Parameters

Parameter	Value
Rated Voltage	$24.01\ V$
Rated Current	$1.16\ A$
Resistance (L-L)	$4.03\ \Omega$
Inductance (L-L)	$4.60\ mH$
Torque Constant	$0.06913\ N.m/A$
Voltage Constant	$7.24\ V/Krpm$
Rotor Inertia	$4.4346 \times 10^{-6}\ kg.m^2$
No. of Poles	10

Table A.9: BLDC Motor Ratings

Controller Gains

Note: The same gains are used for the PI controller in hybrid and standalone modes.

Gain	Value
Proportional	0.05
Integral	320

Table A.10: PI Controller Gains

Commutation Table

Hall Signals			Switch closed		Phase Current		
Hc	Hb	Ha			A	B	C
0	0	1	S1	S6	+	off	-
0	1	0	S4	S5	off	-	+
0	1	1	S1	S4	+	-	off
1	0	0	S2	S3	-	+	off
1	0	1	S3	S6	off	+	-
1	1	0	S2	S5	-	off	+

Table A.11: Commutation Table for the Hurst BLDC Motor Drive

REFERENCES

[1] A. Damen and S. Weiland, "Robust Control," *Lecture Notes on Robust Control, Department of Electrical Engineering, Eindhoven University of Technology*, 2002.

[2] C.-H. Lien, "Robust Observer-Based Control of Systems With State Perturbations Via LMI Approach," *IEEE Transactions on Automatic Control*, vol. 49, no. 8, pp. 1365–1370, Aug. 2004.

[3] J. Daafouz, G. Bara, F. Kratz, and J. Ragot, "State observers for discrete-time LPV systems: an interpolation based approach," in *Proceedings of the 39th IEEE Conference on Decision and Control (Cat. No.00CH37187)*, vol. 5. IEEE, 2000, pp. 4571–4572.

[4] S. Ibaraki and M. Tomizuka, "Taming internal dynamics by mismatched and H_∞-optimized state observer," in *Proceedings of the 2000 American Control Conference. ACC (IEEE Cat. No.00CH36334)*. IEEE, 2000, pp. 715–719 vol.1.

[5] B.-S. Hong, "Observer-based parameterized LPV L2-gain control synthesis," in *Proceedings of the 2002 American Control Conference (IEEE Cat.*

No.CH37301), vol. 6. American Automatic Control Council, 2002, pp. 4427–4432.

[6] E. Prempain, I. Postlethwaite, and A. Benchaib, "A linear parameter variant H_∞ control design for an induction motor," *Control Engineering Practice*, vol. 10, no. 6, pp. 633–644, Jun. 2002.

[7] J. Chen and C. M. Lagoa, "Robust Observer Design for a Class of Switched Systems," in *Proceedings of the 45th IEEE Conference on Decision and Control*. IEEE, 2006, pp. 1659–1664.

[8] S. Aubouet, L. Dugard, and O. Sename, "H_∞/LPV observer for an industrial semi-active suspension," in *2009 IEEE International Conference on Control Applications*. IEEE, Jul. 2009, pp. 756–763.

[9] B. Gerard, H. Souley Ali, M. Zasadzinski, and M. Darouach, "H_∞ Filter for Bilinear Systems Using LPV Approach," *IEEE Transactions on Automatic Control*, vol. 55, no. 7, pp. 1668–1674, Jul. 2010.

[10] W. P. M. H. Heemels, J. Daafouz, and G. Millerioux, "Observer-Based Control of Discrete-Time LPV Systems With Uncertain Parameters," *IEEE Transactions on Automatic Control*, vol. 55, no. 9, pp. 2130–2135, Sep. 2010.

[11] F. A. Shirazi, J. Mohammadpour Velni, and K. M. Grigoriadis, "An LPV Design Approach for Voltage Control of an Electrostatic MEMS Actuator," *Journal of Microelectromechanical Systems*, vol. 20, no. 1, pp. 302–311, Feb. 2011.

[12] S. Fergani, L. Menhour, O. Sename, L. Dugard, and B. D. Novel, "A new LPV/H_∞semi-active suspension control strategy with performance adaptation to roll behavior based on non linear algebraic road profile estimation," in *52nd IEEE Conference on Decision and Control*. IEEE, Dec. 2013, pp. 3511–3516.

[13] C.-H. Lien, "An efficient method to design robust observer-based control of uncertain linear systems," *Applied Mathematics and Computation*, vol. 158, no. 1, pp. 29–44, Oct. 2004.

[14] S. Ibrir, "Convex Optimization Approach to Observer-Based Stabilization of Uncertain Linear Systems," *Journal of Dynamic Systems, Measurement, and Control*, vol. 128, no. 4, p. 989, 2006.

[15] Z. Song and J. Zhao, "Observer-based robust H-infinity control for uncertain switched systems," *Journal of Control Theory and Applications*, vol. 5, no. 3, pp. 278–284, Aug. 2007.

[16] R. Zhang, T. Li, and L. Guo, "Disturbance observer based H-infinity control for flexible spacecraft with time-varying input delay," *Advances in Difference Equations*, vol. 2013, no. 1, p. 142, 2013.

[17] M. Belguith and A. Benabdallah, "Robust Observer Based Control for Stability of Linear Systems: Application to Polytopic Systems," *Journal of Dynamic Systems, Measurement, and Control*, vol. 136, no. 1, p. 014504, Sep. 2013.

[18] Q.-K. Li, G. M. Dimirovski, and J. Zhao, "Observer based tracking control for switched linear systems with time-delay," in *2008 American Control Conference*. IEEE, Jun. 2008, pp. 1570–1575.

[19] H.-H. Wang and G.-Y. Tang, "Observer-based optimal output tracking for discrete-time systems with multiple state and input delays," *International Journal of Control, Automation and Systems*, vol. 7, no. 1, pp. 57–66, Mar. 2009.

[20] Q.-K. Li, J. Zhao, X.-J. Liu, and G. M. Dimirovski, "Observer-based tracking control for switched linear systems with time-varying delay," *International Journal of Robust and Nonlinear Control*, vol. 21, no. 3, pp. 309–327, Feb. 2011.

[21] D. Zhang and Q.-L. Han, "Observer-based output tracking control for a class of linear networked control systems," in *Proceedings of the 2011 American Control Conference*. IEEE, Jun. 2011, pp. 1656–1661.

[22] H. Zhang, Y. Shi, and J. Wang, "Observer-based tracking controller design for networked predictive control systems with uncertain Markov delays," *International Journal of Control*, vol. 86, no. 10, pp. 1824–1836, Oct. 2013.

[23] B. Wang, J.-Y. Zhai, and S.-M. Fei, "Output feedback tracking control for a class of switched nonlinear systems with time-varying delay," *International Journal of Automation and Computing*, vol. 11, no. 6, pp. 605–612, Nov. 2014.

[24] B.-S. Chen, Y.-P. Lin, and Y.-J. Chuang, "Robust H_∞ observer-based tracking control of stochastic immune systems under environmental disturbances and

measurement noises," *Asian Journal of Control*, vol. 13, no. 5, pp. 667–690, Sep. 2011.

[25] H. Ghorbel, A. El Hajjaji, M. Souissi, and M. Chaabane, "Improvement on observer-based H_∞ tracking control for TS fuzzy systems with unmeasurable premise variables," in *52nd IEEE Conference on Decision and Control*. IEEE, Dec. 2013, pp. 6124–6129.

[26] ——, "Robust Tracking Control for TakagiSugeno Fuzzy Systems With Unmeasurable Premise Variables: Application to Tank System," *Journal of Dynamic Systems, Measurement, and Control*, vol. 136, no. 4, p. 041011, Apr. 2014.

[27] M. C. Rabhi and N. M'Sirdi, "H_∞ Tracking Observer-Based Control of the Buck Power Converters," in *Sustainability in Energy and Buildings*, 2012, pp. 169–176.

[28] J. Dong and G.-H. Yang, "Static Output Feedback Control Synthesis for Linear Systems With Time-Invariant Parametric Uncertainties," *IEEE Transactions on Automatic Control*, vol. 52, no. 10, pp. 1930–1936, Oct. 2007.

[29] M. M. Komnatska, "Flight control system design via static output feedback: LMI-approach," in *2013 IEEE 2nd International Conference Actual Problems of Unmanned Air Vehicles Developments Proceedings (APUAVD)*. IEEE, Oct. 2013, pp. 184–186.

[30] A. Fujimori, "Optimization of Static Output Feedback Using Substitutive LMI Formulation," *IEEE Transactions on Automatic Control*, vol. 49, no. 6, pp. 995–999, Jun. 2004.

[31] J. Gadewadikar, A. Bhilegaonkar, and F. Lewis, "Bounded L2 Gain Static Output Feedback: Controller Design and Implementation on an Electromechanical System," *IEEE Transactions on Industrial Electronics*, vol. 54, no. 5, pp. 2593–2599, Oct. 2007.

[32] J. Rubió-Massegú, F. Palacios-Quiñonero, J. M. Rossell, and H. R. Karimi, "Static Output-Feedback Control for Vehicle Suspensions: A Single-Step Linear Matrix Inequality Approach," *Mathematical Problems in Engineering*, vol. 2013, pp. 1–12, 2013.

[33] X.-H. Chang and G.-H. Yang, "New Results on Output Feedback Hinf Control for Linear Discrete-Time Systems," *IEEE Transactions on Automatic Control*, vol. 59, no. 5, pp. 1355–1359, May 2014.

[34] J. Dong and G.-H. Yang, "Robust static output feedback control synthesis for linear continuous systems with polytopic uncertainties," *Automatica*, vol. 49, no. 6, pp. 1821–1829, Jun. 2013.

[35] F. Leibfritz, "An LMI-Based Algorithm for Designing Suboptimal Static H2/Hinf Output Feedback Controllers," *SIAM Journal on Control and Optimization*, vol. 39, no. 6, pp. 1711–1735, Jan. 2001.

[36] Y.-Y. CAO, J. LAM, and Y.-X. SUN, "Static Output Feedback Stabilization: An ILMI Approach," *Automatica*, vol. 34, no. 12, pp. 1641–1645, Dec. 1998.

[37] F. Hao and X. Zhao, "Linear matrix inequality approach to static output-feedback stabilisation of discrete-time networked control systems," *IET Control Theory & Applications*, vol. 4, no. 7, pp. 1211–1221, Jul. 2010.

[38] C. Wang and T. Huang, "Static output feedback control for positive linear continuous-time systems," *International Journal of Robust and Nonlinear Control*, vol. 23, no. 14, pp. 1537–1544, Sep. 2013.

[39] J. Rubió-Massegú, J. Rossell, H. Karimi, and F. Palacios-Quiñonero, "Static output-feedback control under information structure constraints," *Automatica*, vol. 49, no. 1, pp. 313–316, Jan. 2013.

[40] G. Chesi, "Robust Static Output Feedback Controllers via Robust Stabilizability Functions," *IEEE Transactions on Automatic Control*, vol. 59, no. 6, pp. 1618–1623, Jun. 2014.

[41] G. G. Rigatos, "Model-based and model-free control of flexible-link robots: A comparison between representative methods," *Applied Mathematical Modelling*, vol. 33, no. 10, pp. 3906–3925, 2009.

[42] V. Moudgal, W. Kwong, K. Passino, and S. Yurkovich, "Fuzzy learning control for a flexible-link robot," *IEEE Transactions on Fuzzy Systems*, vol. 3, no. 2, pp. 199–210, 1995.

[43] A. Yazdizadeh, K. Khorasani, and R. V. Patel, "Identification of a two-link flexible manipulator using adaptive time delay neural networks." *IEEE transactions on systems, man, and cybernetics. Part B, Cybernetics : a publication of the IEEE Systems, Man, and Cybernetics Society*, vol. 30, no. 1, pp. 165–172, 2000.

[44] Z. Su and K. Khorasani, "A neural-network-based controller for a single-link flexible manipulator using the inverse dynamics approach," *IEEE Transactions on Industrial Electronics*, vol. 48, no. 6, pp. 1074–1086, 2001.

[45] L. Tian and C. Collins, "Adaptive neuro-fuzzy control of a flexible manipulator," *Mechatronics*, vol. 15, no. 10, pp. 1305–1320, 2005.

[46] R. J. Wai and M. C. Lee, "Intelligent Optimal Control of Single-Link Flexible Robot Arm," *IEEE Transactions on Industrial Electronics*, vol. 51, no. 1, pp. 201–220, 2004.

[47] J. M. Renno, "Inverse dynamics based tuning of a fuzzy logic controller for a single-link flexible manipulator," *Journal of Vibration and Control*, vol. 13, no. 12, pp. 1741–1759, 2007.

[48] V. Donescu, D. Neacsu, and G. Griva, "Design of fuzzy logic speed controller for brushless DC motor drives," in *Proceedings of IEEE International Symposium on Industrial Electronics*, vol. 1. IEEE, 1996, pp. 404–408.

[49] A. Rubaai, D. Ricketts, and M. Kankam, "Experimental verification of a hybrid fuzzy control strategy for a high-performance brushless DC drive system," *IEEE Transactions on Industry Applications*, vol. 37, no. 2, pp. 503–512, 2001.

[50] C. Xia, P. Guo, T. Shi, and M. Wang, "Speed control of brushless DC motor using genetic algorithm based fuzzy controller," in *2004 International Conference on Intelligent Mechatronics and Automation, 2004. Proceedings.* IEEE, 2004, pp. 460–464.

[51] Z. Pan and F. Luo, "Steady state reference current determination technique for brushless DC motor drive system," *IEE Proceedings - Electric Power Applications*, vol. 152, no. 6, p. 1585, 2005.

[52] A. Rubaai, M. J. Castro-Sitiriche, and A. R. Ofoli, "Design and Implementation of Parallel Fuzzy PID Controller for High-Performance Brushless Motor Drives: An Integrated Environment for Rapid Control Prototyping," *IEEE Transactions on Industry Applications*, vol. 44, no. 4, pp. 1090–1098, 2008.

[53] R. Shanmugasundram, K. M. Zakariah, and N. Yadaiah, "Implementation and Performance Analysis of Digital Controllers for Brushless DC Motor Drives," *IEEE/ASME Transactions on Mechatronics*, vol. 19, no. 1, pp. 213–224, Feb. 2014.

[54] K. Premkumar and B. Manikandan, "Adaptive Neuro-Fuzzy Inference System based speed controller for brushless DC motor," *Neurocomputing*, vol. 138, pp. 260–270, Aug. 2014.

[55] A. Ajami and S. Hosseini, "Application of a Fuzzy Controller for Transient Stability Enhancement of AC Transmission System by STATCOM," *2006 SICE-ICASE International Joint Conference*, 2006.

[56] A. Ghafouri, M. R. Zolghadri, and M. Ehsan, "Power system stability improvement using self-tuning fuzzy logic controlled STATCOM," in *EUROCON 2007 - The International Conference on Computer as a Tool*, 2007, pp. 1444–1449.

[57] N. Henini, F. Benzerafa, and A. Tlemcani, "Design and simulation of five-level inverter based DSTATCOM using fuzzy logic," in *IREC2015 The Sixth International Renewable Energy Congress*, 2015, pp. 1–6.

[58] S. Hosseini, R. Rahnavard, and Y. Ebrahimi, "Reactive Power Compensation in Distribution Networks with STATCOM by Fuzzy Logic Theory Application," in *2006 CES/IEEE 5th International Power Electronics and Motion Control Conference*, vol. 2, 2006.

[59] S. Mohagheghi, G. Venayagamoorthy, and R. Harley, "An Interval Type-II Robust Fuzzy Logic Controller for a Static Compensator in a Multimachine Power System," in *The 2006 IEEE International Joint Conference on Neural Network Proceedings*, 2006.

[60] S. Mohagheghi, G. K. Venayagamoorthy, S. Rajagopalan, and R. G. Harley, "Hardware implementation of a mamdani fuzzy logic controller for a static compensator in a multimachine power system," *IEEE Transactions on Industry Applications*, vol. 45, no. 4, pp. 1535–1544, 2009.

[61] S. Mohagheghi, G. K. Venayagamoorthy, and R. G. Harley, "Adaptive critic design based neuro-fuzzy controller for a static compensator in a multimachine

power system," *IEEE Transactions on Power Systems*, vol. 21, no. 4, pp. 1744–1754, 2006.

[62] S. Nagarajan and N. Kumar, "Fuzzy logic based control of STATCOM for mitigation of SSR," in *2012 IEEE 5th India International Conference on Power Electronics (IICPE)*, 2012, pp. 1–6.

[63] G. Shahgholian, M. Mahdavian, A. Emami, and B. Ahmadzade, "Improve power quality using static synchronous compensator with fuzzy logic controller," in *2011 International Conference on Electrical Machines and Systems*, 2011, pp. 1–5.

[64] L. Wang and D. N. Truong, "Stability enhancement of DFIG-based offshore wind farm fed to a multi-machine system using a STATCOM," *IEEE Transactions on Power Systems*, vol. 28, no. 3, pp. 2882–2889, 2013.

[65] B.-S. C. B.-S. Chen, C.-S. T. C.-S. Tseng, and H.-J. U. H.-J. Uang, "Mixed H_2/H_∞ fuzzy output feedback control design for nonlinear dynamic systems: an LMI approach," *IEEE Transactions on Fuzzy Systems*, vol. 8, no. 3, pp. 249–265, 2000.

[66] C. W. Scherer, "An efficient solution to multi-objective control problems with LMI objectives," *Systems & Control Letters*, vol. 40, pp. 43–57, 2000.

[67] B. S. Chen and W. Zhang, "Stochastic H_2/H_∞ control with state-dependent noise," *IEEE Transactions on Automatic Control*, vol. 49, no. 1, pp. 45–57, 2004.

[68] H. R. Karimi and H. Gao, "Mixed H_2/H_∞ output-feedback control of second-order neutral systems with time-varying state and input delays," *ISA Transactions*, vol. 47, no. 3, pp. 311–324, 2008.

[69] H. Gao, J. Lam, and C. Wang, "Mixed H_2/H_∞ filtering for continuous-time polytopic systems: A parameter-dependent approach," *Circuits, Systems, and Signal Processing*, vol. 24, no. 6, pp. 689–702, 2005.

[70] H. G. H. Gao, J. Lam, L. X. L. Xie, and C. W. C. Wang, "New approach to mixed H_2/H_∞ filtering for polytopic discrete-time systems," *IEEE Transactions on Signal Processing*, vol. 53, no. 8, pp. 3183–3192, 2005.

[71] S. M. de Oca and V. Puig, "Fault-Tolerant Control design using a virtual sensor for LPV systems," in *2010 Conference on Control and Fault-Tolerant Systems (SysTol)*. IEEE, Oct. 2010, pp. 88–93.

[72] H. Zhang, Y. Shi, and A. Mehr, "Parameter-dependent mixed H_2/H_∞ filtering for linear parameter-varying systems," *IET Signal Processing*, vol. 6, no. 7, pp. 697–703, 2012.

[73] A. White, Z. Ren, G. Zhu, and J. Choi, "Mixed H_2/H_∞ observer-based LPV control of a hydraulic engine cam phasing actuator," *IEEE Transactions on Control Systems Technology*, vol. 21, no. 1, pp. 229–238, 2013.

[74] H. Zhang, J. Wang, and Y.-Y. Wang, "Robust mixed H_2/H_∞ gain-scheduling observer design for removal of NOx sensor ammonia cross sensitivity in selective

catalytic reduction systems," in *American Control Conference (ACC)*, 2013, pp. 2177 – 2182.

[75] X. Wei and M. Verhaegen, "Mixed H-/Hinf fault detection observer design for LPV systems," in *2008 47th IEEE Conference on Decision and Control*. IEEE, 2008, pp. 1073–1078.

[76] X. Chen and K. Zhou, "Multiobjective H_2/H_∞ Control Design," *SIAM Journal on Control and Optimization*, vol. 40, pp. 628–660, 2001.

[77] H. R. Karimi, "Observer-Based Mixed H_2/H_∞ Control Design for Linear Systems with Time-Varying Delays: An LMI Approach," *International Journal of Control, Automation and Systems*, vol. 6, no. 1, pp. 1–14, 2008.

[78] L. Yuzhi and L. Muguo, "Robust observer-based mixed H_2/H_∞ control design for uncertain linear discrete-time systems," in *Control Conference (CCC), 2013 32nd Chinese*, 2013, pp. 2769 – 2774.

[79] S. Ibrir, W. F. Xie, and C.-Y. Su, "Observer-based control of discrete-time Lipschitzian non-linear systems: application to one-link flexible joint robot," *International Journal of Control*, vol. 78, pp. 385–395, 2005.

[80] H. Li, "Observer-based mixed H_2/H_∞ tracking control for continuous-time systems with integral action and pole placement," *Discrete Dynamics in Nature and Society*, vol. 2012, pp. 1–13, 2012.

[81] C. Scherer, "Mixed H_2/H_∞ Control," *Trends in Control: A European Perspective*, 1995.

[82] M. Ge, M.-S. Chiu, and Q.-G. Wang, "Robust PID controller design via LMI approach," *Journal of Process Control*, vol. 12, no. 1, pp. 3–13, Jan. 2002.

[83] A. Delibasi, I. B. Kucukdemiral, and G. Cansever, "A robust PID like state-feedback control via LMI approach: An application on a Double Inverted Pendulum System," in *2007 International Symposium on Computational Intelligence in Robotics and Automation*. IEEE, Jun. 2007, pp. 374–379.

[84] S. Lei and Y. Jianying, "Smooth Switching Output Tracking Control for a Class of Linear Time-Varying Systems: An LMI Approach," in *29th Chinese Control Conference (CCC)*, 2010, pp. 1977 – 1982.

[85] R. Conway, J. Choi, R. Nagamune, and R. Horowitz, "Robust track-following controller design in hard disk drives based on parameter dependent lyapunov functions," *IEEE Transactions on Magnetics*, vol. 46, no. 4, pp. 1060–1068, 2010.

[86] K. Baghestan, S. M. Rezaei, H. A. Talebi, and M. Zareinejad, "Robust force control in a novel electro-hydraulic structure using polytopic uncertainty representation." *ISA transactions*, vol. 53, no. 6, pp. 1873–80, Nov. 2014.

[87] S. Ibrir and M. Bettayeb, "New sufficient conditions for observer-based control of fractional-order uncertain systems," *Automatica*, vol. 59, pp. 216–223, Sep. 2015.

[88] L. Zadeh, "Fuzzy Sets," *Information and Control*, vol. 8, no. 3, pp. 338–353, 1965.

[89] MATLAB, "R2013b Fuzzy Logic Toolbox Documentation," *Matlab R2013b*, 2013.

[90] B. Bose, *Power Electronics and Motor Drives*, 1st ed. Elsevier Inc., 2006.

[91] R. Krishnan, *Permanent Magnet Synchronous and Brushless DC Motor Drives*, 1st ed. CRC Press, 2010.

[92] S. Baldursson, "BLDC Motor Modelling and Control - A Matlab/Simulink Implementation," Ph.D. dissertation, 2005.

[93] C.-L. Xia, *Permanent Magnet Brushless DC Motor Drives and Controls*, 1st ed. Wiley, 2012.

[94] K.-H. Park, T.-S. Kim, S.-C. Ahn, and D.-S. Hyun, "Speed control of high-performance brushless DC motor drives by load torque estimation," in *IEEE 34th Annual Conference on Power Electronics Specialist, 2003. PESC '03.*, vol. 4. IEEE, 2003, pp. 1677–1681.

[95] H.-x. Wu, S.-k. Cheng, and S.-m. Cui, "A controller of brushless DC motor for electric vehicle," *IEEE Transactions on Magnetics*, vol. 41, no. 1, pp. 509–513, Jan. 2005.

[96] C.-t. Pan and E. Fang, "A Phase-Locked-Loop-Assisted Internal Model Adjustable-Speed Controller for BLDC Motors," *IEEE Transactions on Industrial Electronics*, vol. 55, no. 9, pp. 3415–3425, Sep. 2008.

[97] V. Bist and B. Singh, "Improved power quality bridgeless Cuk converter fed brushless DC motor drive for air conditioning system," *IET Power Electronics*, vol. 6, no. 5, pp. 902–913, May 2013.

[98] C. L. P. Swamy, B. Singh, and B. P. Singh, "Investigations on Dynamic Behavior of Permanent Magnet Brushless Dc Motor Drive," *Electric Machines & Power Systems*, vol. 23, no. 6, pp. 689–701, Nov. 1995.

[99] P. Pillay and R. Krishnan, "Modeling, simulation, and analysis of permanent-magnet motor drives. II. The brushless DC motor drive," *IEEE Transactions on Industry Applications*, vol. 25, no. 2, pp. 274–279, 1989.

[100] H. Chen, M. Huang, C. Liaw, Y. Chang, P. Yu, and J. Huang, "Robust current control for brushless DC motors," *IEE Proceedings - Electric Power Applications*, vol. 147, no. 6, p. 503, 2000.

[101] K.-H. Kim, I.-C. Baik, S.-K. Chung, and M.-J. Youn, "Robust speed control of brushless DC motor using adaptive inputoutput linearisation technique," *IEE Proceedings - Electric Power Applications*, vol. 144, no. 6, p. 469, 1997.

[102] H.-S. Choi, Y.-H. Park, Y. Cho, and M. Lee, "Global sliding-mode control. Improved design for a brushless DC motor," *IEEE Control Systems Magazine*, vol. 21, no. 3, pp. 27–35, Jun. 2001.

[103] T. Shi, N. Lu, Q. Zhang, and C. Xia, "Brushless DC motor sliding mode control with Kalman Filter," in *2008 IEEE International Conference on Industrial Technology*, no. 05. IEEE, Apr. 2008, pp. 1–6.

[104] C.-Y. Chen, W.-C. Chan, T.-C. Ou, S.-H. Yu, and T.-W. Liu, "Sliding mode speed control of Brushless DC Motor using Pulse-Width-Modulated current regulator," in *2009 IEEE/ASME International Conference on Advanced Intelligent Mechatronics*. IEEE, Jul. 2009, pp. 1395–1399.

[105] H. Lin, W. Yan, J. Wang, Y. Yao, and B. Gao, "Robust nonlinear speed control for a brushless DC motor using model reference adaptive backstepping approach," in *2009 International Conference on Mechatronics and Automation*. IEEE, Aug. 2009, pp. 335–340.

[106] Y. Liu, J. Zhao, M. Xia, and H. Luo, "Model Reference Adaptive Control-Based Speed Control of Brushless DC Motors With Low-Resolution Hall-Effect Sensors," *IEEE Transactions on Power Electronics*, vol. 29, no. 3, pp. 1514–1522, Mar. 2014.

[107] F. Rodriguez and A. Emadi, "A Novel Digital Control Technique for Brushless DC Motor Drives," *IEEE Transactions on Industrial Electronics*, vol. 54, no. 5, pp. 2365–2373, Oct. 2007.

[108] A. Sathyan, N. Milivojevic, M. Krishnamurthy, and A. Emadi, "An FPGA-Based Novel Digital PWM Control Scheme for BLDC Motor Drives," *IEEE Transactions on Industrial Electronics*, vol. 56, no. 8, pp. 3040–3049, Aug. 2009.

[109] J. Dixon and L. Leal, "Current control strategy for brushless DC motors based on a common DC signal," *IEEE Transactions on Power Electronics*, vol. 17, no. 2, pp. 232–240, Mar. 2002.

[110] G.-R. Yu and R.-C. Hwang, "Optimal PID speed control of brush less DC motors using LQR approach," in *2004 IEEE International Conference on Systems, Man and Cybernetics (IEEE Cat. No.04CH37583)*, vol. 1. IEEE, 2004, pp. 473–478.

[111] C. Xia, J. Liu, W. Yu, and Z. Li, "Variable structure control of BLDCM based on extended state observer," in *IEEE International Conference Mechatronics and Automation, 2005*, vol. 2, no. July. IEEE, 2005, pp. 568–571.

[112] P. Thirusakthimurugan and P. Dananjayan, "A novel robust speed controller scheme for PMBLDC motor." *ISA transactions*, vol. 46, no. 4, pp. 471–7, Oct. 2007.

[113] C.-Y. Chen, M. H.-M. Cheng, and C.-F. Yang, "Modified Sliding Mode Speed Control of Brushless DC Motor Using Quantized Current Regulator," in *2009 Fourth International Conference on Innovative Computing, Information and Control (ICICIC)*. IEEE, Dec. 2009, pp. 926–929.

[114] H. Okumu, H. Kahveci, and M. Ekici, "Improved brushless DC motor speed controller with digital signal processor," *Electronics Letters*, vol. 50, no. 12, pp. 864–866, Jun. 2014.

[115] S. Singh and B. Singh, "A Voltage-Controlled PFC Cuk Converter-Based PMBLDCM Drive for Air-Conditioners," *IEEE Transactions on Industry Applications*, vol. 48, no. 2, pp. 832–838, Mar. 2012. [Online]. Available: http://ieeexplore.ieee.org/lpdocs/epic03/wrapper.htm?arnumber=6121901

[116] C. Xia, Z. Li, and T. Shi, "A Control Strategy for Four-Switch Three-Phase Brushless DC Motor Using Single Current Sensor," *IEEE Transactions on Industrial Electronics*, vol. 56, no. 6, pp. 2058–2066, Jun. 2009.

[117] B. Singh, A. Reddy, and S. Murthy, "Hybrid fuzzy logic proportional plus conventional integral-derivative controller for permanent magnet brushless DC motor," in *Proceedings of IEEE International Conference on Industrial Technology 2000 (IEEE Cat. No.00TH8482)*, vol. 1. Jaico Publishing House, 2000, pp. 185–191.

[118] B. Singh, R. Saha, A. Chandra, and K. Al-Haddad, "Static synchronous compensators (STATCOM): a review," p. 297, 2009.

[119] D. L. D. Lijie, L. Y. L. Yang, and M. Y. M. Yiqun, "Comparison of High Capacity SVC and STATCOM in Real Power Grid," *Intelligent Computation Technology and Automation (ICICTA), 2010 International Conference on*, vol. 1, 2010.

[120] H. Wang, "Phillips-Heffron model of power systems installed with STATCOM and applications," *IEE Proceedings - Generation, Transmission and Distribution*, vol. 146, no. 5, p. 521, 1999.

[121] Y. Y. Y. Yu, C. J. C. Jianye, and H. Y. H. Yingduo, "STATCOM modeling and analysis in damping power system oscillations," *Collection of Technical Papers. 35th Intersociety Energy Conversion Engineering Conference and Exhibit (IECEC) (Cat. No.00CH37022)*, vol. 2, 2000.

[122] M. Abido, "Analysis and assessment of STATCOM-based damping stabilizers for power system stability enhancement," *Electric Power Systems Research*, vol. 73, no. 2, pp. 177–185, Feb. 2005.

[123] S. A. Al-Baiyat, "Power system transient stability enhancement by STATCOM with nonlinear H_∞ stabilizer," *Electric Power Systems Research*, vol. 73, no. 1, pp. 45–52, 2005.

[124] F. S. Al-Ismail, M. A. Hassan, and M. A. Abido, "RTDS implementation of STATCOM-based power system stabilizers," *Canadian Journal of Electrical and Computer Engineering*, vol. 37, no. 1, pp. 48–56, 2014.

[125] K. R. Padiyar and N. Prabhu, "Design and performance evaluation of subsynchronous damping controller with STATCOM," *IEEE Transactions on Power Delivery*, vol. 21, no. 3, pp. 1398–1405, 2006.

[126] K. Li, J. Liu, Z. Wang, and B. Wei, "Strategies and operating point optimization of STATCOM control for voltage unbalance mitigation in three-phase three-wire systems," *IEEE Transactions on Power Delivery*, vol. 22, no. 1, pp. 413–422, 2007.

[127] M. Molinas, J. A. Suul, and T. Undeland, "Low voltage ride through of wind farms with cage generators: STATCOM versus SVC," *IEEE Transactions on Power Electronics*, vol. 23, no. 3, pp. 1104–1117, 2008.

[128] A. Moharana, R. K. Varma, and R. Seethapathy, "SSR Alleviation by STATCOM in Induction-Generator-Based Wind Farm Connected to Series Compen-

sated Line," *IEEE Transactions on Sustainable Energy*, vol. 5, no. 3, pp. 947–957, 2014.

[129] T. L. Lee, S. H. Hu, and Y. H. Chan, "D-STATCOM with positive-sequence admittance and negative-sequence conductance to mitigate voltage fluctuations in high-level fenetration of distributed-generation systems," *IEEE Transactions on Industrial Electronics*, vol. 60, no. 4, pp. 1417–1428, 2013.

[130] C. Wessels, N. Hoffmann, M. Molinas, and F. W. Fuchs, "StatCom control at wind farms with fixed-speed induction generators under asymmetrical grid faults," *IEEE Transactions on Industrial Electronics*, vol. 60, no. 7, pp. 2864–2873, 2013.

[131] B. Singh, S. S. Murthy, and R. S. R. Chilipi, "STATCOM-Based Controller for a Three-Phase SEIG Feeding Single-Phase Loads," *IEEE Transactions on Energy Conversion*, vol. 29, no. 2, pp. 320–331, 2014.

[132] R. Varma, S. Rahman, and T. Vanderheide, "New Control of PV Solar Farm as STATCOM (PV-STATCOM) for Increasing Grid Power Transmission Limits During Night and Day," *IEEE Transactions on Power Delivery*, pp. 1–1, 2014.

[133] Y. Xu and F. Li, "Adaptive PI control of STATCOM for voltage regulation," *IEEE Transactions on Power Delivery*, vol. 29, no. 3, pp. 1002–1011, 2014.

[134] A. K. Jain, A. Behal, X. T. Zhang, D. M. Dawson, and N. Mohan, "Nonlinear controllers for fast voltage regulation using STATCOMs," *IEEE Transactions on Control Systems Technology*, vol. 12, no. 6, pp. 827–842, 2004.

[135] N. Mariun, S. Aizam, H. Hizam, and N. Wahab, "Design of pole placement controller in D-STATCOM for unbalanced faults mitigation," in *2005 International Power Engineering Conference*, 2005.

[136] S. Eshtehardiha, G. Shahgholian, and H. Mahmoodian, "Coordinating the multivariable state-feedback controller on static synchronous compensator with genetic algorithm," in *2007 International Conference on Intelligent and Advanced Systems, ICIAS 2007*, 2007, pp. 864–869.

[137] A. Shukla, A. Ghosh, and A. Joshi, "State feedback control of multilevel inverters for DSTATCOM applications," *IEEE Transactions on Power Delivery*, vol. 22, no. 4, pp. 2409–2418, 2007.

[138] V. Spitsa, A. Alexandrovitz, and E. Zeheb, "Robust pole placement technique for STATCOM controller design," in *IEEE Convention of Electrical and Electronics Engineers in Israel, Proceedings*, 2008, pp. 95–99.

[139] V. Spitsa, A. Alexandrovitz, and E. Zeheb, "Design of a robust state feedback controller for a STATCOM using a zero set concept," *IEEE Transactions on Power Delivery*, vol. 25, no. 1, pp. 456–467, 2010.

[140] M. Miranbeigi, Y. Neyshabouri, and H. Iman-Eini, "State feedback control strategy and voltage balancing scheme for a transformer-less STATic synchronous COMpensator based on cascaded H-bridge converter," *IET Power Electronics*, vol. 8, no. 6, pp. 906–917, 2015.

[141] S. Boyd, L. E. Ghaoui, E. Feron, and V. Balakrishnan, *Linear Matrix Inequalities in System and Control Theory*, 1st ed. Society for Industrial and Applied Mathematics, 1994.

[142] D. Luenberger, "An introduction to observers," *IEEE Transactions on Automatic Control*, vol. 16, no. 6, pp. 596–602, Dec. 1971.

[143] S. Boyd and L. Vandenberghe, *Convex Optimization*, 1st ed. Cambridge University Press, 2004.

[144] R. Toscano, "Signal and System Norms," in *Structured Controllers for Uncertain Systems*. Springer, 2013, ch. 2, pp. 25–44.

[145] C. Crusius and A. Trofino, "Sufficient LMI conditions for output feedback control problems," *IEEE Transactions on Automatic Control*, vol. 44, no. 5, pp. 1053–1057, May 1999.

[146] J. Lofberg, "YALMIP : a toolbox for modeling and optimization in MATLAB," in *2004 IEEE International Conference on Robotics and Automation (IEEE Cat. No.04CH37508)*. IEEE, 2004, pp. 284–289.

[147] MathWorks, "MATLAB/Simulink R2013b," 2013.

[148] D. Retzmann, "Design of a rule-based controller for STATCOM," in *IECON '98. Proceedings of the 24th Annual Conference of the IEEE Industrial Electronics Society (Cat. No.98CH36200)*, vol. 1. IEEE, 1998, pp. 467–472.

[149] C.-T. Chen, *Linear System Theory and Design*, 3rd ed. Oxford University Press, 1999.

[150] T. J. Ross, *Fuzzy Logic with Engineering Applications*. John Wiley & Sons, 2010.

[151] C. Edwards and S. K. Spurgeon, *Sliding Mode Control: Theory and Applications*, 1st ed. Taylor & Francis, 1998.

[152] Microchip, "dsPICDEM MCLV-2 Development Board User's Guide," *Microchip Technology Inc.*, 2012.

[153] Hurst, "NT Dynamo Brushless DC Motor, DMB0224C10002," *Hurst MFG.*, 2002. [Online]. Available: http://www.hurst-motors.com/

[154] Microchip, "MPLAB 16-Bit Device Blocks for Simulink," *Microchip Technology Inc.*, 2014. [Online]. Available: http://www.microchip.com/SimulinkBlocks, [Accessed: May 30, 2015]

[155] HIOKI E.E. CORPORATION, "HIOKI 3197 Power Quality Analyzer," *User Manual*. [Online]. Available: https://www.hioki.com/products/power_current_sensor/power_meters/1444, [Accessed: May 30, 2015]

[156] Microchip, "MPLAB ICD-3 In-Circuit Debugger User's Guide," *Microchip Technology Inc.*, 2012.

[157] A. Abdullah and M. Zribi, "Sensor-Fault-Tolerant Control for a Class of Linear Parameter Varying Systems With Practical Examples," *IEEE Transactions on Industrial Electronics*, vol. 60, no. 11, pp. 5239–5251, Nov. 2013.

[158] F. Lopez-Estrada, J.-C. Ponsart, D. Theilliol, C. Astorga-Zaragoza, and Y. Zhang, "Robust sensor fault diagnosis and tracking controller for a UAV modelled as LPV system," in *2014 International Conference on Unmanned Aircraft Systems (ICUAS)*. IEEE, May 2014, pp. 1311–1316.

[159] C. Guo and X.-G. Liang, "Disturbance-Observer-Based Robust H_∞ Switching Tracking Control for Near Space Interceptor," *International Journal of Aeronautical and Space Sciences*, vol. 15, no. 2, pp. 153–162, Jun. 2014.

Vitae

- Name: Adeel Sabir
- Nationality: Pakistan
- Date of Birth: 30 October, 1981
- Permanent Address: 26-B Mumtazabad, Multan 60600, Pakistan
- Phone: (+966) 507832892
- Email: *adeel_sabir@hotmail.com*

- M.S. Electrical Engineering, May 2009
- B.S. Electrical Engineering, May 2006